

# Greedification Operators for Policy Optimization: Investigating Forward and Reverse KL Divergences

Alan Chan

Hugo Silva

Sungsu Lim

Tadashi Kozuno

A. Rupam Mahmood

Martha White

ACHAN4@UALBERTA.CA

HUGOLUIS@UALBERTA.CA

SUNGSU@UALBERTA.CA

KOZUNO@UALBERTA.CA

ARMAHMOOD@UALBERTA.CA

WHITEM@UALBERTA.CA

*Department of Computing Science, Alberta Machine Intelligence Institute (Amii)*

*University of Alberta*

*Edmonton, Alberta, Canada*

## Abstract

Approximate Policy Iteration (API) algorithms alternate between (approximate) policy evaluation and (approximate) greedification. Many different approaches have been explored for approximate policy evaluation, but less is understood about approximate greedification and what choices guarantee policy improvement. In this work, we investigate approximate greedification when reducing the KL divergence between the parameterized policy and the Boltzmann distribution over action values. In particular, we investigate the difference between the forward and reverse KL divergences, with varying degrees of entropy regularization. We show that the reverse KL has stronger policy improvement guarantees, but that reducing the forward KL can result in a worse policy. We also demonstrate, however, that a large enough reduction of the forward KL can induce improvement under additional assumptions. Empirically, we show on simple continuous-action environments that the forward KL can induce more exploration, but at the cost of a more suboptimal policy. No significant differences were observed in the discrete-action setting or on a suite of benchmark problems. Throughout, we highlight that many policy gradient methods can be seen as an instance of API, with either the forward or reverse KL for the policy update, and discuss next steps for understanding and improving our policy optimization algorithms.

**Keywords:** reinforcement learning, policy gradient, policy iteration, kl divergence

## 1. Introduction

A canonical approach to learn policies in reinforcement learning (RL) is Policy Iteration (PI). PI interleaves policy evaluation—understanding how a policy is currently performing by computing a value function—and policy improvement—making the current policy better based on the value function. The policy improvement step is sometimes called the *greedification* step, because typically the policy is set to a greedy policy. That is, the policy is set to take the action that maximizes the current action-value function, in each state. In the tabular setting, this procedure is guaranteed to result in iteratively better policies and converge to the optimal policy (Bertsekas, 2019). The greedification step can also be soft, in that some probability is placed on all other actions. In certain such cases, like with entropy regularization, PI converges to the optimal soft policy (Geist et al., 2019).

Practically, however, it is not always feasible to perform each step to completion. Approximate PI (API) (Bertsekas, 2011; Scherrer, 2014) allows for each step to be done incompletely, and still maintain convergence guarantees in some cases. The agent can perform an approximate policy evaluation step, where it obtains an improved estimate of the values without achieving the true values. The agent can also only perform approximate greedification by updating the policy to be closer to the (soft) greedy policy under the current values. The first approximation underlies algorithms like Sarsa, where the action-value estimates are updated with one new sample, upon which the new policy is immediately set to the soft greedy policy (approximate evaluation, exact greedification).

It is not as common to consider approximate greedification. One of the reasons is that obtaining the (soft) greedy policy is straightforward for discrete actions.<sup>1</sup> For continuous actions, however, obtaining the greedy action for given action-values is non-trivial, requiring the computation of the maximum value (or supremum) over the continuous domain. Some methods have considered optimization approaches to compute it, to get continuous-action Q-learning methods (Ryu et al., 2020; Gu, 2019). It is more common, though, to instead turn to policy gradient methods and learn a parameterized policy.

This switch to parameterized policies, however, does not evade the question of how to perform approximate greedification. Indeed, many policy gradient (PG) methods can actually be seen as instances of API, which involves both approximate greedification and approximate evaluation. The connection between PG and API arises because the efficient implementation of PG methods requires the estimation of a value function, in the absence of exact calculation. In REINFORCE (Williams, 1992), one performs approximate policy evaluation through Monte Carlo rollouts, while most actor-critic methods estimate an action-value function through temporal-difference methods (Sutton and Barto, 2018). We explicitly show in this work that the basic actor-critic method can be seen as API with a particular approximate greedification step. In general, numerous papers have already linked PG methods to policy iteration (Sutton et al., 1999; Kakade and Langford, 2002; Perkins and Pendrith, 2002; Perkins and Precup, 2003; Wagner, 2011, 2013; Scherrer and Geist, 2014; Bhandari and Russo, 2019), including recent work connecting maximum-entropy PG and value-based methods (O’Donoghue et al., 2017; Nachum et al., 2017b; Schulman et al., 2017a; Nachum et al., 2019).

Moreover, most so-called PG methods used in practice are better thought of as API methods, rather than as PG methods. Many PG methods in fact use a biased estimate of the policy gradient (Nota and Thomas, 2020). The correct state weighting is not used in either the on-policy setting (Thomas, 2014; Nota and Thomas, 2020) or the off-policy setting (Imani et al., 2018). Additionally, the use of function approximators to estimate action-values generally results in biased gradient estimates without any further guarantees, such as a compatibility condition (Sutton et al., 1999). This bias can be reduced by using  $n$ -step return estimates for the policy update, but is not completely removed. Understanding

---

1. Even under discrete actions, there is a reasonable argument that approximate greedification may be preferable, even if exact greedification is possible. We typically only have estimates of the value function, and exact greedification on the estimates can potentially harm the agent’s performance (Kakade and Langford, 2002). Further, having an explicit parameterized policy, even under discrete actions, can be beneficial to avoid an effect known as delusional bias (Lu et al., 2018), where directly computing the greedy value in action-value updates can result in inconsistent action choices.

approximate greedification within API, therefore, is one direction for better understanding the PG methods actually used in practice.

The next question, then, is what approximate greedification approach should be used. For tabular policies, policy greedification is straightforward: at each state, we set the policy to place unit mass on the greedy action (or mass spread arbitrarily around the greedy actions), with zero mass on non-greedy actions. If a new policy is greedy with respect to the action-value function of an old policy, the classical policy improvement theorem (Sutton and Barto, 2018) guarantees that the new policy is at least as good as the old policy. For parameterized policies (e.g., neural-network policies), however, exact greedification in each state is rarely possible as not all policies will be representable by a given function approximator class.

Instead, we can define a desired target policy, that would provide policy improvement if we could represent it, and learn a policy to approximate that target. One choice is to minimize the Kullback-Leibler (KL) divergence of the current policy to a Boltzmann distribution over the action values. This Boltzmann policy has certain policy improvement guarantees (Haarnoja et al., 2018), which we further extend in this work. Further, the KL divergence is a convenient choice because stochastic estimation of this objective only requires the ability to sample from the distributions and evaluate them at single points.

It is unclear, however, whether to use the reverse or the forward KL divergence, here also called RKL and FKL respectively. That is, should the first argument of the KL divergence be policy  $\pi$ , or should it be the Boltzmann distribution over the action values? Neumann (2011) argues in favour of the reverse KL divergence as such a resulting policy would be cost-averse, while Norouzi et al. (2016) uses the forward KL divergence to induce a policy that is more exploratory (i.e., has a more diverse state visitation distribution). The typical default is the reverse KL. The reverse KL without entropy regularization corresponds to a standard Actor-Critic update and is easy to compute, as we show in Section 3.2. More recently, it was shown that the reverse KL guarantees policy improvement when the KL can be minimized separately for each state (Haarnoja et al., 2018, p. 4). This finding served to motivate the development of Soft-Actor Critic, one of the state-of-the-art PG methods.

Despite the fact that both have been used and advocated, there is no comprehensive investigation into the differences between these two choices for approximate greedification. The closest work is Neumann (2011), but they do KL divergence reduction in the context of EM-based policy search using the variational inference framework, whereas we frame the problem as approximate policy iteration, which leads to different optimization processes and cost functions. Their reverse KL target, for example, is a reward weighted trajectory distribution, which is different from the Boltzmann distribution we use here and they minimize the KL divergence with respect to the variational distribution, while we minimize it directly with respect to the policy. Their work does not provide any theoretical results and their experimental settings are limited to single step decision making, whereas we experiment on sequential decision making.

The goal of this work is to investigate the differences between using a forward or reverse KL divergence, primarily in the context of entropy regularization, for approximate greedification. We ask, given that we optimize a policy to reduce either the forward or the reverse KL divergence to a Boltzmann distribution over the action values, what is the

quality of the resulting policy? We provide some clarity on this question with the following contributions.

1. We highlight four choices for greedification: forward KL (FKL) or reverse KL (RKL) to a Boltzmann distribution on the action-values, with or without entropy regularization. We show that many existing methods can be categorized into one of these four quadrants, and particularly show that the standard Actor-Critic update corresponds to using the RKL.
2. We extend the policy improvement result for the RKL (Haarnoja et al., 2018) to the case where, instead of reducing the RKL for all states, we only need to reduce it on average.
3. We show via a counterexample that merely reducing the FKL is not sufficient to guarantee improvement and discuss additional sufficient conditions for improvement.
4. On small-scale experiments, we find that, particularly under continuous actions, (a) the RKL can converge faster, but sometimes to suboptimal local minima solutions, but (b) the optimal solution of the FKL can be worse than the corresponding RKL, particularly under higher entropy regularization.
5. We show that the FKL promotes more exploration under continuous actions, by maintaining a higher variance in the learn policy, but that for discrete actions, exploration is very similar for the RKL and FKL.
6. On benchmark environments, we find that (a) the dominant factor is the degree of entropy regularization, (b) both divergences perform similarly for the same temperatures, though for the few cases where there was a notable difference, the FKL outperformed the RKL and (c) they have relatively similar sensitivities to hyperparameters.

## 1.1 Additional Related Work

Actor-Critic methods (Sutton, 1984; Konda and Tsitsiklis, 2000) have recently seen a surge of renewed interest given their ease of application in high-dimensional, continuous action spaces when combined with neural networks (Schulman et al., 2016; Wang et al., 2017; Mnih et al., 2016). Recent developments include learning deterministic policies (Silver et al., 2014; Lillicrap et al., 2016), trust-regions (Schulman et al., 2015, 2017b), continuous-action extensions of Q-learning (Haarnoja et al., 2017; Lim et al., 2018; Ryu et al., 2020), probabilistic approaches (Abdolmaleki et al., 2018; Fellows et al., 2019), and entropy regularization (Ziebart et al., 2008; Ziebart, 2010; Rawlik et al., 2013; Haarnoja et al., 2017, 2018; Levine, 2018).

Theoretical and empirical work into PG is growing. For theoretical work, CPI (Kakade and Langford, 2002) is an early example of insights into obtaining guaranteed policy improvement with PG. More recently, Agarwal et al. (2019a) derive finite-sample and approximation bounds for a variety of PG methods; Mei et al. (2020) show that, with a softmax policy parameterization, entropy-regularized PG converges faster than unregularized PG; Neu et al. (2017); Liu et al. (2019); Shani et al. (2020) reformulate TRPO as mirror descent and prove convergence; Ahmed et al. (2019) show that entropy regularization may

lead to smoother optimization landscapes; and Bhandari and Russo (2019) show global optimality of local minima under certain restrictions on the MDP.<sup>2</sup>

Recent investigations have also unveiled some of the shortcomings of current PG methods. Many implementations of PG in practice use biased gradient estimates (Thomas, 2014; Imani et al., 2018; Nota and Thomas, 2020). Somewhat unfortunately, the apparent superiority of some more modern PG methods seems to be due to techniques that could have been used in all algorithms, like reward normalization, rather than advances specific to the algorithm being proposed (Henderson et al., 2018; Ilyas et al., 2020; Engstrom et al., 2019).

Though the policy update for many PG methods can be seen as optimizing a reverse KL, some work has employed the forward KL (Norouzi et al., 2016; Nachum et al., 2017a; Agarwal et al., 2019b; Vieillard et al., 2020b), including implicitly some of the work in classification for RL (Lagoudakis and Parr, 2003; Lazaric et al., 2010; Farahmand et al., 2015). For contextual bandits, Chen et al. (2019) showed improved performance when using a surrogate, forward KL objective for the smoothed risk. Some works also use the forward KL ostensibly to prevent mode collapse, given that the forward KL is mode-covering (Agarwal et al., 2019b; Mei et al., 2019). The forward KL divergence is also used in supervised learning, in the form of the cross-entropy loss.<sup>3</sup>

In Inverse Reinforcement Learning and Imitation Learning, Ghasemipour et al. (2020) have shown that, under the cost regularized framework proposed by Ho and Ermon (2016), most methods can be categorized as reducing some divergence. Notably among them is behavior cloning, which corresponds to a FKL reduction between policies, whereas AIRL (Fu et al., 2018), one of the state-of-the-art methods, reduces the RKL between occupancy measures. The paper then proposes a variant of AIRL based on reducing the FKL, obtaining competitive results.

Recently, Ghosh et al. (2020) have reformulated standard policy gradient updates in terms of two steps: (1) a policy improvement operator applied to the current policy and (2) a forward KL projection step to the result of (1). The two steps are reminiscent of policy iteration as one may view the composition of improvement and projection as an approximate greedification step. Interestingly, they rederive PPO (Schulman et al., 2017b) and MPO (Abdolmaleki et al., 2018) using this operator perspective, and suggest a path to new policy gradient algorithms by considering different policy improvement operators.

In the context of variational inference, RKL is often used due to tractability, but the popular expectation propagation framework is based on reducing the FKL (Bishop, 2006). Furthermore, when combining variational inference with importance sampling, the proposal distribution is commonly obtained via RKL reduction. This, however, was recently shown to be inferior to the method proposed by Jerfel et al. (2021), based on FKL reduction. The cause was likely the underestimation of the tail of the target distribution that occurs when

---

2. We note that the results in Bhandari and Russo (2019) bear a striking resemblance to earlier results in Scherrer and Geist (2014). In particular, both works rely on convex policy classes and a closure of the policy class under greedification.

3. We emphasize that we use the KL divergence to project the target policy to the space of parameterized policies. Some previous works use the KL (or Bregman) divergence to regularize policy updates to force a new policy be close to a previous one (Peters et al., 2010; Schulman et al., 2015; Abdolmaleki et al., 2018; Geist et al., 2019; Vieillard et al., 2020a). While such regularization changes the target policy and may confer benefits to algorithms (Schulman et al., 2015; Vieillard et al., 2020a), there still remains a question of how to project the target policy, which is the main theme of the present paper.

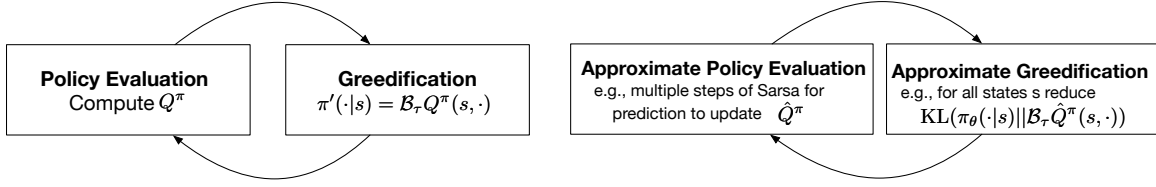


Figure 1: **Contrasting Policy Iteration (PI) and Approximation PI (API)**, left and right respectively. **[Left-hand Side]** In PI, the policy evaluation step and the greedification step are done exactly. In the policy evaluation step, the action values for the current policy  $\pi$  are computed. In the greedification step—also called the policy improvement step—the policy  $\pi'$  is set to the (soft) greedy policy. This  $\pi'$  is handed off to the policy evaluation step, as the new  $\pi$ , and the new action values are computed. In this work, the soft greedy policy that we consider is the Boltzmann policy,  $\mathcal{B}_\tau Q^\pi$ , defined in Equation (4). We discuss why this choice for greedification provides policy improvement in Section 3.1.

**[Right-hand Side]** In API, we use the same target policy for greedification—namely the Boltzmann policy—but we only approximate this target policy. We formalize this approximation goal by minimizing a KL divergence to the target policy. This approximation can be done by fully minimizing this KL divergence, to get the best parameterized  $\pi_\theta$  that approximates  $\mathcal{B}_\tau Q^\pi$ . This learned  $\pi_\theta$  corresponds to the new policy  $\pi'$  that is handed back to the approximate policy evaluation step. The approximate greedification step can also only reduce the KL, rather than fully minimizing it. The approximate policy evaluation step has a similar choice: we can either obtain the best approximate action-values with a batch algorithm like least-squares TD, or we can simply improve the estimate from the existing estimate using multiple stochastic updates to the action-values under the new policy.

reducing RKL, in contrast with FKL, which overestimates the tail of the target. We believe that understanding FKL properties in the context of sequential decision making may allow researchers to better leverage the benefits FKL has shown in other areas to propose better algorithms in the future.

## 2. Problem Formulation

We formalize the reinforcement learning problem (Sutton and Barto, 2018) as a Markov Decision Process (MDP): a tuple  $(\mathcal{S}, \mathcal{A}, \gamma, r, p)$  where  $\mathcal{S}$  is the state space;  $\mathcal{A}$  is the action space;  $\gamma \in [0, 1]$  is the discount factor;  $r : \mathcal{S} \times \mathcal{A} \rightarrow \mathbb{R}$  is the reward function; and, for every  $(s, a) \in \mathcal{S} \times \mathcal{A}$ ,  $p(\cdot | s, a)$  gives the conditional transition probabilities over  $\mathcal{S}$ . A *policy* is a mapping  $\pi : \mathcal{S} \rightarrow \Delta_{\mathcal{A}}$ , where  $\Delta_{\mathcal{A}}$  is the space of probability distributions over  $\mathcal{A}$ . At every discrete time step  $t$ , an agent observes a state  $S_t$ , from which it draws an action from its policy:  $A_t \sim \pi(\cdot | S_t)$ . The agent sends the action  $A_t$  to the environment, from which it receives the reward signal  $r(S_t, A_t)$  and the next state  $S_{t+1}$ .

In this work we focus on the episodic problem setting, where the goal of the RL agent is to maximize the *expected return*—the expectation of a discounted sum of rewards—from the set of start states. To formalize this goal, we define the *value function*  $V^\pi$  for policy  $\pi$  as

$$V^\pi(s) := \mathbb{E}_\pi \left[ \sum_{k=0}^{\infty} \gamma^k r(S_k, A_k) \mid S_0 = s \right].$$

The expectation above is over the trajectory  $(S_0, A_0, S_1, A_1, \dots)$  induced by  $\pi$  and the transition kernel  $p$ . For simplicity, we omit  $p$  in the subscript, because the expectation is always according to  $p$ . We similarly define the *action-value function*:

$$\begin{aligned} Q^\pi(s, a) &:= \mathbb{E}_\pi \left[ \sum_{k=0}^{\infty} \gamma^k r(S_k, A_k) \mid S_0 = s, A_0 = a \right] \\ &= r(s, a) + \gamma \mathbb{E}[V^\pi(S') \mid S = a, A = a] \end{aligned}$$

A common objective in policy optimization is the value of the policy  $\pi_\theta$  averaged over the start state distribution  $\rho_0$ :

$$\eta(\pi_\theta) := \int_{\mathcal{S}} \rho_0(s) \int_{\mathcal{A}} \pi_\theta(a|s) Q^{\pi_\theta}(s, a) \, da \, ds. \quad (1)$$

The policy gradient theorem gives us the gradient of  $J(\theta)$  (Sutton et al., 1999),

$$\nabla_\theta \eta(\pi_\theta) = \frac{1}{1-\gamma} \int_{\mathcal{S}} d^{\pi_\theta}(s) \int_{\mathcal{A}} Q^{\pi_\theta}(s, a) \nabla_\theta \pi_\theta(a \mid s) \, da \, ds, \quad (2)$$

where  $d^{\pi_\theta}(s) := (1-\gamma) \sum_{t=0}^{\infty} \gamma^t p(S_t = s \mid S_0 \sim \rho_0)$  is the normalized discounted state visitation distribution.

Because we do not have access to  $Q^{\pi_\theta}$ , we instead approximate. For example, in REINFORCE (Williams, 1992), a sampled return from  $(s, a)$  is used as an unbiased estimate of  $Q^{\pi_\theta}(s, a)$ . This method, however, assumes on-policy returns and tends to be sample inefficient. Commonly, a biased but lower-variance choice is to use a learned estimate  $Q$  of  $Q^{\pi_\theta}$ , obtained through policy evaluation algorithms like SARSA (Sutton and Barto, 2018). In these Actor-Critic algorithms, the actor—the policy—updates with a (biased) estimate of the above gradient, given by this  $Q$ —the critic.

This procedure can be interpreted as Approximate Policy Iteration (API). API methods alternate between approximate policy evaluation to obtain a new  $Q$  and approximate greedification to get a policy  $\pi$  that is more greedy with respect to  $Q$ . We depict this approach in Figure 1, and contrast it to PI. As we show in the next section, the gradient in Equation (2) can be recast as the gradient of a KL divergence to a policy peaked at maximal actions under  $Q$ ; reducing this KL divergence updates the policy to increase its own probabilities of these maximal actions, and so become more greedy with respect to  $Q$ . Under this view, we obtain a clear separation between estimating  $Q$  and greedifying  $\pi$ . We can be agnostic to the strategy for updating  $Q$ —we can even use soft action values (Ziebart, 2010) or Q-learning (Watkins and Dayan, 1992)—and focus on answering: for a given  $Q$ , how can we perform an approximate greedification step and which approaches are most effective?

Before we continue our discussion about greedification, it will be necessary to introduce a measure of distance between  $\pi$  and some target policy  $\pi_{target}$ , which is presumably “better” than  $\pi$ . If we can close the distance between  $\pi$  and  $\pi_{target}$ , then we will hopefully end up with a better policy. However, we must first make sense of how to define the distance between probability distributions.

One common choice is to use the Kullback–Leibler (KL) divergence. Given two probability distributions  $p, q$  on  $\mathcal{A}$ , the KL divergence between  $p$  and  $q$  is defined as

$$\text{KL}(p \parallel q) := \int_{\mathcal{A}} p(a) \log \frac{p(a)}{q(a)} da, \quad (3)$$

where  $p$  is assumed to be absolutely continuous (Billingsley, 2008) with respect to  $q$  (i.e.  $p$  is never nonzero where  $q$  is zero), to ensure that the KL divergence exists. The KL divergence is zero iff  $p = q$  almost everywhere, and is always non-negative. Stochastic estimation of the KL divergence has the advantage of requiring just the ability to sample from  $p$  and to calculate  $p$  and  $q$ . This feature is in contrast to the Wasserstein metric<sup>4</sup> for example, which generally requires solving an optimization problem just to compute it.

The KL divergence is not symmetric; for example,  $\text{KL}(p \parallel q)$  may be defined while  $\text{KL}(q \parallel p)$  may not even exist if  $q$  is not absolutely continuous with respect to  $p$ . This asymmetry leads to the two possible choices for measuring differences between distributions: the reverse KL and the forward KL. Assume that  $p$  is a true distribution that we would like to match with our learned distribution  $q_\theta$ , where  $q_\theta$  is smooth with respect to  $\theta \in \mathbb{R}^k$ . The *forward* KL divergence is  $\text{KL}(p \parallel q_\theta)$  and the *reverse* KL divergence is  $\text{KL}(q_\theta \parallel p)$ . This work investigates the impact of choosing either the forward or reverse KL divergences, for approximate greedification.

### 3. Approximate Greedification

We return to the subject of greedification. A (soft) greedy policy is one that concentrates probability on high-value actions, for a given action-value  $Q(s, a)$ . Given access to such a policy  $\pi_{target}$ , we can update our existing policy  $\pi$  to be closer to  $\pi_{target}$ , using the KL divergence. Such an update allows for approximate greedification, as we only move closer to  $\pi_{target}$ . As we further discuss below, approximate greedification can be desirable for computational efficiency and to avoid full greedification on estimated action-values that are constantly updated.

In this section, we formalize how to do approximate greedification. First, we discuss an appropriate choice for the (soft) greedy policy  $\pi_{target}$ . Then we present the four divergences we will use throughout the paper, and derive the updates under each choice. Finally, we discuss the importance of the state weighting in the final objective, which weights the divergence to the target policy in each state.

---

4. Some interesting work has explored the benefits of the Wasserstein metric. (Arjovsky et al., 2017) show that the Wasserstein metric induces a weaker notion of convergence than the KL divergence, allowing for better stability and convergence during GAN training.



### 3.1 Defining a Target Policy

A reasonable choice for the target policy is the Boltzmann distribution, as we motivate in this section. The Boltzmann distribution we use here is also common in pseudo-likelihood methods (Kober and Peters, 2008; Neumann, 2011; Levine, 2018), ensuring that one has a target distribution based on the action-values.

Let  $Q$  be an action-value function estimate. For a given  $\tau > 0$ , the Boltzmann distribution  $\mathcal{B}_\tau Q(s, \cdot)$  for a state  $s$  is defined as

$$\mathcal{B}_\tau Q(s, a) := \frac{\exp(Q(s, a)\tau^{-1})}{\int_{\mathcal{A}} \exp(Q(s, b)\tau^{-1}) db}. \quad (4)$$

We write  $Z(s)$  for the denominator in Equation (4), otherwise known as the partition function. Note that the definition in Equation (4) does not depend upon a particular policy; in other words, we can input any function  $Q$  that is a function of states and actions. For larger  $\tau$ , the Boltzmann distribution is more stochastic: it has higher entropy.

In fact, this distribution can be derived by solving for the entropy-regularized greedy policy on  $Q$ . To see why, recall the definition of the entropy of a distribution, which captures how spread out the distribution is:

$$\mathcal{H}(\pi(\cdot | s)) := - \int_{\mathcal{A}} \pi(a | s) \log \pi(a | s) da.$$

The higher the entropy, the less the probability mass of  $\pi(\cdot | s)$  is concentrated in any particular area. Let  $\mathcal{F}$  be the set of all nonnegative functions on  $\mathcal{A}$  that integrate to 1. At a given state, the entropy-regularized greedy policy is given by

$$\pi_{\text{target}}(\cdot | s) := \arg \max_{p \in \mathcal{F}} \int p(a) (Q(s, a) - \tau \log p(a)) da.$$

The integrand can be rewritten as follows:

$$\begin{aligned} p(a) (Q(s, a) - \tau \log p(a)) &= \tau p(a) \log \frac{\exp(Q(s, a)/\tau)}{p(a)} \\ &= \tau p(a) \log \frac{\mathcal{B}_\tau Q(s, a)}{p(a)} + \tau p(a) \log \int \exp\left(\frac{Q(s, a)}{\tau}\right) da. \end{aligned}$$

The right summand becomes a constant when integrated, so  $\pi_{\text{target}}(\cdot | s)$  can be rewritten as

$$\begin{aligned} \pi_{\text{target}}(\cdot | s) &= \arg \min_{p \in \mathcal{F}} \int p(a) \log \frac{p(a)}{\mathcal{B}_\tau Q(s, a)} da \\ &= \arg \min_{p \in \mathcal{F}} \text{KL}(p \parallel \mathcal{B}_\tau Q(s, \cdot)) \\ &= \mathcal{B}_\tau Q(s, \cdot). \end{aligned}$$

The use of entropy-regularization avoids obtaining deterministic, greedy policies that can be problematic in policy gradient methods. Instead, this approach allows for soft greedification, giving the most greedy policy under the constraint that the entropy of the

policy remains non-negligible. This policy can be shown to provide guaranteed policy improvement, but under a different criteria: according to soft value functions (Ziebart, 2010).

Soft value functions are value functions where an entropy term is added to the reward.

$$V_\tau^\pi(s) := \mathbb{E}_\pi \left[ \sum_{k=0}^{\infty} \gamma^k [r(S_k, A_k) + \tau \mathcal{H}(\pi(\cdot | S_k))] \mid S_0 = s \right]$$

We can define the soft action-value function in terms of the soft value function.

$$Q_\tau^\pi(s, a) := r(s, a) + \gamma \mathbb{E}[V_\tau^\pi(S') \mid S = s, A = a]$$

We can also write the state-value function in terms of the action-value function.

$$V_\tau^\pi(s) = \mathbb{E}_\pi [Q_\tau^\pi(s, A) - \tau \log \pi(A \mid s)].$$

These soft value functions corresponds to a slightly different RL problem described as entropy-regularized MDPs (Geist et al., 2019).

For these soft value functions, we can guarantee policy improvement under greedification with the Boltzmann distribution. If we set  $\pi'(\cdot | s) = \mathcal{B}_\tau Q^\pi(s, \cdot)$  for all  $s \in \mathcal{S}$ , then  $Q_\tau^{\pi'}(s, a) \geq Q_\tau^\pi(s, a)$  for all  $(s, a)$  (Haarnoja et al., 2017, Theorem 4). This parallels the classical policy improvement result in policy iteration (Sutton and Barto, 2018). This guaranteed policy improvement is a motivation for using  $\mathcal{B}_\tau Q$  as a target policy for greedification. We extend this policy improvement result to hold under weaker conditions in Section 6, and also show that it guarantees convergence to an optimal policy.

### 3.2 Approximate Greedification with the KLs

In this section we discuss how to use a KL divergence to bring  $\pi_\theta$  closer to  $\mathcal{B}_\tau Q$ . One might wonder why we should not just set  $\pi(\cdot | s) = \mathcal{B}_\tau Q(s, \cdot)$ . Indeed, for discrete action spaces, we can draw actions from  $\mathcal{B}_\tau Q(s, \cdot)$  easily at each time step. However, for continuous actions, even calculating  $\mathcal{B}_\tau Q(s, \cdot)$  requires approximating a generally intractable integral. Furthermore, even in the discrete-action regime, using  $\mathcal{B}_\tau Q$  might not be desirable as  $Q$  is usually just an action-value *estimate*. Greedifying with respect to an action-value estimate does not guarantee greedification with respect to the action-value.

We define the **Reverse KL** (RKL) for greedification on  $Q$  at a given state  $s$  as

$$\text{RKL}(\pi_\theta(\cdot | s), \mathcal{B}_\tau Q(s, \cdot)) := \text{KL}(\pi_\theta(\cdot | s) \parallel \mathcal{B}_\tau Q(s, \cdot)).$$

This  $Q$  is any action-value on which we perform approximate greedification; it can be a soft action value or not. We can rewrite the RKL as follows:

$$\begin{aligned} \text{RKL}(\pi_\theta(\cdot | s), \mathcal{B}_\tau Q(s, \cdot)) &= \int_{\mathcal{A}} \pi_\theta(a | s) \log \frac{\pi_\theta(a | s)}{\mathcal{B}_\tau Q(s, a)} da \\ &= \int_{\mathcal{A}} \pi_\theta(a | s) \left( \log \pi_\theta(a | s) - \frac{Q(s, a)}{\tau} + \log Z(s) \right) da \\ &= -\mathcal{H}(\pi_\theta(\cdot | s)) - \int_{\mathcal{A}} \pi_\theta(a | s) \frac{Q(s, a)}{\tau} da + \log Z(s), \end{aligned}$$

with gradient

$$\nabla_{\theta} \text{RKL}(\pi_{\theta}(\cdot | s), \mathcal{B}_{\tau} Q(s, \cdot)) = -\nabla_{\theta} \mathcal{H}(\pi_{\theta}(\cdot | s)) - \int_{\mathcal{A}} \nabla_{\theta} \pi_{\theta}(a | s) \frac{Q(s, a)}{\tau} da.$$

If we scale by  $\tau$  to get  $\tau \text{RKL}(\theta; s, Q)$ , we can see that  $\tau$  plays the role of an entropy regularization parameter:<sup>5</sup> a larger  $\tau$  results in more entropy regularization on  $\pi_{\theta}(\cdot | s)$ .

In the case of a finite action space, we can perform the following limit to get the **Hard Reverse KL**<sup>6</sup>.

$$\begin{aligned} \lim_{\tau \rightarrow 0} \tau \text{RKL}(\pi_{\theta}(\cdot | s), \mathcal{B}_{\tau} Q(s, \cdot)) &= \lim_{\tau \rightarrow 0} \tau \sum_a \pi(a | s) \log \pi(a | s) - \tau \sum_a \pi_{\theta}(a | s) \log \mathcal{B}_{\tau} Q(s, a) \\ &= 0 - \lim_{\tau \rightarrow 0} \tau \sum_a \pi_{\theta}(a | s) \log \mathcal{B}_{\tau} Q(s, a) \\ &= - \lim_{\tau \rightarrow 0} \sum_a \pi_{\theta}(a | s) \left( Q(s, a) - \tau \log \sum_b \exp(Q(s, b) \tau^{-1}) \right) \\ &= \left( - \sum_a \pi_{\theta}(a | s) Q(s, a) \right) + \lim_{\tau \rightarrow 0} \tau \log \sum_b \exp(Q(s, b) \tau^{-1}) \\ &= \left( - \sum_a \pi_{\theta}(a | s) Q(s, a) \right) + \max_a Q(s, a). \end{aligned}$$

Since the last term of the RHS does not depend on  $\pi_{\theta}$ , we define the Hard Reverse KL as follows, for both finite and infinite action spaces.

$$\text{Hard RKL}(\pi_{\theta}(\cdot | s), \mathcal{B}_{\tau} Q(s, \cdot)) := - \int_{\mathcal{A}} \pi_{\theta}(a | s) Q(s, a) da,$$

with gradient

$$\nabla_{\theta} \text{Hard RKL}(\pi_{\theta}(\cdot | s), \mathcal{B}_{\tau} Q(s, \cdot)) = - \int_{\mathcal{A}} \nabla_{\theta} \pi_{\theta}(a | s) Q(s, a) da.$$

If  $Q$  is equal to  $Q^{\pi_{\theta}}$ , then this gradient is exactly the negative of the inner term of the policy gradient in Equation (2).<sup>7</sup> This similarity in form means that the typical policy gradient update in actor-critic can be thought of as a greedification step with the Hard RKL.

Similarly, we can define the **Forward KL** (FKL) for greedification:

$$\text{FKL}(\pi_{\theta}(\cdot | s), \mathcal{B}_{\tau} Q(s, \cdot)) := \text{KL}(\mathcal{B}_{\tau} Q(s, \cdot) \| \pi_{\theta}(\cdot | s)).$$

- 
5. For a fixed  $\mathcal{B}_{\tau} Q$ , the policy that minimizes the RKL is the same regardless of the scaling by a constant in front, so we use the more standard unscaled KL to define the RKL.
  6. When investigating  $\tau \rightarrow 0$ , it is not straightforward to extend the calculations we do here to integrals, so we derive them for the discrete case and extrapolate to the continuous case.
  7. We are unaware of a previous statement of this result in the literature, though similar results have been reported. For example, Kober and Peters (2008) derive the policy gradient update from a pseudo-likelihood method. Belousov and Peters (2019) also derive it as a special case of f-divergence constrained relative entropy policy search (Peters et al., 2010). Some references to a connection between value-based methods with entropy regularization and policy gradient can be found in (Nachum et al., 2017b).

We can rewrite the FKL as

$$\begin{aligned}
 \text{FKL}(\pi_\theta(\cdot | s), \mathcal{B}_\tau Q(s, \cdot)) &= \int_{\mathcal{A}} \mathcal{B}_\tau Q(s, a) \log \frac{\mathcal{B}_\tau Q(s, a)}{\pi_\theta(a | s)} da \\
 &= \int_{\mathcal{A}} \mathcal{B}_\tau Q(s, a) \log \mathcal{B}_\tau Q(s, a) da - \int_{\mathcal{A}} \mathcal{B}_\tau Q(s, a) \log \pi_\theta(a | s) da \\
 &= -\mathcal{H}(\mathcal{B}_\tau Q(s, \cdot)) - \int_{\mathcal{A}} \mathcal{B}_\tau Q(s, a) \log \pi_\theta(a | s) da
 \end{aligned}$$

with gradient

$$\nabla_\theta \text{FKL}(\pi_\theta(\cdot | s), \mathcal{B}_\tau Q(s, \cdot)) = - \int_{\mathcal{A}} \mathcal{B}_\tau Q(s, a) \nabla_\theta \log \pi_\theta(a | s) da.$$

We can again consider the limit  $\tau \rightarrow 0$  in the case of a finite action space (in this case there is no need to multiply the KL divergence by  $\tau$ ). Assume that there are  $A^*$  maximizing actions of  $Q(s, \cdot)$ , indexed by  $a_i^*$ .

$$\begin{aligned}
 \lim_{\tau \rightarrow 0} \text{FKL}(\pi_\theta(\cdot | s), \mathcal{B}_\tau Q(s, \cdot)) &= - \lim_{\tau \rightarrow 0} \mathcal{H}(\mathcal{B}_\tau Q(s, \cdot)) - \lim_{\tau \rightarrow 0} \sum_a \frac{\exp(Q(s, a)\tau^{-1})}{\sum_b \exp(Q(s, b)\tau^{-1})} \log \pi_\theta(a | s) \\
 &= 0 - \sum_a \lim_{\tau \rightarrow 0} \frac{\exp(Q(s, a)\tau^{-1})}{\sum_b \exp(Q(s, b)\tau^{-1})} \log \pi_\theta(a | s) \\
 &= -\frac{1}{A^*} \sum_{i=1}^{A^*} \log \pi_\theta(a_i^* | s)
 \end{aligned}$$

We define the **Hard Forward KL** as

$$\text{Hard FKL}(\pi_\theta(\cdot | s), \mathcal{B}_\tau Q(s, \cdot)) := -\frac{1}{A^*} \sum_{i=1}^{A^*} \log \pi_\theta(a_i^* | s)$$

In the case of a continuous action space, we may replace the  $\arg \max$  with a  $\arg \sup$ . The gradient for the Hard FKL is

$$\nabla_\theta \text{Hard FKL}(\pi_\theta(\cdot | s), \mathcal{B}_\tau Q(s, \cdot)) = -\frac{1}{A^*} \sum_{i=1}^{A^*} \nabla_\theta \log \pi_\theta(a_i^* | s)$$

The Hard FKL expression looks quite similar to the cross-entropy loss in supervised classification, if one views the maximum action of  $Q(s, \cdot)$  as the correct class of state  $s$ . We are unaware of any literature that analyzes the Hard FKL for approximate greedification.

We summarize the main expressions, gradients and results in Table 1. Many existing policy gradient methods have policy updates that fit into one of these four quadrants; we provide this categorization in Section 5.

KL	Formula	Gradient	Comment
RKL	$\text{KL}(\pi_\theta(\cdot   s) \parallel \mathcal{B}_\tau Q(s, \cdot))$	$-\int_{\mathcal{A}} \nabla_\theta \pi_\theta(a   s) \tau^{-1} Q(s, a) \, da - \nabla_\theta \mathcal{H}(\pi_\theta(\cdot   s))$	A likelihood-based Soft Actor-Critic. <sup>8</sup>
Hard RKL	$-\int_{\mathcal{A}} \pi_\theta(a   s) Q(s, a) \, da$	$-\int_{\mathcal{A}} \nabla_\theta \pi_\theta(a   s) Q(s, a) \, da$	Equivalent to vanilla actor-critic if action value is unregularized.
FKL	$\text{KL}(\mathcal{B}_\tau Q(s, \cdot) \parallel \pi_\theta(\cdot   s))$	$-\int_{\mathcal{A}} \mathcal{B}_\tau Q(s, a) \nabla_\theta \log \pi_\theta(a   s) \, da$	Like classification with cross-entropy loss and $\mathcal{B}_\tau Q$ the distribution over the correct label.
Hard FKL	$-\frac{1}{A^*} \sum_{i=1}^{A^*} \log \pi_\theta(a_i^*   s)$	$-\frac{1}{A^*} \sum_{i=1}^{A^*} \nabla_\theta \log \pi_\theta(a_i^*   s)$	Like classification with cross-entropy loss and $a_i^*$ the correct labels.

Table 1: This table summarizes the four KL variants for greedification, including the objective, gradient, and a descriptive comment. We fix a state  $s$  and define  $a_i^* \in \arg \max_a Q(s, a)$  with  $A^*$  maximal actions.

### 3.3 Differences between the FKL and RKL

Although switching  $\pi_\theta$  and  $\mathcal{B}_\tau Q$  might seem like a small change, there are several differences in terms of the optimization and the solution itself. In terms of the optimization behavior, it can be simpler to sample the gradient of the RKL, because actions can be sampled according to  $\pi_\theta$ . The FKL, on the other hand, requires actions to be sampled from the  $\mathcal{B}_\tau Q$ , which can be expensive. But, favourably for the FKL, if  $\pi_\theta(a | s) \propto \exp(\theta_a)$ , then the FKL is convex with respect to  $\theta$  because  $\log \sum_i \exp(\theta_i)$  is convex.<sup>9</sup> The RKL, on the other hand, is generally not convex with respect to  $\theta$ , even if  $\pi_\theta$  is parameterized with a Boltzmann distribution.

The other critical difference is in terms of the solution itself. If  $\mathcal{B}_\tau Q$  is representable by  $\pi_\theta$  for some  $\theta$ , then the FKL and RKL both have the same solution:  $\mathcal{B}_\tau Q$ . Otherwise, they make different trade-offs. Of particular note is the well-known fact that the forward KL causes mean-seeking behavior and the reverse KL causes mode-seeking behavior (Bishop, 2006). To understand the reason, we look at the expressions for each divergence. For a target distribution  $Q$ , the forward KL is  $\int_x Q(x) \log \left( \frac{Q(x)}{P(x)} \right) dx$ . If there is an  $x$  where  $Q(x) \gg 0$  (i.e.  $Q(x)$  is significantly greater than zero) and  $P(x)$  is very close to zero, then  $Q(x) \log \left( \frac{Q(x)}{P(x)} \right)$  is large. In fact, as  $P(x) \rightarrow 0$ , we have that  $Q(x) \log \left( \frac{Q(x)}{P(x)} \right) \rightarrow \infty$ . Therefore, to keep the forward KL small, whenever  $Q(x) \gg 0$  then we also need  $P(x) \gg 0$ .

9. This fact can be seen by showing that the Hessian is positive semi-definite, for example.

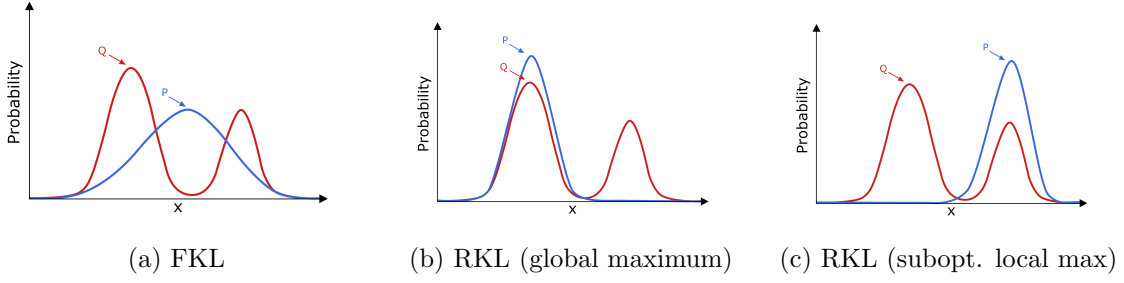


Figure 2: Mean-seeking (FKL) and mode-seeking (RKL) behavior.

This can result in  $P$  that is quite different from  $Q$  if  $P$  is parameterized in a way where it cannot represent  $Q$ . Particularly, if  $Q$  is multimodal and  $P$  is unimodal, then the  $P^*$  that minimizes the forward KL will try to cover all of the modes simultaneously, even if the cost for that is placing high mass in regions where  $Q(x) \approx 0$ . For us, this corresponds to regions where the action-values are low. This forward KL solution, which is called M-projection (the M stands for moment), is also known to be moment-matching. In the case that the family of distributions parameterizing  $P$  is exponential and has some element whose moments match those of  $Q$ , then the moments of  $P^*$  and  $Q$  will match (Koller and Friedman, 2009).

The reverse KL, on the other hand, has the expression  $\int_x P(x) \log \left( \frac{P(x)}{Q(x)} \right) dx$ . Even if  $Q(x) \gg 0$ , we can choose  $P(x) = 0$  without causing  $P(x) \log \left( \frac{P(x)}{Q(x)} \right)$  to get big. This means that  $P$  can select one mode, if  $Q$  is multi-modal. This can be desirable in RL, because it can concentrate the action probability on the region with highest value, even if there is another region with somewhat high action values.

However, the reverse KL can get stuck in sub-optimal solutions. If  $Q(x)$  is near zero for some  $x$ , and we pick  $P(x) \gg 0$ , then  $P(x) \log \left( \frac{P(x)}{Q(x)} \right)$  can be large. As  $Q(x)$  gets closer to zero, this number goes to infinity. Therefore, reducing the reverse KL will lead to  $P$  such that when  $Q(x) \approx 0$  then  $P(x) \approx 0$ . Because of this, the reverse KL is sometimes called zero-forcing or cost-averse. Similarly to the forward KL, this has certain consequences if  $P$  is parameterized in a way that cannot represent  $Q$ . In the multimodal target example we used for the forward KL,  $P^*$  that minimizes the reverse KL, often called I-projection (the I stands for information), will try to avoid placing mass in regions where  $Q(x) \approx 0$ . This means that  $P$  may end up in a sub-optimal mode when reducing the reverse KL via gradient descent. Both behaviors are illustrated in Figure 2.

When approximating some distribution by reducing the FKL, the mean-seeking behavior causes overestimation of the tail of the target, whereas reducing the RKL underestimates it because of the mode-seeking behavior. In variational inference, one wants to approximate the posterior distribution by using a variational distribution. Importance sampling (IS) can be used to debias estimates obtained from some Bayesian inference procedures. In this context, the IS proposal distribution is commonly obtained by minimizing the RKL. However, because of this underestimation of the tail of the target, the quality of the IS estimates sometimes suffer, and a proposal distribution that overestimates the tail of the target is more desirable. Recent work (Jerfel et al., 2021) has shown that the FKL can be

superior in this case. Better understanding the implications of reducing the FKL in the context of approximate policy improvement will facilitate incorporate such advantages into future RL algorithms.

### 3.4 The Weighting over States

The above greedification objectives, and corresponding gradients, are defined per state. To specify the full greedification objective across states, we need a weighting  $d : \mathcal{S} \rightarrow \mathbb{R}^+$  on the relative importance of each state. Under function approximation, the agent requires this distribution to trade-off accuracy of greedification across states. The full objective for the RKL is

$$\int_{\mathcal{S}} d(s) \text{RKL}(\theta; s, Q) \, ds.$$

The other objectives are specified similarly.

The state weighting specifies how function approximation resources should be allocated for greedification. If there are no trade-offs, such as if the Boltzmann policy can be perfectly represented in each state, then the state weighting plays almost no role. It simply needs to be positive in a state to ensure the KL is minimized for that state. Otherwise, it may be the case that to make the policy closer to the Boltzmann policy in one state, it has to make it further in another state. The state weighting specifies which states to prioritize in this trade-off.

For most algorithms in practice that use a replay buffer, the state weighting implicitly corresponds to the state frequency in the replay buffer. The agent samples transitions from the buffer, to compute policy updates for a given state. This weighting is constantly changing. We might expect early on that the implicit weighting is similar to the state visitation distribution under a random policy, and later becomes more similar to the state visitation under a near-optimal policy—if learning is effective. The ramifications of allowing  $d$  to be chosen implicitly by the replay buffer are as yet not well understood. In practice, algorithms seem to perform reasonably well, even without carefully controlling this weighting, possibly in part due to the fact that large neural networks are used to parameterize the policy that are capable of representing the target policy.

There is, however, some evidence that the weighting can matter, particularly from theoretical work on policy gradient methods. This role of the weighting might seem quite different from the typical role in the policy gradient, but there are some clear connections. When averaging the gradient of the Hard RKL with weighting  $d$ , we have

$$- \int_{\mathcal{S}} d(s) \int_{\mathcal{A}} Q(s, a) \nabla \pi_{\theta}(a \mid s) \, da \, ds.$$

If  $d = d^{\pi_{\theta}}$  and  $Q = Q^{\pi_{\theta}}$ , then this update corresponds to the true policy gradient; otherwise, for different weightings  $d$ , it may not correspond to the gradient of any function (Nota and Thomas, 2020). A similar issue has been highlighted for the off-policy policy gradient setting (Imani et al., 2018), where using the wrong weighting results in convergence to a poor stationary point. These counterexamples have implications for API, as they suggest that with accurate policy evaluation steps, the iteration between evaluation and greedification—the policy gradient step—may converge to poor solutions, without carefully selecting the state weighting.

At the same time, this does not mean that the weighting must correspond to the policy state visitation distribution. Outside these counterexamples, many other choices could result in good policies. In fact, the work on CPI indicates that the weighting with  $d^\pi$  can require a large number of samples to get accurate gradient estimates, and moving to a more uniform weighting over states can be significantly better (Kakade and Langford, 2002). The choice of weighting remains an important open question. For this work, we do not investigate this question, and simply opt for the typical choice in practice—using replay.

#### 4. An API Algorithm with FKL or RKL

In this section, we provide a concrete algorithm which can use either the FKL or RKL for policy improvement within an API framework. The algorithm most closely resembles Soft Actor-Critic (SAC) (Haarnoja et al., 2018), which was originally described as a policy iteration algorithm. The key choices in the algorithm include (1) how to learn the (soft) action-values, (2) how to obtain an estimate of the RKL or FKL for a given state, and (3) how to sample states.

To sample states, we use the standard strategy of maintaining a buffer of the most recent experience. We sample states uniformly from this buffer. To obtain an estimate of the FKL or RKL for a given state, we need to estimate the gradient that has a sum or integral over actions. For the discrete action setting, we can simply sum over all actions. The **All-Actions** updates from a state  $s$  correspond to

$$\begin{aligned} \text{RKL} : \nabla_\theta \sum_{a \in \mathcal{A}} \pi_\theta(a | s) \log \pi_\theta(a | s) - \sum_{a \in \mathcal{A}} \nabla_\theta \pi_\theta(a | s) \log \mathcal{B}_\tau Q(a | s) \\ = - \sum_{a \in \mathcal{A}} \nabla_\theta \pi_\theta(a | s) \left[ \frac{Q(s, a)}{\tau} - \log \pi_\theta(a | s) \right] \end{aligned} \quad (5)$$

$$\text{FKL} : - \sum_{a \in \mathcal{A}} \mathcal{B}_\tau Q(a | s) \nabla_\theta \log \pi_\theta(a | s) \quad (6)$$

$$\text{Hard RKL} : - \sum_{a \in \mathcal{A}} \nabla_\theta \pi_\theta(a | s) Q(s, a) \quad (7)$$

$$\text{Hard FKL} : - \nabla_\theta \log \pi_\theta \left( \arg \max_b Q(s, b) | s \right). \quad (8)$$

For the Hard FKL, when there is more than one maximal action, we assume that ties are broken randomly and the cross-entropy optimization maximizes the likelihood of all maximal actions. For the continuous action setting, we can try to estimate the All-Actions update with numerical integration. In our experiments in small environments, we calculate the the All-Actions update exactly.

More practically, however, the simple strategy is to sample actions for the continuous action setting. This is more straightforward for the RKL than the FKL. For the RKL and Hard RKL, we simply need to sample actions from the policy. In this case, we assume we sample  $n$  actions  $a_1, \dots, a_n$  from  $\pi_\theta(\cdot | s)$  and, using  $\nabla_\theta \pi_\theta(a | s) = \pi_\theta(a | s) \nabla_\theta \log \pi_\theta(a | s)$  and  $\sum_{a \in \mathcal{A}} \pi_\theta(a | s) \nabla_\theta \log \pi_\theta(a | s) \approx \sum_{i=1}^n \frac{\nabla_\theta \log \pi_\theta(a_i | s)}{n}$ , compute a **Sampled-Action** update,



where we also change  $Q$  to  $Q - V$

$$\mathbf{RKL} : -\frac{1}{n} \sum_{i=1}^n \nabla_{\theta} \log \pi_{\theta}(a_i | s) \left( \frac{Q(s, a_i) - V(s)}{\tau} - \log \pi_{\theta}(a_i | s) \right) \quad (9)$$

$$\mathbf{Hard RKL} : -\frac{1}{n} \sum_{i=1}^n \nabla_{\theta} \log \pi_{\theta}(a_i | s) (Q(s, a_i) - V(s)) \quad (10)$$

The inclusion of a baseline  $V$  reduces variance due to sampling actions and does not introduce bias. Alternatively, for certain distributions, we can use the reparametrization trick and compute alternative sampled-action updates. For the case where the policy is parametrized as a multivariate normal, with  $\pi_{\theta}(\cdot | s) \sim \mathcal{N}(\mu_{\theta}(s), \text{Diag}(\sigma_{\theta}(s)))$ , where  $\text{Diag}(\cdot)$  converts a vector to a diagonal matrix, an action sampled  $a \sim \pi_{\theta}(\cdot | s)$  can be written as  $a = a_{\theta}(s, a') = \mu_{\theta}(s) + \text{Diag}(\sigma_{\theta}(s))a'$  for  $a' \sim \mathcal{N}(0, I)$ . This reparameterization allows gradients to flow through sampled actions by using the chain rule. We can write:

$$\begin{aligned} \nabla_{\theta} \mathbb{E}_{\pi_{\theta}}[f(\pi_{\theta}(\cdot | s))] &= \nabla_{\theta} \int_a \pi_{\theta}(a | s) f(\pi_{\theta}(a | s)) da \\ &= \nabla_{\theta} \int_{a'} p(a') f(\pi_{\theta}(a_{\theta}(s, a') | s)) da' \\ &= \int_{a'} p(a') \nabla_{\theta} f(\pi_{\theta}(a_{\theta}(s, a') | s)) da' \\ &\approx \frac{1}{N} \sum_{i=1}^N \nabla_{\theta} f(\pi_{\theta}(a_{\theta}(s, a'_i) | s)) \end{aligned}$$

Applying this to the formulas in Table 1, the updates then become

$$\mathbf{RKL} : \frac{1}{n} \sum_{i=1}^n \nabla_{\theta} \log(\pi_{\theta}(a_{\theta}(s, a'_i) | s)) - \left( \frac{\nabla_{\theta} Q(s, a_{\theta}(s, a'_i))}{\tau} \right) \quad (11)$$

$$\mathbf{Hard RKL} : -\frac{1}{n} \sum_{i=1}^n \nabla_{\theta} Q(s, a_{\theta}(s, a'_i)) \quad (12)$$

For the FKL, we need to sample according to  $\mathcal{B}_{\tau}Q(\cdot | s)$ , which can be expensive. Instead, we will use weighted importance sampling, similarly to a previous method that minimizes FKL (Nachum et al., 2017a). We can sample actions from  $\pi_{\theta}$ , and compute importance sampling ratios  $\rho_i := \frac{\mathcal{B}_{\tau}Q(a_i | s)}{\pi_{\theta}(a_i | s)} \propto \frac{\exp(Q(s, a_i)\tau^{-1})}{\pi(a_i | s)}$ . To reduce variance, we use weighted importance sampling with  $\tilde{\rho}_i := \frac{\rho_i}{\sum_{j=1}^n \rho_j}$ , to get the update

$$\mathbf{FKL} : -\sum_{i=1}^n \tilde{\rho}_i \nabla_{\theta} \log \pi_{\theta}(a_i | s) \quad (13)$$

The Hard FKL update is the same as in the discrete action setting, with the additional complication that computing the argmax action is more difficult for continuous actions. The Hard FKL is generally impractical in the continuous action setting.

Finally, we use a standard bootstrapping approach to learn the soft action-values. We perform bootstrapping as per the recommendations in Pardo et al. (2018). For a non-terminal transition  $(s, a, r, s')$ , the action values  $Q(s, a)$  are updated with the bootstrap target  $r + \gamma V(s')$ . For a terminal transition, the target is simply  $r$ . Note that an episode cut-off—where the agent is teleported to a start state if it reaches a maximum number of steps in the episode—is not a terminal transition and is updated with the usual  $r + \gamma V(s')$ .

To compute this bootstrap target, we learn a separate  $V$ . It is possible to instead simply use  $Q(s', a') - \tau \log(\pi(a' | s'))$  for the bootstrap target, but this has higher variance. Instead, a lower variance approach is to use the idea behind Expected Sarsa, which is to compute the expected value for the given policy in the next state.  $V(s')$  is a direct estimate of this expected value, rather than computing it from  $Q$ , which can be expensive in the continuous action setting. To update  $V$ , we can use the same bootstrap target for  $Q$ , but need to incorporate an importance sampling ratio to correct the distribution over actions. To avoid using importance sampling, another option is to use the approach in SAC, where the target for  $V(s)$  is  $Q(s, a) - \tau \log(\pi(a | s))$ . The complete algorithm, putting this all together, is in Algorithm 1.

---

**Algorithm 1** Approximate Policy Iteration (API) with KL Greedification

---

**Input:** choice of KL divergence; temperature  $\tau \geq 0$ ; learning rates  $\alpha_\theta, \alpha_v, \alpha_w$   
Initialize: policy  $\pi_\theta$  (parameters  $\theta$ ); action-value estimate  $Q_\beta$  (parameters  $\beta$ ); state-value estimate  $V_w$  (parameters  $w$ ); experience replay buffer  $\mathcal{B}$  Get initial state  $s_0$   
**for**  $t = 0, \dots$  **do**  
    Draw  $a_t \sim \pi_\theta(\cdot | s_t)$   
    Apply action  $a_t$  and observe  $r, s_{t+1}, \text{done}$   
     $\mathcal{B} = \mathcal{B} \cup (s_t, a_t, s_{t+1}, r, \text{done})$   
    **if**  $|\mathcal{B}| \geq \text{batch\_size}$  **then**  
        Draw minibatch  $\mathcal{D} \sim \mathcal{B}$   
        Calculate  $g_\theta \approx \mathbb{E}_{\mathcal{D}}[\nabla_\theta KL]$  using one of Equations 5 - 13  
        Calculate  $g_w, g_v$  using Algorithm 2  
         $\theta = \theta - \alpha_\theta g_\theta$   
         $w = w - \alpha_w g_w$   
         $v = v - \alpha_v g_v$

---



---

**Algorithm 2** GetValueUpdates

---

Given: policy  $\pi_\theta$  (parameters  $\theta$ ); action-value estimate  $Q_\beta$  (parameters  $\beta$ ); state-value estimate  $V_w$  (parameters  $w$ ); temperature  $\tau \geq 0$ ; batch of data  $\mathcal{D}$   
 $g_w \leftarrow 0, g_v \leftarrow 0$   
**for**  $(s, a, r, s')$  in  $\mathcal{D}$  **do**  
    Draw  $\tilde{a} \sim \pi_\theta(\cdot | s)$ .  
     $g_w \leftarrow g_w - (Q_\beta(s, \tilde{a}) - \tau \log \pi_\theta(\tilde{a} | s) - V_w(s)) \nabla_w V_w(s)$   
     $g_v \leftarrow g_v - (r + \gamma \cdot (1 - \text{done}) \cdot V_w(s') - Q_\beta(s, a)) \nabla_v Q_\beta(s, a)$   
 $g_w \leftarrow \frac{g_w}{|\mathcal{D}|}, g_v \leftarrow \frac{g_v}{|\mathcal{D}|}$

---

## 5. Categorizing Existing Algorithms by their Greedification Operators

There are many existing policy optimization algorithms. As we motivated in the introduction, many of these can actually be seen as doing API, though they are typically described as policy gradient methods. In this section, we categorize these methods based on which of these four KLs underly their policy update.

### 5.1 RKL without Entropy Regularization

Many actor-critic approaches that do not have entropy regularization are implicitly optimizing a hard RKL when performing a policy update.

**Vanilla Actor-Critic** (Sutton and Barto, 2018) uses the gradient of the Hard RKL for its policy update, in a given state. For the episodic objective  $\eta(\pi_\theta)$  given in Equation (1), the policy gradient theorem shows that gradient is

$$\nabla_\theta \eta(\pi_\theta) = \int_S d^{\pi_\theta}(s) \int_A Q^{\pi_\theta}(s, a) \nabla_\theta \pi_\theta(a | s) da ds.$$

For each state, the inner update is exactly the Hard RKL. By selecting  $d = d^{\pi_\theta}$ , the Hard RKL averaged across all states exactly equals the policy gradient underlying actor-critic. This weighting is obtained by simply acting on-policy and weighting the update by the discount raised to the power of the step in the episode (Thomas, 2014). In practice, this weighting by the discount is often omitted and the Hard RKL update performed in each state visited under the policy.

**Trust Region Policy Optimization (TRPO)** (Schulman et al., 2015) has the same hard RKL objective as vanilla actor-critic, but with an additional constraint that the policy should not change too much after an update. This strategy builds on the earlier Conservative Policy Iteration (CPI) algorithm (Kakade and Langford, 2002), which motivates that the old policy and old action-values can be used in the objective. This objective is sometimes called the linearized objective; with the addition of the constraint, the objective corresponds to

$$J(\theta) = \mathbb{E}_{S \sim d^{\pi_{\theta_{old}}}, A \sim \pi_\theta} [Q^{\pi_{\theta_{old}}}(S, A)] = \mathbb{E}_{S \sim d^{\pi_{\theta_{old}}}, A \sim \pi_{\theta_{old}}} \left[ \frac{\pi_\theta(A|S)}{\pi_{\theta_{old}}(A|S)} Q^{\pi_{\theta_{old}}}(S, A) \right]$$

subject to  $\delta \geq \mathbb{E}_{S \sim d^{\pi_{\theta_{old}}}} [\text{KL}(\pi_{\theta_{old}}(\cdot|S) || \pi_\theta(\cdot|S))]$

For a given state sampled from  $d^{\pi_{\theta_{old}}}$ , the inner optimization is precisely a hard RKL to the action-values for the old policy. The objective can be written with actions sampled either according to  $\pi_\theta$  or according to  $\pi_{\theta_{old}}$  with an importance sampling ratio.

Note, though, that the actual TRPO algorithm uses an approximation that results in a natural policy gradient update, rather than a gradient of the above objective. So, though it is motivated by optimizing the above (Equation (14) in their work), it actually solves (Schulman et al., 2015, Equation 17).

**Proximal Policy Optimization (PPO)** (Schulman et al., 2017b) the baseline they compare against uses the same objective as TRPO, but uses a KL penalty instead of a constraint. The policy objective with the KL penalty is

$$J(\theta) = \mathbb{E}_{S \sim d^{\pi_{\theta_{old}}}, A \sim \pi_{\theta_{old}}} \left[ \frac{\pi_\theta(A|S)}{\pi_{\theta_{old}}(A|S)} Q^{\pi_{\theta_{old}}}(S, A) \right] - \beta \mathbb{E}_{S \sim d^{\pi_{\theta_{old}}}} [\text{KL}(\pi_{\theta_{old}}(\cdot|S) || \pi_\theta(\cdot|S))]$$

The greedification component of this objective—the first term—can again be seen as using  $d = d^{\pi_{old}}$  with a Hard RKL to action-values  $Q^{\pi_{old}}$ . The second term simply modifies how the Hard RKL is optimized, because the convergence point is unchanged: when  $\theta_{old}$  is optimal, setting  $\theta = \theta^*$  maximizes the first term while keeping the second term 0.

The actual objective used in PPO clips hyperparameter  $\epsilon \geq 0$  and is written as

$$J(\theta) = \mathbb{E}_{\pi_{\theta_{old}}} \left[ \min \left( \frac{\pi_{\theta}(a|s)}{\pi_{\theta_{old}}(a|s)} \hat{A}^{\pi}(s, a), \text{clip} \left( \frac{\pi_{\theta}(a|s)}{\pi_{\theta_{old}}(a|s)}, 1 - \epsilon, 1 + \epsilon \right) \hat{A}^{\pi}(s, a) \right) \right]$$

The clipped objective forces the probability ratio  $\frac{\pi_{\theta}(a|s)}{\pi_{\theta_{old}}(a|s)}$  to stay within  $[1 - \epsilon, 1 + \epsilon]$ .

**Other trust region policy optimization methods** can be also understood as minimizing the Hard RKL. Maximum a posteriori policy optimization (Abdolmaleki et al., 2018) resembles TRPO, but uses a different direction of KL divergence as a policy update constraint. Mirror descent policy iteration, which is mirror descent modified policy iteration (Geist et al., 2019) with  $m = \infty$ , uses the Bregman divergence as a policy update regularization. Another policy optimization algorithm based on the trust region method is relative entropy policy search (Peters et al., 2010).

**Deep Deterministic Policy Gradient (DDPG)** (Silver et al., 2014; Lillicrap et al., 2016) can be viewed as a “degenerate” Hard RKL with a deterministic policy, taking care to differentiate through the action.

## 5.2 RKL with Entropy Regularization

The RKL has been used for an actor-critic algorithm and a continuous action Q-learning algorithm.

**Soft Actor-Critic (SAC)** (Haarnoja et al., 2018) minimizes the RKL, but is written slightly differently because it subsumes the temperature inside the reward and scales the reward to control the temperature. The policy objective is

$$J(\theta) = \mathbb{E}_{S \sim \mathcal{D}} \left[ \text{KL} \left( \pi_{\theta}(\cdot|S) \parallel \frac{\exp(Q^{\pi_{old}}(S, \cdot))}{Z(S)} \right) \right]$$

where the states  $s$  are sampled from a dataset given by  $\mathcal{D}$ . We note that A3C (Mnih et al., 2016) updates the policy with the same objective, but does not learn the soft value functions.

**Soft Q-learning (SQL)** (Haarnoja et al., 2017) introduces a soft Bellman optimality update, that iterates towards a soft optimal action-value  $Q^*$  using a soft maximization. To avoid sampling the Boltzmann policy, which is expensive, they proposed using Stein variational gradient descent. This approach requires introducing an approximate sampling network, which can be alternatively seen as a policy. The resulting objective corresponds exactly to an RKL, with the Boltzmann policy defined on  $Q^*$

$$J(\theta) = \mathbb{E}_{S \sim \mathcal{D}} \left[ \text{KL} \left( \pi_{\theta}(\cdot|S) \parallel \frac{\exp(Q^*(S, \cdot) \tau^{-1})}{Z(S)} \right) \right]$$

Two other approaches are similar to SQL, but for discrete actions. Asadi and Littman (2017) propose generalized value iteration with the mellomax operator, where the maximum-entropy mellomax policy is a Boltzmann policy with state-dependent temperature. Conservative value iteration (Kozuno et al., 2019) can be seen as a variant of SQL in which a trust region method is used, formally proven in (Vieillard et al., 2020a).

### 5.3 FKL without Entropy Regularization

The FKL without entropy regularization and Boltzmann target policy has not previously been explored. However, the FKL to other target distributions has been considered.

**Deep Conservative Policy Iteration (DCPI)** (Vieillard et al., 2020b) learns both an action value function  $Q$  and a policy  $\pi_\theta$ , with target networks  $Q^-$  and  $\pi^-$  for each. To update the policy, DCPI minimizes a forward KL loss between  $\pi_\theta$  and a regularized greedification of  $Q$ . In other words, DCPI uses a forward KL, but to different target distribution than the Boltzmann distribution.

$$J(\theta) := \mathbb{E}_{S \sim \mathcal{D}} [\text{KL}((1 - \alpha)\pi^-(\cdot|S) + \alpha\mathcal{G}(Q(S, \cdot)) \parallel \pi_\theta(\cdot|S))]$$

for  $\alpha \in [0, 1]$  and  $\mathcal{G}(Q(S, \cdot))$  the greedy policy w.r.t.  $Q$  for a given state  $S$ .

**Policy Greedification as Classification** uses multi-class classification, where actions that maximize  $Q(s, a)$  at each state are labeled positive, and the policy is updated to predict that greedy action for every state (Lagoudakis and Parr, 2003; Lazaric et al., 2010; Farahmand et al., 2015). This approach is related to using the Hard FKL, because the FKL corresponds to the cross-entropy loss which can be used for classification. Other classification methods, however, like SVMs, are not directly related.

### 5.4 FKL with Entropy Regularization

**Under-appreciated Reward EXploration (UREX)** (Nachum et al., 2017a) optimizes a mixture of forward and reverse KLs. Their reverse KL is the usual vanilla actor-critic objective, while the forward KL is given by  $\text{KL}(\pi^* \parallel \pi_\theta)$ , where they approximate  $\pi^* \propto \exp(\tau^{-1}G - \log \pi_\theta)$ , where  $G$  is the return received at the end of the episode. Subsequent work in Agarwal et al. (2019b) also employs both a forward and reverse KL, where the forward KL is initially used to collect diverse trajectories, and the reverse KL is used to learn a robust policy, which performs well in sparse and under-specified reward settings.

**Exploratory Conservative Policy Optimization (ECPO)** (Mei et al., 2019) splits policy optimization into a *project* and a *lift* step. The project step minimizes the forward KL divergence to a target policy  $\bar{\pi}_{\tau, \tau'}$  that is the optimal policy under the entropy-regularized objective, with a KL penalty to the old policy.

$$\begin{aligned} \text{Project} : \arg \min_{\pi_\theta} \text{KL}(\bar{\pi}_{\tau, \tau'} \parallel \pi_\theta) \\ \text{Lift} : \bar{\pi}_{\tau, \tau'} = \arg \max_{\pi} \mathbb{E}_{S_0} [V^{\pi_{old}}(S_0)] - \tau \text{KL}(\pi \parallel \pi_{old}) + \tau' \mathcal{H}(\pi) \end{aligned}$$

There have also been relevant works in supervised learning using entropy regularization and forward KL. In **Reward Augmented Maximum Likelihood (RAML)** (Norouzi et al., 2016), instead of optimizing over the traditional maximum likelihood framework (Hard FKL), a target reward distribution is defined, and the model distribution minimizes the forward KL to that target distribution.

## 6. Theoretical Results on Policy Improvement Guarantees

In this section, we study the theoretical policy improvement guarantees under the RKL and FKL. We start with definitions and by motivating the choice of the entropy regularized

setting. We then consider the guarantees, or lack thereof, for the RKL and FKL. To the best of our knowledge, there is as yet only one analysis with guarantees: the RKL when assuming exact minimization in each state (Haarnoja et al., 2018, Lemma 2). We provide an extension of this result to rely only upon RKL minimization *on average* across states. Next, we provide a counterexample where optimizing the FKL *does not* induce policy improvement. Finally, we discuss further assumptions that can be made to ensure that FKL does induce policy improvement. All proofs are contained in Appendix A.

## 6.1 Definitions and Assumptions

We characterize performance of the policy in the entropy regularized setting. First, it will be useful to introduce some concepts for unregularized MDPs and then present their counterparts for entropy regularized MDPs. Throughout, we assume that the class of policies  $\Pi$  consists of policies whose entropies are finite. This assumption is not restrictive for finite action-spaces, as entropy is always finite in that setting. The assumption of finite entropies is necessary to ensure that the soft value functions are well-defined. For some of the theoretical results for the FKL, we will restrict our attention further to only finite action-spaces, just to ensure we have non-negative entropies and to use the total variation distance for discrete sets.

**Assumption 1.** *Every  $\pi \in \Pi$  has finite entropy:  $\mathcal{H}(\pi(\cdot|s))$  for all  $s \in \mathcal{S}$ .*

**Definition 2** (Unregularized Performance Criterion). *For a start state distribution  $\rho_0$ , the performance criterion is defined as*

$$\eta(\pi) := \mathbb{E}_{\rho_0}[V^\pi(S)].$$

**Definition 3** (Unregularized Advantage). *For any policy  $\pi$ , the advantage is*

$$A^\pi(s, a) := Q^\pi(s, a) - V^\pi(s).$$

The advantage asks, what is the average benefit if I take action  $a$  in state  $s$ , as opposed to drawing an action from  $\pi$ ? The soft extensions of these quantities are as follows.

**Definition 4** (Soft Performance Criterion). *For a start state distribution  $\rho_0$  and temperature  $\tau > 0$ , the soft performance criterion is defined as*

$$\eta_\tau(\pi) := \mathbb{E}_{\rho_0}[V_\tau^\pi(S)].$$

It will also be helpful to have a soft version of the advantage. An intuition for the advantage in the non-soft setting is that it should be zero when averaged over  $\pi$ . To enforce this requirement in the soft setting, we require a small modification.

**Definition 5** (Soft Advantage). *For a policy  $\pi$  and temperature  $\tau > 0$ , the soft advantage is*

$$A_\tau^\pi(s, a) := Q_\tau^\pi(s, a) - \tau \log \pi(a | s) - V_\tau^\pi(s).$$

If  $\tau = 0$ , we recover the usual definition of the advantage function. It is also true that  $\mathbb{E}_\pi[A_\tau^\pi(s, A)] = 0$ , by definition of the soft value functions.

Finally, for target distribution  $q$  for a given state, we will refer to the reverse KL as  $\text{RKL}(p, q) := \text{KL}(p \parallel q)$  and the forward KL as  $\text{FKL}(p, q) := \text{KL}(q \parallel p)$ .

## 6.2 Why use the entropy regularized framework?

Since the actual goal of RL is to optimize the unregularized objective, it might sound unnatural to instead study guarantees in its regularized counterpart. We can view the entropy regularized setting as a surrogate for the unregularized setting, or simply of alternative interest. In the first case, it may be too difficult to optimize  $\eta(\pi)$ ; entropy regularization can improve the optimization landscape and potentially promote exploration. Optimizing  $\eta_\tau(\pi)$  is more feasible and can still get us close enough to a good solution of  $\eta(\pi)$ . In the second case, we may in fact want to reason about optimal stochastic policies, obtained through entropy regularization. In either setting, it is sensible to understand if we can obtain policy improvement guarantees under entropy regularization.

There have been several recent papers highlighting that entropy regularization can improve the optimization behavior of policy gradient algorithms. Mei et al. (2020) studied how entropy regularization affects convergence rates in the tabular case, considering policies parametrized by a softmax. By using a proof technique based on Łojasiewicz inequalities, they were able to show that policy gradients without entropy regularization converge to the optimal policy at a  $O(1/t)$  rate. Furthermore, they also showed a  $\Omega(1/t)$  bound for this same method, concluding that the bound is unimprovable for vanilla policy gradients. By adding entropy regularization, the convergence rate can be improved to  $O(e^{-t})$ .

Ahmed et al. (2019) empirically studied how adding entropy regularization changes the optimization landscape for policy gradient methods. By sampling multiple directions in parameter space for some suboptimal policy and visualizing scatter plots of curvature and gradient values around that policy, combined with visualization techniques that linearly interpolate policies, they concluded that adding entropy regularization likely connects local optima. The optimization landscape can be made smoother, while also allowing the use of higher learning rates.

Finally, Ghosh et al. (2020) provided theoretical justification that (nearly) deterministic policies can stall learning progress. They first provide an operator view of policy gradient methods, particularly showing that REINFORCE can be seen as a repeated application of an improvement operator and a projection operator (Ghosh et al., 2020, Proposition 1). They then showed (Ghosh et al., 2020, Proposition 5) that the performance of the (non-projected) improved policy  $\pi'$ ,  $\eta(\pi')$ , is equal to  $\eta(\pi_{\text{old}})$  times a term including the variance:  $\eta(\pi') = \eta(\pi_{\text{old}})(1 + \frac{\text{Variance of Return under } \pi_{\text{old}}}{\text{Expected Return under } \pi_{\text{old}}}) \geq \eta(\pi_{\text{old}})$ . This means that if the variance under  $\pi_{\text{old}}$  is near zero, then  $\eta(\pi') \approx \eta(\pi_{\text{old}})$ . In that sense, having higher variance can help the algorithm make consistent progress. A common way of achieving higher variance is by adding entropy regularization.

Finally, there is some theoretical work relating the solutions under the unregularized and regularized objectives. From (Geist et al., 2019, Proposition 3), if the entropy is bounded for all policies with constants  $L_\tau, U_\tau$  giving  $L_\tau \leq -\tau \mathcal{H}(\pi) \leq U_\tau$ , then we know that

$$V^\pi(s) - \frac{U_\tau}{1-\gamma} \leq V_\tau^\pi(s) \leq V^\pi(s) - \frac{L_\tau}{1-\gamma}.$$

Using this result, we can take expectations across the state space with respect to the starting state distribution, to get

$$\eta(\pi) - \frac{U_\tau}{1-\gamma} \leq \eta_\tau(\pi) \leq \eta(\pi) - \frac{L_\tau}{1-\gamma}.$$

Hence, if the upper bound is tight, increasing  $\eta_\tau(\pi)$  will increase  $\eta(\pi)$ . A similar result exists for single-step decision making with discrete actions (Chen et al., 2019, Proposition 2), where the optimal policy under the regularized objective ( $\pi^*_\tau$ ) and unregularized objective ( $\pi^*$ ) satisfy  $\eta(\pi^*_\tau) > \eta(\pi^*) - \tau \log |\mathcal{A}|$ .

### 6.3 Policy Improvement with the RKL

First, we note a strengthening of the original result for policy improvement under RKL reduction (Haarnoja et al., 2018). Their statement is slightly different from how we will present it here. Particularly, they take  $\pi_{new}$  to be the policy that minimizes the RKL to  $\mathcal{B}_\tau Q_\tau^{\pi_{old}}(s, \cdot)$  at every state. Although they take it as the minimizing policy, examining the proof of their Lemma 2 reveals that their new policy  $\pi_{new}$  does not have to be the minimizer; rather, it suffices that  $\pi_{new}$  is smaller in RKL than  $\pi_{old}$  at every state  $s$ . We therefore restate their lemma with this slight modification.

**Lemma 6** (Restatement of Lemma 2 of Haarnoja et al. (2018)). *For  $\pi_{old}, \pi_{new} \in \Pi$ , if for all  $s$*

$$\text{RKL}(\pi_{new}(\cdot | s), \mathcal{B}_\tau Q_\tau^{\pi_{old}}(s, \cdot)) \leq \text{RKL}(\pi_{old}(\cdot | s), \mathcal{B}_\tau Q_\tau^{\pi_{old}}(s, \cdot)),$$

*then  $Q_\tau^{\pi_{new}}(s, a) \geq Q_\tau^{\pi_{old}}(s, a)$  for all  $(s, a)$  and  $\tau > 0$ .*

**Proof** Same proof as in Haarnoja et al. (2018). ■

We extend this result by considering an RKL reduction in average across states, rather than requiring RKL reduction in every state. To prove our result, it will be useful to note a soft counterpart to the classical performance difference lemma (Kakade and Langford, 2002).

**Lemma 7.** *[Soft Performance Difference] For any policies  $\pi_{old}, \pi_{new}$ , the following is true for any  $\tau \geq 0$ .*

$$\eta_\tau(\pi_{new}) - \eta_\tau(\pi_{old}) = \frac{1}{1 - \gamma} \mathbb{E}_{d^{\pi_{new}}} \left[ \mathbb{E}_{\pi_{new}} [A_\tau^{\pi_{old}}(S, A)] - \tau \text{KL}(\pi_{new}(\cdot | S) \parallel \pi_{old}(\cdot | S)) \right].$$

If we set  $\tau = 0$ , we recover the classical performance difference lemma. Now, we can show that reducing the RKL on average is sufficient and necessary for policy improvement.

**Proposition 8.** *[Improvement Under Average RKL Reduction] For  $\pi_{old}, \pi_{new} \in \Pi$ , define*

$$\begin{aligned} \Delta \text{RKL}(\pi_{old}(\cdot | S), \pi_{new}(\cdot | S)) \\ := \text{RKL}(\pi_{old}(\cdot | S), \mathcal{B}_\tau Q_\tau^{\pi_{old}}(S, \cdot)) - \text{RKL}(\pi_{new}(\cdot | S), \mathcal{B}_\tau Q_\tau^{\pi_{old}}(S, \cdot)). \end{aligned}$$

*For  $\tau > 0$ , we can write:*

$$\eta_\tau(\pi_{new}) - \eta_\tau(\pi_{old}) = \frac{\tau}{1 - \gamma} \mathbb{E}_{d^{\pi_{new}}} [\Delta \text{RKL}(\pi_{old}(\cdot | S), \pi_{new}(\cdot | S))]. \quad (14)$$

*Furthermore,  $\eta_\tau(\pi_{new}) \geq \eta_\tau(\pi_{old})$  if and only if*

$$\mathbb{E}_{d^{\pi_{new}}} [\text{RKL}(\pi_{old}(\cdot | S), \mathcal{B}_\tau Q_\tau^{\pi_{old}}(S, \cdot))] \geq \mathbb{E}_{d^{\pi_{new}}} [\text{RKL}(\pi_{new}(\cdot | S), \mathcal{B}_\tau Q_\tau^{\pi_{old}}(S, \cdot))], \quad (15)$$

*or, equivalently,*

$$\mathbb{E}_{d^{\pi_{new}}} [\Delta \text{RKL}(\pi_{old}(\cdot | S), \pi_{new}(\cdot | S))] \geq 0.$$



Notice that the all-state RKL reduction from Lemma 6 implies  $\mathbb{E}_{d^{\pi_{\text{new}}}}[\Delta \text{RKL}(\pi_{\text{old}}(\cdot | S), \pi_{\text{new}}(\cdot | S))] \geq 0$ . Hence, it implies improvement in the regularized objective. Furthermore, we note that improvement in the soft-objective can only be obtained if there is also improvement in RKL under  $d^{\pi_{\text{new}}}$ . In fact, by inspecting Equation (14), we can see that any optimal policy satisfies, for any fixed  $\pi_0$ ,

$$\pi^* = \arg \max_{\pi \in \Pi} \eta_{\tau}(\pi) = \arg \max_{\pi \in \Pi} \eta_{\tau}(\pi) - \eta_{\tau}(\pi_0) = \arg \max_{\pi \in \Pi} \frac{\tau}{1 - \gamma} \mathbb{E}_{d^{\pi}}[\Delta \text{RKL}(\pi_0(\cdot | S), \pi(\cdot | S))]$$

The above result motivates approximate greedification, where we use stochastic gradient descent for the RKL. This procedure reduces the RKL on average across all states, which in turn improves the policy under the start state objective. This procedure is more practical than requiring reduction in every state. It is likely that, due to policies being restricted by some parametrization, reducing the RKL in some states may increase it in others. With sufficient reduction of the average RKL on each step, this iterative procedure between approximate greedification and exact policy evaluation should converge to an optimal policy. Note, however, that we cannot generally guarantee that this procedure will converge to the optimal policy. This is because the average RKL reduction may decrease to zero prematurely, in the sense that  $\lim_{i \rightarrow \infty} \eta_{\tau}(\pi_i)$  may be less than  $\sup_{\pi \in \Pi} \eta_{\tau}(\pi)$ .

## 6.4 Policy Improvement with the FKL

In this section, we study the policy improvement properties of reducing the FKL. First, in Section 6.4.1 we provide a counterexample showing that reducing the FKL leads to a strictly worse policy. The intuition behind this example is that  $\pi_{\text{old}}$  almost always chooses the good action, but is made close to deterministic and thus arbitrarily large in FKL to  $\mathcal{B}_{\tau} Q_{\tau}^{\pi_{\text{old}}}$ , while  $\pi_{\text{new}}$ , by being less deterministic, reduces the FKL to  $\mathcal{B}_{\tau} Q_{\tau}^{\pi_{\text{old}}}$  but it almost always chooses the bad action, thus being worse in the soft-objective. Second, in Section 6.4.2 we provide a sufficient condition on the FKL reduction to ensure policy improvement. The plots in that section show that this bound is non-trivial, but yet the reduction required is close to the maximum possible reduction. Third, in Section 6.4.3, we discuss when reducing the FKL may be used as a surrogate for reducing the RKL, in particular by providing an upper bound for the RKL in terms of the FKL. It will turn out that reducing the FKL alone is insufficient for reducing the RKL because this bound involves not only the FKL, but another term that depends upon  $\pi_{\text{new}}$ .

### 6.4.1 COUNTEREXAMPLE FOR POLICY IMPROVEMENT UNDER FKL REDUCTION

Unfortunately, the FKL does not enjoy the same policy improvement guarantees as the RKL. In the next proposition, we provide a counterexample where reducing the FKL makes the policy worse. Again we use the notation

$$\Delta \text{FKL}(\pi_{\text{old}}(\cdot | s), \pi_{\text{new}}(\cdot | s)) := \text{FKL}(\pi_{\text{old}}(\cdot | s), \mathcal{B}_{\tau} Q_{\tau}^{\pi_{\text{old}}}(s, \cdot)) - \text{FKL}(\pi_{\text{new}}(\cdot | s), \mathcal{B}_{\tau} Q_{\tau}^{\pi_{\text{old}}}(s, \cdot))$$

where  $\Delta \text{FKL}(\pi_{\text{old}}(\cdot | s), \pi_{\text{new}}(\cdot | s)) > 0$  means we obtained FKL reduction: the new policy has lower FKL than the old policy.

**Proposition 9.** *[Counterexample for Improvement with FKL] For any  $\tau \geq 0$ , and  $\gamma \in [0, 1)$ , there exists a pair of policies  $(\pi_{\text{old}}, \pi_{\text{new}})$  such that at every state  $s \in \mathcal{S}$  we have*

$\Delta\text{FKL}(\pi_{\text{old}}(\cdot|s), \pi_{\text{new}}(\cdot|s)) > 0$  but the new policy has lower value:  $Q_{\tau}^{\pi_{\text{new}}}(s, a) < Q_{\tau}^{\pi_{\text{old}}}(s, a)$  at every state-action pair  $(s, a) \in \mathcal{S} \times \mathcal{A}$ ,  $V_{\tau}^{\pi_{\text{new}}}(s) < V_{\tau}^{\pi_{\text{old}}}(s)$  at every state  $s \in \mathcal{S}$ , and  $\eta_{\tau}(\pi_{\text{new}}) < \eta_{\tau}(\pi_{\text{old}})$ .

It is possible to extend this to an MDP with multiple states. Consider a case where  $\mathcal{S} = \{s_1, s_2, s_3, \dots, s_N\}$ , and at each  $s_n \in \mathcal{S}$  except  $s_N$ , a state transition to  $s_{n+1}$  occurs. At state  $s_N$ , the transition is back to itself. Setting the reward,  $\pi_{\text{old}}$ , and  $\pi_{\text{new}}$  similarly to the environment in Proposition 9, we can show the same result with multiple states.

#### 6.4.2 POLICY IMPROVEMENT UNDER SUFFICIENT FKL REDUCTION

Although mere FKL reduction is not sufficient to guarantee improvement, we know that, assuming we can represent all policies, maximum FKL reduction will guarantee improvement, since then we would have  $\pi_{\text{new}} = \mathcal{B}_{\tau}Q_{\tau}^{\pi_{\text{old}}}$ , which guarantees  $\eta_{\tau}(\pi_{\text{new}}) \geq \eta_{\tau}(\pi_{\text{old}})$ . One might hope that, under some additional conditions, reduction in the FKL implies a reduction in the RKL, which as we have already seen implies policy improvement.

We first motivate that RKL reduction is necessary to obtain improvement in the bandit setting, and so motivate aiming for sufficient FKL reduction to ensure RKL reduction. We then show that with sufficient FKL reduction, we can ensure policy improvement in: (1) the bandit setting, (2) when considering improvement per state and (3) in average across states.

**Definition 10** (Entropy-Regularized Bandits Setting). *We denote  $\boldsymbol{\pi}$  as a vector in  $\mathbb{R}^{|\mathcal{A}|}$  that satisfies  $\boldsymbol{\pi} \geq \mathbf{0}$  and  $\boldsymbol{\pi}^{\top} \mathbf{1} = 1$ , with  $\mathbf{1}$  and  $\mathbf{0}$  being vectors containing respectively only entries equal to 1 and 0. Further, we consider a single state and denote the corresponding action-values as a vector  $\mathbf{q} \in \mathbb{R}^{|\mathcal{A}|}$ . The objective is then defined as  $\eta_{\tau}(\boldsymbol{\pi}) = \boldsymbol{\pi}^{\top}(\mathbf{q} - \tau \log(\boldsymbol{\pi}))$ . Moreover,  $\mathcal{B}_{\tau}Q = \mathcal{B}_{\tau}\mathbf{q} = \frac{\exp(\frac{\mathbf{q}}{\tau})}{Z}$  with  $Z = \exp(\frac{\mathbf{q}}{\tau})^{\top} \mathbf{1}$  being the normalizing constant. We also have  $\text{FKL}(\boldsymbol{\pi}, \mathcal{B}_{\tau}Q) = \mathcal{B}_{\tau}Q^{\top} \log\left(\frac{\mathcal{B}_{\tau}Q}{\boldsymbol{\pi}}\right)$  and  $\text{RKL}(\boldsymbol{\pi}, \mathcal{B}_{\tau}Q) = \boldsymbol{\pi}^{\top} \log\left(\frac{\boldsymbol{\pi}}{\mathcal{B}_{\tau}Q}\right)$ .*

By inspecting Proposition 8 and noting that the entropy regularized bandits setting is a subset of the case studied there, we can conclude that RKL reduction is necessary for improvement in bandits. This result motivates that, when choosing to use the FKL, it is reasonable to understand if sufficient FKL reduction can guarantee RKL reduction. While in principle this may look like FKL is a worse choice for improvement, we will see in the experiments that it has a smoother optimization landscape than the RKL, which means it may be easier to reduce the FKL, even if the amount of reduction needed is larger.

The maximal possible FKL reduction is obtained by moving  $\pi_{\text{new}}$  all the way to  $\mathcal{B}_{\tau}Q_{\tau}^{\pi_{\text{old}}}$ , to give  $\Delta\text{FKL} = \text{FKL}(\pi_{\text{old}}, \mathcal{B}_{\tau}Q_{\tau}^{\pi_{\text{old}}})$ ; for this  $\pi_{\text{new}}$ , we can guarantee RKL reduction. The question is if we can still obtain RKL reduction, even without stepping all the way to this maximal possible FKL reduction. We provide a condition on how much FKL reduction is sufficient to ensure that we obtain policy improvement, first in the bandit setting and then generalized to the MDP setting.

**Proposition 11** (Sufficient FKL Reduction in Bandits). *For two policies  $\pi_{old}, \pi_{new} \in \mathbb{R}^{|\mathcal{A}|}$  in the bandit setting, if*

$$\begin{aligned} & \Delta \text{FKL}(\pi_{old}, \pi_{new}) \\ & \geq \max \left\{ 0, \text{FKL}(\pi_{old}, \mathcal{B}_\tau Q) - \frac{1}{2} \left( \frac{\tau}{\|\mathbf{q}\|_\infty} \left( \text{RKL}(\pi_{old}, \mathcal{B}_\tau Q) + \mathcal{B}_\tau Q^\top \log(\pi_{old}) \right) \right)^2 \right\} \end{aligned}$$

and

$$\text{RKL}(\pi_{old}, \mathcal{B}_\tau Q) + \mathcal{B}_\tau Q^\top \log(\pi_{old}) \geq 0,$$

then  $\Delta \text{RKL}(\pi_{old}, \pi_{new}) \geq 0$  and  $\eta_\tau(\pi_{new}) \geq \eta_\tau(\pi_{old})$ .

It is straightforward to extend this result to MDPs when we have reduction in every state.

**Corollary 12** (All-state Sufficient FKL reduction). *Assume the action set is finite. If the following condition is satisfied for all  $s \in \mathcal{S}$ , we have that  $Q_\tau^{\pi_{new}}(s, a) \geq Q_\tau^{\pi_{old}}(s, a)$  for all states and actions and also that  $\eta_\tau(\pi_{new}) \geq \eta_\tau(\pi_{old})$ .*

$$\begin{aligned} & \Delta \text{FKL}(\pi_{old}(\cdot|s), \pi_{new}(\cdot|s)) \geq \text{FKL}(\pi_{old}(\cdot|s), \mathcal{B}_\tau Q_\tau^{\pi_{old}}(s, \cdot)) \\ & - \frac{1}{2} \left( \frac{\tau}{\|Q_\tau^{\pi_{old}}(s, \cdot)\|_\infty} \left( \text{RKL}(\pi_{old}(\cdot|s), \mathcal{B}_\tau Q_\tau^{\pi_{old}}(s, \cdot)) + \mathbb{E}_{\mathcal{B}_\tau Q_\tau^{\pi_{old}}} [\log(\pi_{old}(\cdot|s))] \right) \right)^2, \quad (16) \end{aligned}$$

and  $\Delta \text{FKL}(\pi_{old}(\cdot|s), \pi_{new}(\cdot|s)) \geq 0$ .

**Proof** We know that reducing the RKL in all states will lead to  $Q_\tau^{\pi_{new}}(s, a) \geq Q_\tau^{\pi_{old}}(s, a)$  for all  $(s, a)$ . From our RKL results, we also know that it implies  $\eta_\tau(\pi_{new}) \geq \eta_\tau(\pi_{old})$ . Therefore, FKL reduction following Equation (16) in all states will also lead to these improvements, since, by the same argument as Proposition 11, it leads to RKL reduction in all states. ■

We can also extend it to the case where FKL reduction happens on average under  $d^{\pi_{new}}$ .

**Proposition 13** (Improvement Under Average Sufficient FKL Reduction). *Assume the action set is finite. If*

$$\mathbb{E}_{d^{\pi_{new}}} [\text{RKL}(\pi_{old}(\cdot|S), \mathcal{B}_\tau Q_\tau^{\pi_{old}}(S, \cdot))] + \mathbb{E}_{d^{\pi_{new}}} \left[ \mathbb{E}_{\mathcal{B}_\tau Q_\tau^{\pi_{old}}} [\log(\pi_{old}(\cdot|S))] \right] \geq 0 \quad (17)$$

and

$$\begin{aligned} & \mathbb{E}_{d^{\pi_{new}}} [\Delta \text{FKL}(\pi_{old}(\cdot|S), \pi_{new}(\cdot|S))] \geq \mathbb{E}_{d^{\pi_{new}}} [\text{FKL}(\pi_{old}(\cdot|S), \mathcal{B}_\tau Q_\tau^{\pi_{old}}(S, \cdot))] \\ & - \frac{1}{2} \left( \frac{\tau}{\|Q_\tau^{\pi_{old}}\|_\infty} \left( \mathbb{E}_{d^{\pi_{new}}} [\text{RKL}(\pi_{old}(\cdot|S), \mathcal{B}_\tau Q_\tau^{\pi_{old}}(S, \cdot))] + \mathbb{E}_{d^{\pi_{new}}} \left[ \mathbb{E}_{\mathcal{B}_\tau Q_\tau^{\pi_{old}}} [\log(\pi_{old}(\cdot|S))] \right] \right) \right)^2, \end{aligned}$$

then  $\eta_\tau(\pi_{new}) \geq \eta_\tau(\pi_{old})$ .

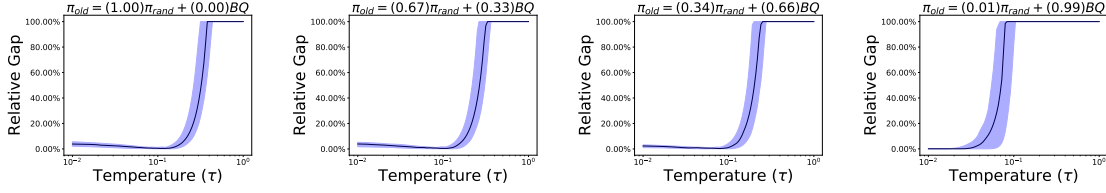


Figure 3: Gap between the maximal  $\Delta\text{FKL}$  and our bound. The solid line is the median over 30 runs, with the shaded region showing the 25% percentile and the 75% percentile. Values close to zero indicate near-maximal reduction is necessary for improvement in the soft objective. The worst  $\pi_{\text{old}}$  is on the left and the best is on the right.

Equation (17) essentially says that on average over  $d^{\pi_{\text{new}}}$ ,  $\mathbb{E}_{d^{\pi_{\text{new}}}} [\text{RKL}(\pi_{\text{old}}(\cdot | S), \mathcal{B}_\tau Q_\tau^{\pi_{\text{old}}}(S, \cdot))] is greater than or equal to  $\mathbb{E}_{d^{\pi_{\text{new}}}} [\text{FKL}(\pi_{\text{old}}(\cdot | S), \mathcal{B}_\tau Q_\tau^{\pi_{\text{old}}}(S, \cdot)) + \mathcal{H}(\mathcal{B}_\tau Q_\tau^{\pi_{\text{old}}}(S, \cdot))]$ . When might the RKL be larger than the FKL and the entropy? If  $\mathcal{B}_\tau Q_\tau^{\pi_{\text{old}}}$  has low entropy across states, then  $\mathcal{B}_\tau Q_\tau^{\pi_{\text{old}}}$  will have low probability mass placed on certain actions. If  $\pi_{\text{old}}$  places probability mass on these actions, the RKL will likely be high because the RKL incentivizes mode-matching.$

The above result gives a condition on the level of FKL reduction to ensure we have improvement. We can test numerically how much less strict this condition is than maximal FKL reduction. We run the experiment in the bandit setting, using  $|\mathcal{A}| = 5$ . We test different  $\pi_{\text{old}}$  calculated as:

$$\pi_{\text{old}} = (1 - \lambda)\pi_{\text{rand}} + (\lambda)\mathcal{B}_\tau Q$$

for  $\lambda \in \{0, 1/3, 2/3, 0.99\}$  and  $\pi_{\text{rand}}$  the random policy. Defining  $\pi_{\text{old}}$  like this and varying  $\lambda$  allows us to know how the bound does for both bad values of  $\pi_{\text{old}}$  (i.e. random) as well as good values (i.e. close to  $\mathcal{B}_\tau Q$  according to the linear interpolation). Then, we vary the range of temperatures and plot the gap between the maximum possible FKL reduction (i.e.  $\Delta\text{FKL} = \text{FKL}(\pi_{\text{old}}, \mathcal{B}_\tau Q)$ ) and our bound as a percentage of this maximum reduction. Values close to zero indicate near-maximal reduction is necessary for improvement in the soft objective. We include the results for 30 seeds in Figure 3.

We can see that the bound is very conservative and a near-maximum FKL reduction is necessary for many temperatures. These plots suggest that additional conditions are needed for FKL reduction to guarantee improvement. We hypothesize that the nature of these conditions has to do with the mean-seeking and mode-seeking behavior. Approximating a target distribution via RKL reduction is very sensitive to placing non-negligible probabilities in regions where the target distribution is close to zero. The FKL, on the other hand, focuses on placing high probabilities in the regions where the target probability is high. It is not hard to see that reducing FKL can increase RKL, if for example we approximate a bimodal distribution with a unimodal one, or if we use a Gaussian parameterization and the target distribution is highly skewed. It remains an open question to understand the conditions that guarantee improvement, and when FKL reduction does not give RKL reduction.

### 6.4.3 UPPER BOUNDING THE RKL IN TERMS OF THE FKL

In this section we show that the FKL times a term that depends on the new and old policies gives an upper bound on the RKL. We discuss how this connection provides insight into why FKL reduction may not result in improvement. We omit dependence on the state in the following result, but it holds per state. This result is a straightforward application of a result from Sason and Verdú (2016). The result uses the Rényi divergence of order  $\infty$ :

$$D_\infty(P \parallel Q) := \log \left( \max_i \frac{p_i}{q_i} \right)$$

where  $P$  and  $Q$  are two discrete probability distributions, with elements  $p_i$  and  $q_i$  respectively, that are absolutely continuous with respect to each other (i.e. one is never nonzero where the other one is zero).

**Lemma 14** (An Upper Bound on RKL in Terms of the FKL). *Assume the action set is finite. For  $\kappa(t) := \frac{t \log t + 1 - t}{t - 1 - \log t}$  where  $\kappa$  is defined on  $(0, 1) \cup (1, \infty)$ ,*

$$\text{RKL}(\pi_{\text{new}}, \mathcal{B}_\tau Q_\tau^{\pi_{\text{old}}}) \leq \kappa(\exp(D_\infty(\pi_{\text{new}} \parallel \mathcal{B}_\tau Q_\tau^{\pi_{\text{old}}})) \text{FKL}(\pi_{\text{new}}, \mathcal{B}_\tau Q_\tau^{\pi_{\text{old}}}) \quad (18)$$

**Proof** To obtain this result, we bound the difference between the two choices of KL divergence. Define

$$\beta_1 := \exp(-D_\infty(P \parallel Q)) \quad \text{and} \quad \beta_2 := \exp(-D_\infty(Q \parallel P)),$$

Then, from Equation (161) in Sason and Verdú (2016), as long as  $P \neq Q$ , we have

$$\kappa(\beta_2) \leq \frac{\text{KL}(P \parallel Q)}{\text{KL}(Q \parallel P)} \leq \kappa(\beta_1^{-1}).$$

Setting  $P = \pi_{\text{new}}$  and  $Q = \mathcal{B}_\tau Q_\tau^{\pi_{\text{old}}}$  at a particular state  $s$ , where we omit the dependence on  $s$ , we have

$$\begin{aligned} \text{RKL}(\pi_{\text{new}}, \mathcal{B}_\tau Q_\tau^{\pi_{\text{old}}}) &\leq \kappa(\beta_1^{-1}) \text{FKL}(\pi_{\text{new}}, \mathcal{B}_\tau Q_\tau^{\pi_{\text{old}}}) \\ &= \kappa(\exp(D_\infty(\pi_{\text{new}} \parallel \mathcal{B}_\tau Q_\tau^{\pi_{\text{old}}})) \text{FKL}(\pi_{\text{new}}, \mathcal{B}_\tau Q_\tau^{\pi_{\text{old}}}) \end{aligned} \quad (19)$$

■

To reduce the RKL as a function of  $\pi_{\text{new}}$ , it thus suffices to reduce the right-hand side of the inequality. There are, however, problems with this approach. First, the bound itself may not be tight; even if we could reduce FKL and the multiplicand  $\kappa(\beta_1^{-1})$ , we still may not obtain a reduction in RKL. Second, we have only developed a mechanism to reduce the FKL, rather than the FKL and the multiplicand. A simple proxy could be to just focus on reducing the FKL.

The bound given above includes  $\kappa(\beta_1^{-1})$ , which also depends on  $\pi_{\text{new}}$ . It is possible that in reducing the FKL, we actually also increase  $\kappa(\beta_1^{-1})$ , possibly offsetting our reduction of the FKL. For example, because of limited function approximation capacity, reducing the FKL might result in  $\pi_{\text{new}}$  covering a low-probability region of  $\mathcal{B}_\tau Q_\tau^{\pi_{\text{old}}}$  in order to place some mass at multiple high-probability regions of  $\mathcal{B}_\tau Q_\tau^{\pi_{\text{old}}}$ . While such a  $\pi_{\text{new}}$  might have a moderate value of FKL, the resulting  $D_\infty(\pi_{\text{new}} \parallel \mathcal{B}_\tau Q_\tau^{\pi_{\text{old}}})$  would be large, making  $\beta_1^{-1}$

large. Correspondingly, because  $\kappa$  is a monotone increasing function (Sason and Verdú, 2016),  $\kappa(\beta_1^{-1})$  would also be large. Consequently,  $\kappa(\beta_1^{-1})\text{FKL}(\pi_{\text{new}}, \mathcal{B}_\tau Q_\tau^{\pi_{\text{old}}})$  may not be small enough to enforce a reduction in RKL.

On a more positive note, however, we know that the  $\kappa$  term in Equation (19),

$$\kappa(\beta_1^{-1}) = \kappa(\exp(D_\infty(\pi_{\text{new}} \parallel \mathcal{B}_\tau Q_\tau^{\pi_{\text{old}}})) = \kappa\left(\max_i \frac{(\pi_{\text{new}})_i}{(\mathcal{B}_\tau Q_\tau^{\pi_{\text{old}}})_i}\right),$$

only grows logarithmically with  $\max_i \frac{(\pi_{\text{new}})_i}{(\mathcal{B}_\tau Q_\tau^{\pi_{\text{old}}})_i}$ . Particularly,

$$\lim_{x \rightarrow \infty} \frac{\kappa(x)}{\log(x)} = 1 \quad \text{and so} \quad \kappa(x) = \Theta(\log(x)).$$

Therefore,  $\beta_1^{-1}$  has to increase by orders of magnitude to significantly increase  $\kappa(\beta_1^{-1})$ .

A modification to the FKL reduction strategy could be to use  $\kappa(\beta_1^{-1})\text{FKL}(\pi_{\text{new}}, \mathcal{B}_\tau Q_\tau^{\pi_{\text{old}}})$  as an objective. The main difficulty with this approach is that  $\beta_1$  is not differentiable because of the max operation in the calculation of  $D_\infty(\pi_{\text{new}} \parallel \mathcal{B}_\tau Q)$ . It might be possible to approximate this maximum with smooth operations like LogSumExp, but we leave exploration of this avenue for future work.

## 6.5 Summary and Discussion

There are two key takeaways from the above results. First, the RKL has a stronger policy improvement result than the FKL as it requires only that the RKL of  $\pi_{\text{new}}$  be no greater than the RKL of  $\pi_{\text{old}}$ . In fact, RKL reduction under a certain state-distribution is a necessary and sufficient condition for improvement to occur. Second, the FKL can fail to induce policy improvement, but sufficient reduction guarantees such improvement. The current bounds, although sufficient, are not a necessary condition for improvement to occur.

An important next step is to leverage these policy improvement results to prove convergence to an optimal policy under approximate greedification. When completely reducing the RKL per state, it is known that the iterative procedure between policy evaluation and greedification with RKL minimization converges to the optimal policy in the policy set (Haarnoja et al., 2018, Theorem 1). This result should similarly hold, under only RKL reduction, as long as that reduction is sufficient on each step. A next step is to understand the conditions on how much reduction is needed per step, for both the RKL and FKL, to obtain this result.

Our derivations for the FKL were based on inequalities connecting f-divergences. Although we chose the FKL, there are many other choices, such as the Hellinger distance, the  $\chi^2$ -distance, the JS divergence, and many more. Sason and Verdú (2016) compiled a list of inequalities connecting f-divergences, so it is possible to follow similar steps to the ones we followed here to derive bounds for other divergences as well. Since each divergence has situations where it works best, having theoretical guarantees for all of them will make it easier to design algorithms that work in each case.

Finally, these theoretical results suggest that the FKL is inferior for improving the policy. The settings where the RKL and FKL are significantly different—meaning that FKL reduction can actually cause the RKL to increase—may not be as prevalent in practice. For

example, if the target distributions are unimodal and symmetric, we may find that RKL and FKL have similar empirical performance. We will see in our experiments that the FKL is often able to induce policy improvement in practice, suggesting a gap between the theory developed and the practical performance.

## 7. Optimization Behavior in Microworlds

The goal in this section is to understand differences between FKL and RKL in terms of (1) the loss surface and (2) the behavior of iterates optimized under the losses. By behavior, we mean whether the iterates reach multiple local optima, how stable iterates under that loss are, and how often iterates reach the global optimum (or optima). Given the fine-grained nature of our questions, we focus upon small-scale environments, which we call *microworlds*. Doing so allows us to avoid any possible confounding factors associated with larger, more complicated environments, and furthermore allows us to more fully separate any issues to do with stochasticity.

We use two continuous action low-dimensional microworlds to allow us to visualize and thoroughly investigate behavior. Our first microworld is a **Bimodal Bandit** in Figure 4a. For continuous actions, we designed a continuous bandit with action space  $[-1, 1]$  and reward function  $Q(a) := \exp(-\frac{1}{2}(\frac{2a+1}{0.2})^2) + \frac{3}{2} \exp(-\frac{1}{2}(\frac{2a-1}{0.2})^2)$ . The two unequal modes at -0.5 and 0.5 enable us to test the mean-seeking and mode-seeking behavior as well as simulate a realistic scenario where the agent’s policy parameterization (here, unimodal) cannot represent the true distribution (bimodal).

Our second microworld is the **Switch-Stay** domain in Figure 4b. From  $s_0$ , action 0 (stay) gives a reward of 1 and transitions to state 0. From  $s_1$ , action 0 gives a reward of 2 and transitions to  $s_1$ . From  $s_0$ , action 1 (switch) gives a reward of -1 and transitions to  $s_1$ , while action 1 from  $s_1$  gives a reward of 0 and transitions to  $s_0$ . To adapt this environment to the continuous action setting, we treat actions  $> 0$  as switch and actions  $\leq 0$  as stay.<sup>10</sup> We set  $\gamma = 0.9$  to ensure that the optimal action from  $s_0$  is to switch, which ensures the existence of a short-term/long-term trade-off inherent to realistic RL environments.

### 7.1 Implementation Details

All policies are tabular in the state. To calculate the FKL and RKL under continuous actions, we use the Clenshaw-Curtis (Clenshaw and Curtis, 1960) numerical integration scheme with 1024 points from the package quadpy,<sup>11</sup> excluding the first and the last points at -1 and 1 because of numerical stability. We use the true action-values when calculating the KL losses. In the Bimodal Bandit, the action-value is given by the reward function, while in Switch-Stay it is calculated (i.e., not learned). To calculate the Hard FKL, we use the true maximum action as determined by the environment. For Switch-Stay, we calculate and optimize the mean KL across the two states.

For policy parameterizations, in continuous action settings we use a Gaussian policy with mean and standard deviation learned as  $(\hat{\mu}, \log(1 + \exp(\hat{\sigma})))$ . The action sampled from the learned Gaussian is passed through tanh to ensure that the action is in the feasible

10. Note that we also compared the RKL and FKL for the discrete action variant of Switch-Stay. Under a softmax parameterization, we found no significant differences between the RKL and FKL.

11. <https://pypi.org/project/quadpy/>

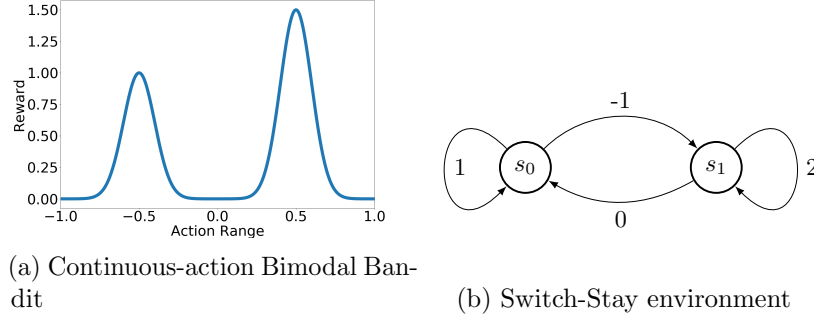


Figure 4: The Microworld environments used to investigate and visualize the optimization behavior of FKL and RKL.

range  $[-1, 1]$  and to avoid the bias induced in the policy gradient when action ranges are not enforced (Chou et al., 2017).

Finally, we use the RMSprop optimizer (Tieleman and Hinton, 2012). Overall trends for Adam (Kingma and Ba, 2015) were similar to those for RMSprop, while results for SGD resulted in slower learning for both FKL and RKL and a wider range of limit points, most likely due to oscillation from the constant step-size. We focus on RMSprop here to avoid any confounding factors associated with momentum.

## 7.2 Continuous Action Results in the Bimodal Bandit

We might expect the FKL to have a smoother loss surface. Given that policies often are part of an exponential family (e.g., softmax policy), having the policy  $\pi$  be the second argument of  $\text{KL}(p \parallel q)$  removes the exponential of  $\pi$ , resulting in an objective that is an affine function of the features. For example, if  $\pi(a \mid s) \propto \exp(\phi(s, a))$  for features  $(s, a)$ , the resulting FKL becomes a sum of a term that is linear in  $\phi(s, a)$  and a term involving  $\text{LogSumExp}(\phi)$ , which is convex.

### 7.2.1 LOSS SURFACE

We visualize the KL loss surfaces in Figure 5 with five different temperatures. The heatmaps depict the loss for each mean and standard deviation pair. The last row depicts the target distribution over which the KL loss is optimized. The surfaces suggest the following.

1) The FKL surface has a single valley, while the RKL surface has two valleys that are separated from one another. In this sense, the FKL surface seems much smoother than the RKL surface, suggesting that iterates under the FKL will more likely reach the global optimum than iterates under the RKL, which seem likely to fall into either of the valleys.

2) The smoothness of the RKL landscape increases with temperature as the gap between the peaks becomes less steep. A higher temperature also causes the valley in the FKL map to become less sharply peaked, and for the optimal  $\mu$  to move closer to 0. The optimal  $\mu$  for the FKL seems to move more quickly to zero, as  $\tau$  increases, than the optimal  $\mu$  for the



RKL, although both eventually reach 0. It is possible that the FKL may become suboptimal sooner than the RKL as  $\tau$  increases.

3) It may seem strange that two valleys exist for the RKL at  $\tau = 0$  given that the target distribution is unimodal. Note, however, that when  $\tau = 0$ , the loss function is no longer a distributional loss; that is, we are no longer minimizing any pseudo-distance between the policy and a distribution.

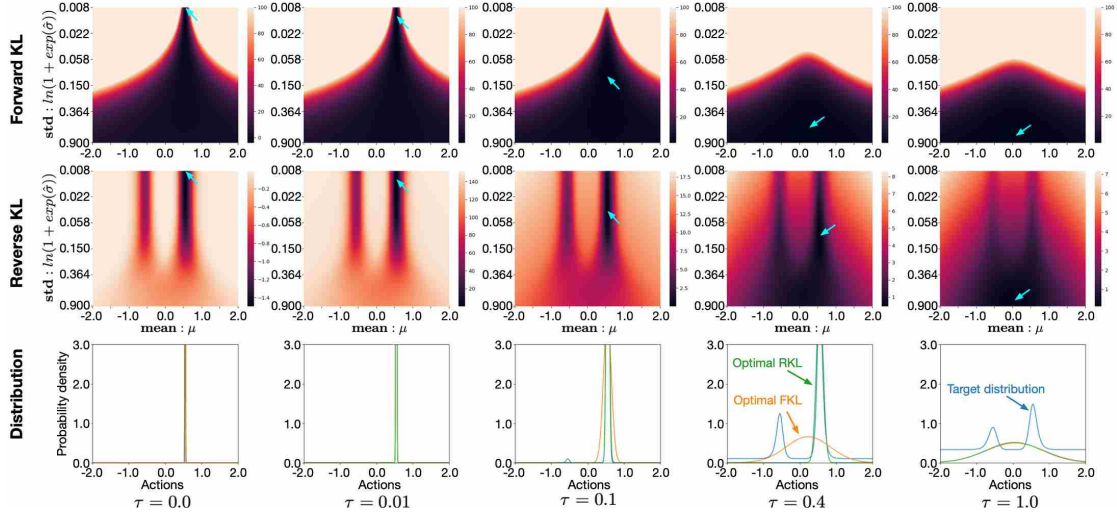


Figure 5: KL loss over mean and standard deviation across temperature. Note that the actual action taken applies  $\tanh$  to the samples of the resulting distribution (i.e., the optimal mean is at  $\tanh^{-1}(0.5) \approx 0.55$ ). FKL loss has been upper-bounded for better visualization of minima. Arrows indicate the global minimum.

### 7.2.2 BEHAVIOR OF ITERATES

To confirm whether our intuitions about the smooth loss surface result in iterates that reach the global optimum, we visualize 1000 random (mean, standard deviation) iterates over 1000 gradient steps to minimize either the FKL or RKL. The mean is initialized uniformly in  $(-0.95, 0.95)$  and  $\hat{\sigma}$  is initialized uniformly in  $(\log(\exp(0.1) - 1), \log(\exp(1) - 1))$ , so that the initial standard deviation  $\sigma_0$  is in  $(0.1, 1)$ . We only show one learning rate, but results are similar for different learning rates. From looking at Figure 6, we observe the following.

For  $\tau \leq 0.4$  (i.e. 4 of the 5 temperatures we used), both the FKL and the RKL have iterates that converge to the global optimum. Indeed, for  $\sigma_0 > 0.3$ , all RKL iterates for  $\tau < 0.4$  (3 of the 5 temperatures) converged to the global optimum. This result suggests that in practice, the fact that the optimization landscape of the RKL may contain more local optima is not necessarily a barrier to convergence to a good local optimum.

We observed an interesting behavioural difference depending upon the initialization of the standard deviation  $\sigma_0$ . While the loss landscapes suggest that the FKL should have no local minima other than the global minimum, the plots in Figure 6 for  $\sigma_0 < 0.3$  show that in fact that FKL iterates fail to converge to the global minimum. This discrepancy persisted

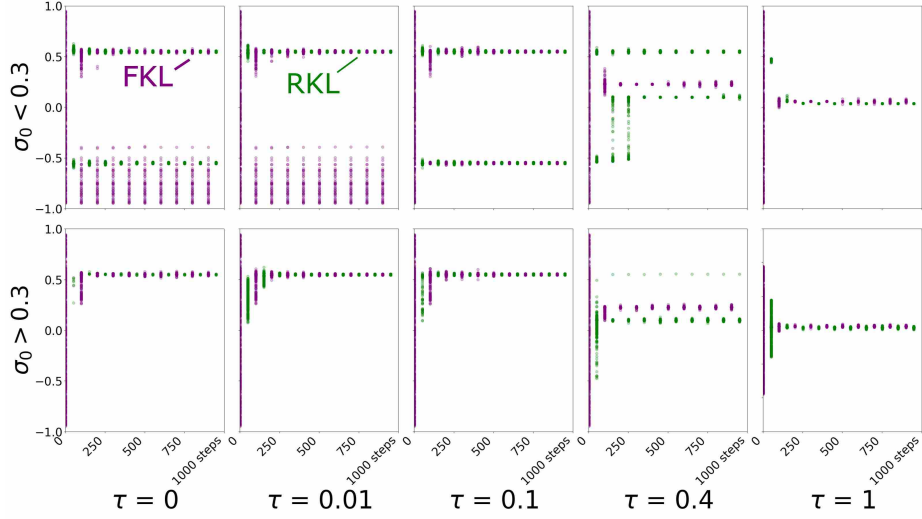


Figure 6: The mean over 1000 gradient steps of each of 1000 iterates under both the FKL and RKL. Each iterate is represented as a translucent, coloured dot with alpha value 0.01. Temperature is varied on the  $x$ -major-axis and initial standard deviation  $\sigma_0$  is varied on the  $y$ -major axis. Learning rate is 0.01.

even with smaller learning rates, suggesting that the problem lies in the loss landscape itself and not in the optimization process.

A possible explanation for this discrepancy is that our loss is not convex with respect to the mean and standard deviation parameters. Although the fact that we push the mean through a tanh does not actually change the log-likelihood of the policy as compared to if we had just used the Gaussian sample directly, the negative log-likelihood of a Gaussian PDF is not convex in the standard deviation. Furthermore, the fact that our standard deviation is parameterized through  $\log(1 + \exp(\hat{\sigma}))$  throws convexity even further into doubt. Why do we have better global convergence for  $\sigma_0 > 0.3$ ? From the heatmaps, the loss landscape becomes smoother for both the RKL and the FKL as the standard deviation increases; intuitively, a higher standard deviation means less committing to bad local minimum.

An earlier version of this experiment used integration points within the range  $[-0.98, 0.98]$ , rather than using all points but  $\{-1, 1\}$ . In this earlier setting, RKL iterates often diverged for  $\sigma_0 > 0.3$  while FKL iterates maintained the same behavior, suggesting that FKL is more robust to this type of bias than RKL. We comment more on the effect of numerical integration error in Section 7.4.

### 7.3 Solution Quality in Switch-Stay

In this section, we investigate the properties of the solutions under the FKL and RKL for an environment with more than one state. Given our previous results, we might expect the FKL to result in better solutions, because FKL iterates can reach the global optimum more easily. But this depends on the quality of this solution. The global minimum of the FKL

objective may not correspond well with the optimal solution of the original, unregularized objective, as we investigate below.

The Switch-Stay environment is appropriate to investigate the quality of the stationary points of the RKL and FKL for two reasons. First, it is a simple instantiation of the full RL problem, we are interested in understanding any possible differences between FKL and RKL in the presence of short-term/long-term trade-offs. In particular, on Switch-Stay, from state 0 one should incur a short-term penalty by switching to state 1 to maximize return, given that  $\gamma = 0.9$ . Second, the Switch-Stay environment facilitates visualization. Since the MDP has only two states, one can plot any value function as a point on a 2-dimensional plane. In particular, one can view the entire space of value functions, shown recently to be a polytope in the discrete-action setting (Dadashi et al., 2019).

We can similarly visualize the value function polytope for continuous actions in Switch-Stay. Recall that we treat any action  $\leq 0$  as stay, and any action  $> 0$  as switch. To calculate the value function corresponding to a continuous policy  $\pi$ , we convert  $\pi$  to an equivalent discrete policy  $\pi_{\text{discrete}}$  of the underlying discrete MDP. The conversion requires the calculation of the probability that  $\pi$  outputs an action  $\leq 0$  in each state, which we do with numerical integration of the policy PDF. We then calculate the value function of  $\pi$  as  $(I - \gamma P_{\pi_{\text{discrete}}})^{-1} r_{\pi_{\text{discrete}}}$ , where  $P_{\pi}$  and  $r_{\pi}$  are respectively the transition matrix and the reward function induced by  $\pi$ .

For the hard FKL, we require access to the greedy action of the action-value function. In the continuous-action setting, this greedy action is usually infeasible to obtain. For the purposes of this experiment, if the greedy action is stay, we represent it in  $[-1, 1]$  by drawing a uniform random number from  $[-1, 0]$ . If the greedy action is switch, we represent it as a uniform random number in  $[0, 1]$ . This design choice is meant to simulate noisy access to the greedy action in practice.

For all of these experiments, we initialized means in the range  $(-0.95, 0.95)$ . All experiments are run for 500 gradient steps and each experiment has 1000 iterates. We plot the value function of the final policy for each iterate and experiment in Figure 7 by visualizing the value function polytope (Dadashi et al., 2019). That is, for finite state and action spaces, the set of all value functions is a polytope (a union of convex polytopes). By plotting the value functions of our policies on the value function polytope, we are able to concisely gauge the performance of an algorithm relative to other algorithms.

**1)** FKL with  $\tau = 0$  converged noticeably slower than the other temperatures, which seems to be an artifact of our encoding of continuous actions to the underlying discrete dynamics of switch-stay, and the fact that we used random tie-breaking when computing the arg max for hard FKL.

**2)** RKL iterates converge slightly faster than FKL iterates across all temperature settings. RKL iterates with  $\tau = 0$  sometimes converged to non-optimal value functions on the corners.

**3)** The limiting value functions of the FKL iterates seem more suboptimal than the limiting value functions of the RKL iterates. The latter are closer to the optimal value function of the original MDP. This result is consistent with our observations in the continuous bandit. Although the FKL optimum may be more easily reached, that optimal point may be suboptimal with respect to the unregularized objective.

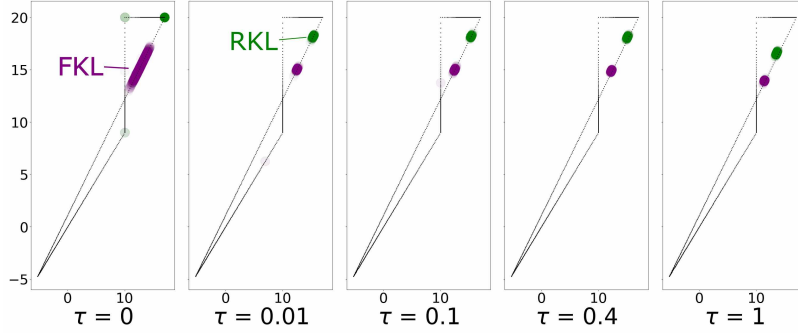


Figure 7: We plot the final value functions on the continuous version of switch-stay after 500 gradient steps with  $\gamma = 0.9$  for 1000 iterates. For clarity, we plot in black the boundary of the value function polytope. All points on the boundary, and all points in the interior of this shape, correspond to value functions of some policy. The top-right corner of the polytope in each subplot is the optimal value function and the bottom-left corner is the pessimal value function. The  $x$ -axis in each subplot corresponds to the value function at state 0 and the  $y$ -axis in each subplot corresponds to the value function at state 1. Each iterate is represented by a translucent dot with alpha value 0.01. RMSprop with an initial learning rate of 0.01 was used for optimization in these plots. Temperature is varied on the  $x$ -major-axis.

#### 7.4 The Impact of Stochasticity in the Update

Although with discrete actions it is practical to sum across all actions when calculating the KL losses, difficulty emerges with high-dimensional continuous action spaces. Quadrature methods scale exponentially with the dimension of the action-space, leaving methods like Clenshaw-Curtis impractical. Monte-Carlo integration—in this case sampling actions from the current policy to estimate the update—seems the only feasible answer in this setting. An important distinction between FKL and RKL, therefore, is how they perform when using a noisier estimate of their updates.

We repeated the continuous-action microworld experiments to understand any differences induced by using Monte-Carlo integration instead of Clenshaw-Curtis quadrature to estimate the update, for a state, averaged across the sampled actions. As discussed in Section 4, we can estimate the gradients of the RKL and FKL using sampled actions rather than full integration. The hard and soft RKL gradient updates are estimated using sampled actions from the current policy  $\pi$ , and the soft FKL gradient update is estimated using weighted importance sampling. Note that since Hard FKL only depends upon the maximum action, we do not modify the algorithm in this experiment.

We examined the differences in both the Bimodal Bandit and Switch-Stay. The overall behavior for the Bimodal Bandit is consistent with the results using Clenshaw-Curtis quadrature. The primary difference is that the iterates take longer to cluster around their limit points. This slow down is natural for both the RKL and FKL, considering each update is more stochastic. Because changing the number of sampled points affected the RKL and

FKL similarly, and otherwise only slowed convergence and did not impact stability, we omit this plot for brevity.

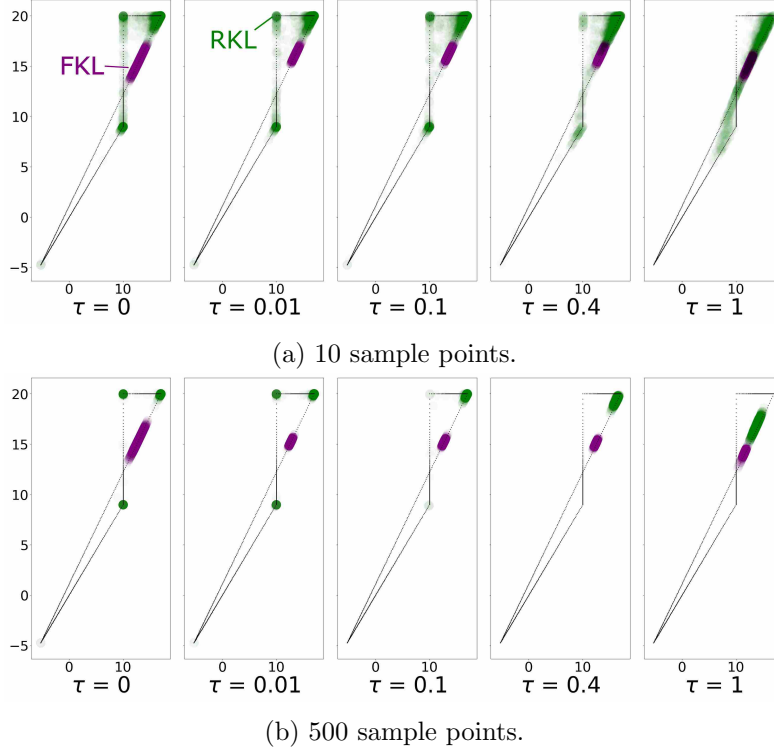


Figure 8: Switch-stay with stochastic estimation of the loss function, learning rate = 0.01, with RMSprop.

On Switch-Stay, more notable differences emerged. RKL iterates converged to minima to which they did not converge in the Clenshaw-Curtis regime, even for larger numbers of sample points. In Figure 8b, there is an interesting trend across temperatures. Temperatures below 0.4 induced many suboptima far from the optimal value function, while temperatures 0.4 and 1 seemed better at clustering RKL iterates near the optimal value function. On the other hand, FKL seemed relatively insensitive both to the temperature and the number of sample points. This relative insensitivity could be due to having a smoother loss landscape to begin with, which tends to direct iterates to a single global optimum. Nevertheless, that global optimum was often quite suboptimal with respect to the unregularized MDP, especially since many RKL iterates were much closer to the optimal policy of the unregularized MDP.

## 8. Exploration Differences between the FKL and RKL

The focus of this section is to study whether there are any significant differences in exploration when using the FKL and RKL. To obtain sufficient exploration, the approach should induce a state visitation distribution whose support is larger, namely that covers more of the state space. Accumulating more transitions from more diverse parts of the state space presumably

allows for more accurate estimates of the action value function, and hence more reliable policy improvement. Entropy-regularized RL, as it is currently formulated, only benefits exploration by proxy, through penalizing the negative entropy of the policy. In the context of reward maximization, entropy is only a means to an end; at times, the means may conflict with the end. A policy with higher entropy may have a more diverse state visitation distribution, but it may be prevented from exploiting that information to the fullest capacity because of the penalty to negative entropy.

There has been some work discussing the potential differences between the FKL and RKL for exploration. Neumann (2011) argues in favour of the reverse KL divergence as such a resulting policy would be cost-averse, but also mentions that the forward KL averages over all modes of the target distribution, which may cause it to include regions of low reward in its policy. While in principle it may seem like a bad idea to include those, we note that the value function estimates can be highly inaccurate (Ilyas et al., 2020), causing this inclusion to possibly be beneficial for exploration. Indeed, Norouzi et al. (2016) use the forward KL divergence to induce a policy that is more exploratory.

We hypothesize that the FKL benefits exploration by causing the agent’s policy to commit more slowly to actions that apparently have high value under the current value function estimate. This could benefit exploration both because it causes the agent to explore more and avoids incorrectly committing too quickly to value function estimates that are inaccurate. This non-committal behavior may help the policy avoid converging quickly to a suboptimal policy. We investigate the differences first in Switch-Stay, under continuous actions, in a continuous environment with a misleading and a correct exits. As few differences were observed for the discrete action experiments, we leave the results to Appendix B.1.

### 8.1 Exploration under Continuous Actions in Switch-Stay

We first revisit the Switch-Stay environment, and examine if the FKL and RKL exhibited differences in the variance of their policies. Recall that we examined the value functions for the final policies under the FKL and RKL, in Figure 7. We noted that the FKL converged to more suboptimal policies than the RKL with the same  $\tau$ , when evaluated under the unregularized objective. A natural hypothesis is that the FKL policy is a more stochastic policy, which is further from the optimal deterministic policy.

To see if this is the case, we plot the final standard deviations of the learned policies for the learning rate of 0.01. In Figure 9, we see that the final FKL iterates have higher standard deviation for each  $\tau$ , meaning that the final policies are further from the optimal deterministic policy of the unregularized MDP. Put informally, the FKL tends to commit less than the RKL. This means that even when using a target Boltzmann policy with the same level of entropy-regularization, that level induces a more stochastic policy under the FKL.

### 8.2 Exploration under Continuous Actions in Misleading Maze

We next investigate exploration behavior in a more difficult exploration problem: a maze with a misleading goal. We also include an experiment in a maze with discrete actions, but find behavior between the FKL and RKL is very similar (see Appendix B.1).

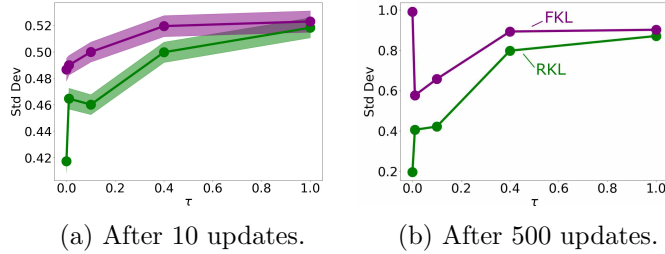


Figure 9: We plot the standard deviation (y-axis) on the continuous version of Switch-Stay, with the temperature varied on the  $x$ -axis. RMSprop is used with learning rate 0.01. Each dot is the mean of 1000 iterates. Shaded areas are standard errors. Temperature is varied on the  $x$ -axis. This plot is for state 0, and recall that every action  $\leq 0$  is treated as “stay” and every action  $> 0$  is treated as “switch”. The large final standard deviation for  $\tau = 0$  with the FKL is an artifact of our encoding of the maximum action as a uniform random point in either  $[0, 1]$  or  $[-1, 0]$ , depending on if the maximum action is respectively stay or switch.

Figure 10a illustrates the maze we use in this section. The agent starts in the center of the green block and has to get close to the center of the blue block. The red blocks are the obstacles and the yellow block corresponds to the misleading exit, which terminates the episode but gives a reward much lower than the real exit. Since the misleading exit is closer to the starting point than the actual exit, the agent can only find out about the higher reward after exploring the maze. The coordinates the agent sees are normalized to the range  $[-1, 1]$ , but its actions are given as a tuple  $(dx, dy)$ , with  $dx, dy \in [-1, 1]$  corresponding to the direction it will try to move (for the actions, 1 corresponds to the length of one block, as opposed to one unit in state-space). The reward is  $-1$  if the agent lands in a normal block,  $-10$  if it hits an obstacle or a wall, 1000 if it lands close to the center of the misleading exit and 100,000 if it lands close to the center of the actual exit. In case the agent hits a wall or obstacle, any attempt to move in a direction that does not point to the opposite direction will result in no movement and a reward of  $-10$ . Additionally, there is a timeout of 10,000 timesteps, after which the agent has its position reset to the starting position without episode termination. To implement this Misleading Maze, we adapt code from GridMap<sup>12</sup>.

The FKL and RKL agents are the same as those used in the following benchmark problems in Section 9, with pseudocode in Section 4. The FKL is used with weighted importance sampling and RKL is used with the reparametrization trick. The actor and critic are both parametrized as two-layer neural networks of size 128 with ReLU activations, with the actor corresponding to an unimodal Gaussian. The critic learning rate is set to  $1\text{E} - 4$  and the actor learning rate is set to  $1\text{E} - 5$ , the optimizer is RMSProp, the batch size is 32 and we sample 128 actions to estimate the gradients. Experiments were done using 30 seeds.

In Figure 10 we show the mean and standard error of the cumulative number of times the correct exit is reached throughout training for multiple temperatures, where FKL and

12. <https://github.com/huyaoyu/GridMap>

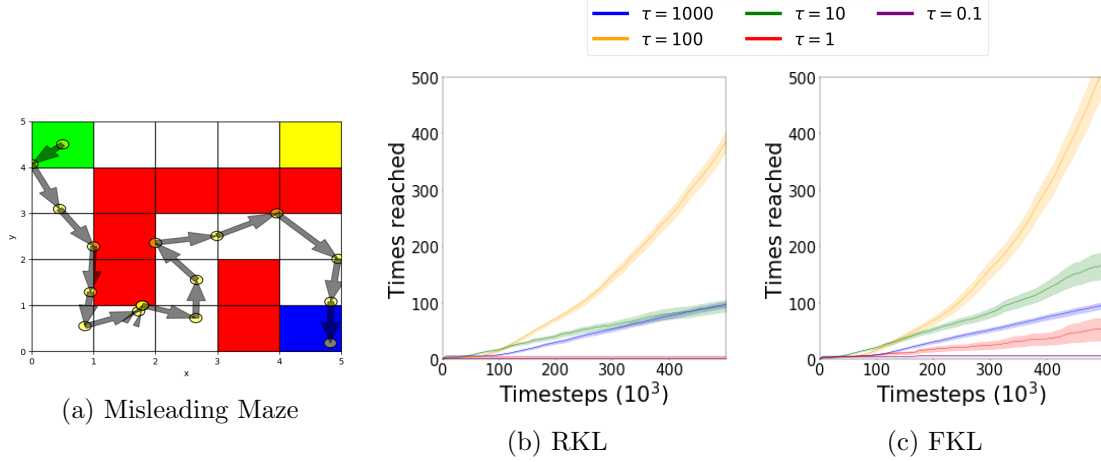


Figure 10: (a) The optimal policy is to go to the blue goal. The yellow goal is misleading, in that it has a positive reward and is easier to get to. Plots in (b) and (c) show the cumulative number of times the correct exit is reached throughout training for multiple temperatures.

RKL are plotted separately. Appendix B.2 gives more detailed plots of these experiments, where we also show the cumulative number of times the misleading exit is reached and plots for 2M timesteps, instead of the 500k steps we show here. From this we conclude that: (1) the FKL seems to be more exploratory than the RKL and (2) the performance when using FKL seems to be a little more robust to the hyperparameters. Also, we note that this is the only experiment in the paper where the higher temperatures such as 10 and 100 performed better than the lower ones. Figure 10a shows a sampled trajectory from one of the resulting FKL policies with temperature 100, trained for 2M timesteps. Although these policies often reach the goal, they are still highly stochastic. A natural next step is to make them more deterministic over time, by using temperature annealing.

## 9. Practical Performance on Benchmark Problems

In this section, we compare the KL methods on benchmark continuous and discrete-action environments, using non-linear function approximation. Here, we wish to understand (1) if our observations from the microworld experiments apply to more complicated environments, (2) if there are any new differences as a result of function approximation or increased environment complexity and (3) if any of the KL divergences is more robust to hyperparameter choices than the other.

### 9.1 Implementation Details

The agents use the API Algorithm with KL Greedification, in Algorithm 1. For the discrete action environments, we use the All-Actions updates, and for the continuous action environments we use the Sampled-Actions update, for both RKL and FKL, with 128 sampled actions. When evaluating the integral of the gradient for the RKL, we tested using the



log-likelihood trick as well as the reparametrization trick. Since the last outperformed the first, we report results using reparametrization. All agents use experience replay with a buffer size of  $10^6$  and use batch sizes of 32.

Hyperparameter sweeps are performed separately for each domain. We use RMSprop for both the actor and critic. In the continuous action-setting, we sweep over the actor learning rates  $\{10^{-5}, 10^{-4}, 10^{-3}, 10^{-2}\}$  and critic learning rates  $\{10^{-5}, 10^{-4}, 10^{-3}, 10^{-2}, 10^{-1}\}$ . In the discrete-action setting we have a shared learning rate because of a shared architecture and the sweep is done over the learning rates  $\{10^{-5}, 10^{-4}, 10^{-3}, 10^{-2}, 10^{-1}\}$ . We sweep temperatures in  $\{10^{-3}, 5 \times 10^{-3}, 10^{-2}, 5 \times 10^{-2}, 10^{-1}, 5 \times 10^{-1}, 1\}$  for the soft action-value methods and additionally include runs with the hard action-value methods. The temperature in  $\mathcal{B}_\tau Q$  and the temperature in the soft action-value function are set to be the same value. For example, if  $\tau = 0.01$ , then we learn a soft action-value function with  $\tau = 0.01$  and use a KL target distribution proportional to  $\exp(Q(s, a)\tau^{-1})$ .

On our continuous-action domains, all policy and value function networks are implemented as two-layer neural networks of size 128, with ReLU activations. On our discrete-action domains, we employ the following architectures. In the OpenAI Gym environments, the architecture is a two-layer neural network of size 128 with ReLU activations, with the policy and value functions as separate heads off of the main two-layer body. In MinAtar, the architecture is a convolutional network into one fully-connected layer for each of the policy, action value function, and state value function. The convolutional layer has 16 3x3 convolutions with stride 1, the same as in Young and Tian (2019). The size of the fully-connected layer is 128, with ReLU activations used between layers.

## 9.2 Performance

For continuous actions, we experiment on Pendulum, Reacher, Swimmer and HalfCheetah (Todorov et al., 2012). For discrete actions, we experiment on OpenAI Gym environments (Brockman et al., 2016) and MinAtar environments (Young and Tian, 2019). In this section, we plot only a summary of the performance, detailed plots showing how it varies throughout training can be found in Appendix B.3. Temperatures  $[1.0, 0.5, 0.1]$  were grouped together and labeled as “High RKL/FK”, whereas  $[0.05, 0.01, 0.005, 0.001, 0.0]$ <sup>13</sup> were grouped together and named “Low RKL/FKL”. For each temperature, 30 seeds were run per hyperparameter setting and the best performing 20% settings were selected, which were then grouped together based on the temperature as “High/Low”. Figures 11 and 12 report the average of the last half of the area under the curve for each group, as well as standard errors between all runs in the group. Returns are normalized between 0 and 1, with 0 corresponding to the lower limit of the returns from the curves in Appendix B.3 and 1 to the highest. There was no striking pattern regarding which temperature is best overall, the choice seems to be highly environment dependent. Furthermore, FKL and RKL seem to perform comparably overall, with no clear dominance of one over the other, although the FKL performed slightly better in the few cases they were different.

---

13. Zero was excluded for FKL with continuous actions, see Appendix B.3

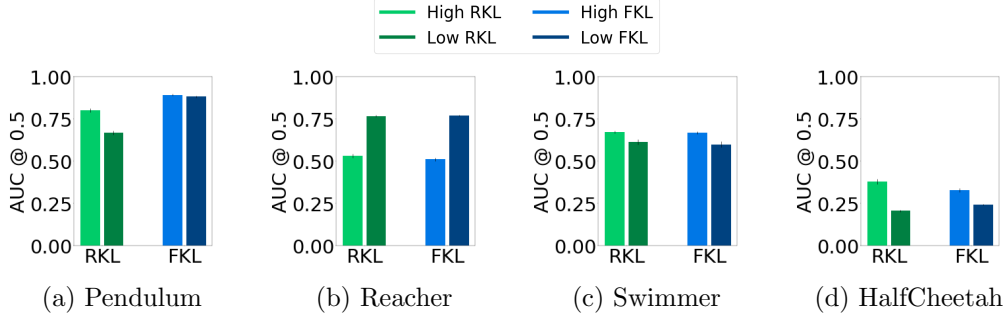


Figure 11: **Average return on the continuous-action environments.** The reported performance is the average return over the last half of learning, normalized between 0 and 1 and averaged over 30 runs with standard errors shown.

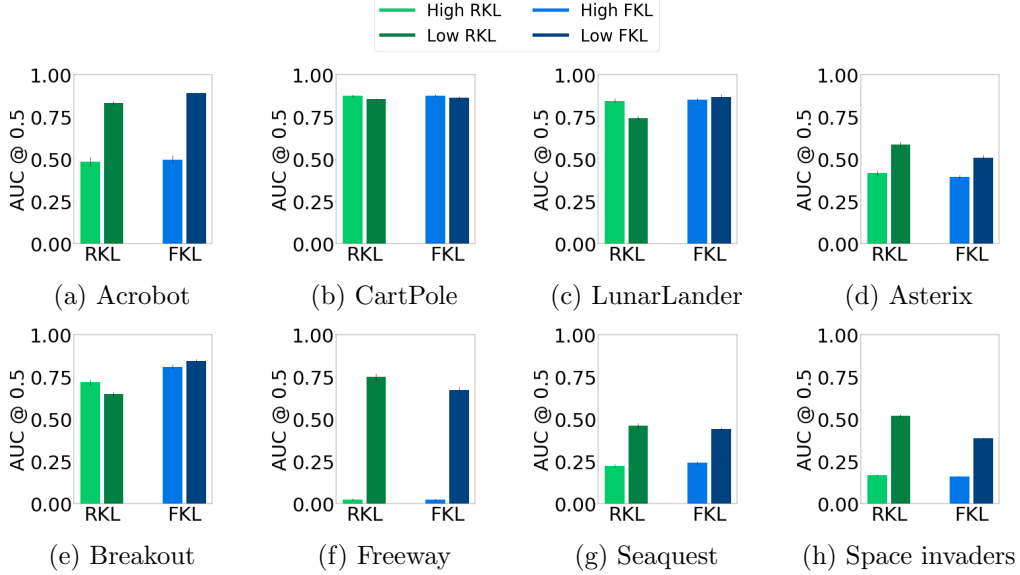


Figure 12: **Average return on the discrete-action environments.** The reported performance is the average return over the last half of learning, normalized between 0 and 1 and averaged over 30 runs with standard errors shown.

### 9.3 Hyperparameter sensitivity

We wrap up the experiments on benchmark problems by investigating the sensitivity of each divergence to hyperparameters. We focus on studying the sensitivity to the ones that seem to influence performance the most: learning rate and temperature. Particularly, we vary learning rates for each different temperature. For the continuous environments, where the actor and critic were separate networks, we have both the actor learning rate and the critic learning rate, whereas for the discrete environments we only have one learning rate.

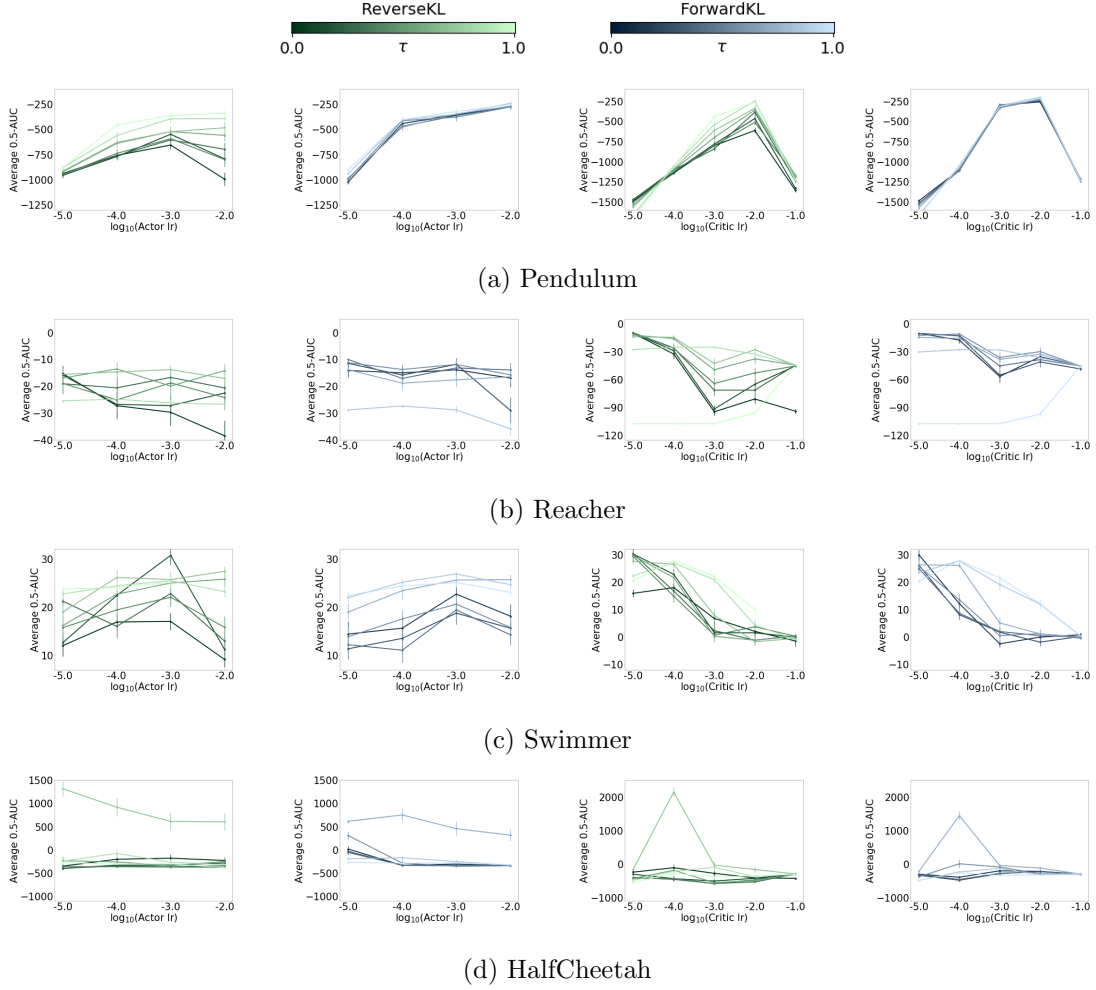


Figure 13: Sensitivity plots for continuous-action environments. The x axis represent the hyperparameter values and the y axis represent the averaged area under the last half of the learning curve. Each point corresponds to the average of the top 20% performing settings that had the corresponding learning rate and temperature

From looking at Figures 13 and 14, we see that both methods are sensitive to the hyperparameters, with the best parameters being highly environment dependent. For a given temperature and environment, RKL and FKL have very similar behavior: if the performance goes up for a certain learning rate for RKL, it also goes up for FKL and the same applies to decreases in performance, with very few exceptions and, even in those cases, the overall tendency is still the same for the two divergences. On Pendulum, represented in Figure 13a, for example, the worst learning rates perform better on FKL than in RKL, but the overall tendency is still for performance to go up as actor learning rates increase to 0.01 and as critic learning rates increase to 0.01, followed by a decrease when critic learning rate further increases to 0.1. The main takeaway is that, for a given choice of environment

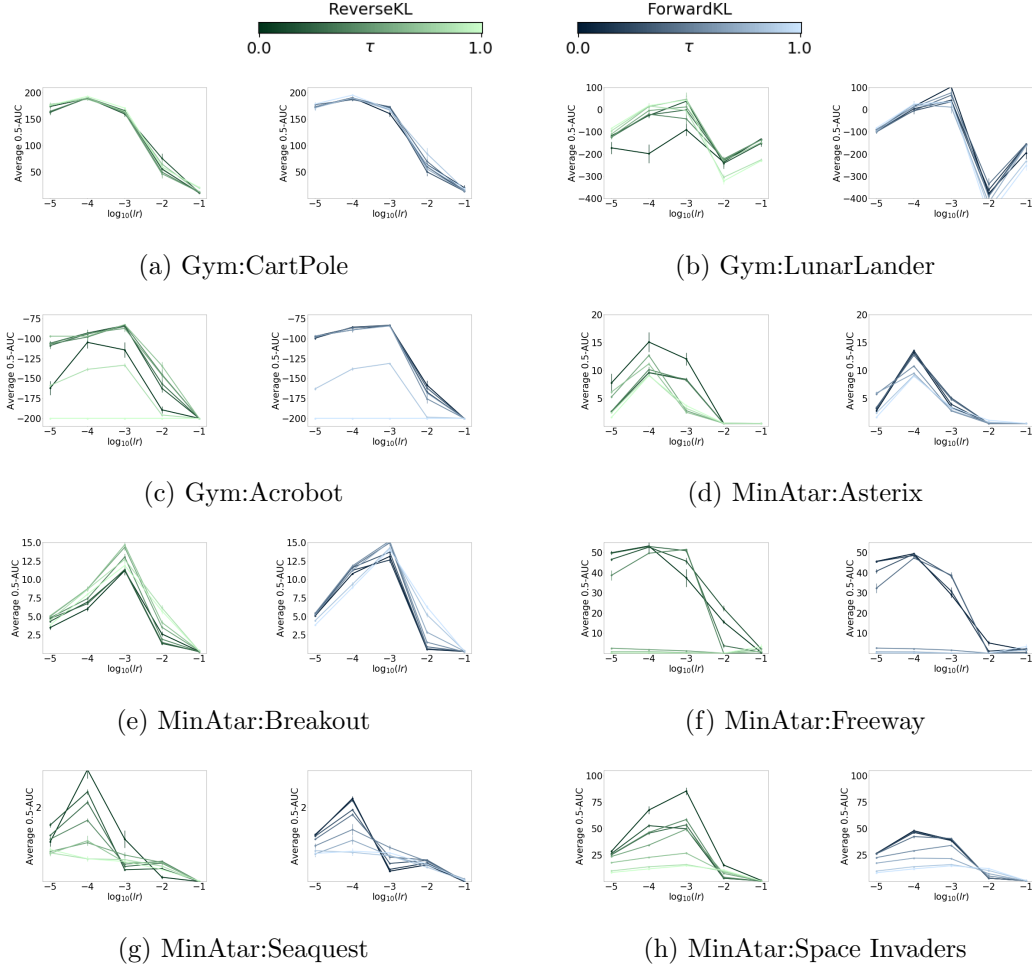


Figure 14: Sensitivity plots for discrete-action environments. Plot settings are identical to Figure 13

and temperature, learning rate sensitivity is not significantly influenced by the choice of divergence.

## 10. Discussion and Conclusion

Based on our theoretical and empirical results, we can summarize our findings as follows.

**Theoretically**, while the FKL may not be guaranteed to induce policy improvement as reliably as the RKL, policy improvement can still occur if a sufficiently high reduction in FKL occurs, or under additional conditions that likely have to do with controlling the Renyi divergence of order  $\infty$ . We hypothesize that the superior policy improvement result of the RKL with true values may be related to its committing to actions with high action-value that we observed in our experiments.

**On the microworld and maze experiments**, there were more differences between FKL and RKL in the continuous-action setting, whereas no significant differences were observed in the discrete-action setting. In the continuous-action setting, the FKL tended to have a smoother loss landscape that directed iterates to a global optimum of the entropy-regularized objective, although this global optimum was sometimes less optimal with respect to the unregularized objective, especially with higher temperatures, than the optima of the RKL. Moreover, the greater suboptimality of the FKL limit points was correlated with the final FKL policies having higher action variance than the corresponding final policies for the RKL. Further experiments supported the claim that the FKL induces more stochastic policies than the RKL, which is consistent with previously described mean-seeking behaviour of the FKL. The fact that significant differences were only observed in the continuous-action regime suggests the important role of policy parameterization.

**On our benchmark experiments**, there did not seem to be much difference between choosing one divergence or the other for most of the environments, with performance being more heavily dictated by the choice of temperature and learning rate. In fact, plots of both performance and sensitivity to learning rates were near mirror images in most cases. The algorithms are sensitive to hyperparameters and the best learning rate-temperature combination was also highly environment dependent.

One conclusion from this work is that, though it has been rarely used, the FKL is a promising direction for policy greedification and warrants further investigation. For  $\tau \neq 0$ , weighted importance sampling allows us to estimate the forward KL objective stochastically, making it practically feasible. Although the FKL performed similarly to the RKL in the benchmark problems, it has properties which can be useful, such as committing less quickly to actions, being more robust to stochastic samples of the gradient of the FKL for a state—which is pertinent as mini-batch estimates will be stochastic—and having a smoother loss surface.

A natural question from this study is why the differences were the largest for continuous actions in our microworld experiments. One potential reason is the policy parameterization: the Gaussian policy is likely more restrictive than the softmax as it cannot capture multimodal structure. Learning the standard deviation of a Gaussian policy may be another source of instability. In contrast, a softmax policy can represent multiple modes, and does not separate the parameterization of the measure of central tendency (e.g., mean) and the measure of variation (e.g., standard deviation). With a Gaussian policy, FKL seems to have a better optimization surface (having smooth and single optima across different temperatures) despite the multimodality of the target distribution in our continuous bandit. However, none of these observations may hold for other policy parameterizations.

A promising next step is to compare FKL and RKL with different policy parameterizations for continuous actions. Recent work into alternative policy parameterizations has explored the Beta distribution (Chou et al., 2017), quantile regression (Richter and Wattenhofer, 2019), and normalizing flows (Ward et al., 2019). While the latter two works in particular have focused on the motivation of multimodality for domains that have multiple goals, we believe that the relevance of multimodality for optimization is as important.

The choice of target distribution in the greedification objective is another sticky issue. The Boltzmann distribution over action values is a natural choice for entropy-regularized RL, but one might not want to be tied this framework, especially given sensitivity to the

temperature parameter and exploration that is undirected. Instead of maximizing the entropy of a distribution over actions, one could try to maximize the entropy of the discounted state visitation distribution (Islam et al., 2019). If the goal is exploration of the state space, perhaps one should let the agent decide how to do so, rather than imposing the proxy of high entropy in the action distribution.

In addition to the choice of target distribution, there are many other possible choices for a greedification objective. Besides the KL divergences, one may consider the Wasserstein distance, Cramér distance, the JS divergence, and many more. One reason we focused on the KL in this work was its ease of optimization, compared to the Wasserstein distance for example. There may, however, be other cogent reasons for selecting an objective. Modeling the quantiles of the policy, for instance, suggests using the quantile loss.

Though we focused on episodic problems in this work, some of the approaches could be used for the continuing setting with average reward. Recent work has analyzed the regret in continuing RL problems for a policy iteration algorithm, called Politex (Abbasi-Yadkori et al., 2019). The policy is a Boltzmann distribution over the sum of all previous action-value function estimates. For continuous actions, a natural alternative is to consider approximate greedification, by approximating this distribution with a parameterized policy. Other work looking at differential action-values for the average reward setting could benefit from explicit policy parameterizations that use approximate greedification with respect to those differential action-values.

Finally, the connection between policy gradients approaches and API could provide new directions to theoretically analyze policy gradient algorithms. A recent global convergence result for policy gradient methods relies on a connection to policy iteration and showing guaranteed policy improvement (Bhandari and Russo, 2019). Of particular relevance is work in API that allows for approximation error in the action-values. Perkins and Precup (2003) proves that API converges with linear function approximation for the action-values and soft policy improvement. This work, though, requires the best linear action-value approximation. More recently, Politex (Abbasi-Yadkori et al., 2019) bounded regret for an API algorithm, with linear action-values learned online. Scherrer (2014) provides error propagation analyses of many variants of API; these analyses could be extended to finite-sample guarantees by following (Scherrer et al., 2015). Finite-sample analyses for LSPI (Lazaric et al., 2012) and classification-based PI (Lazaric et al., 2016) also exist. These approaches are designed for approximate policy evaluation, and exact greedification. An important next step is to investigate if this theory can be extended to approximate greedification.

## Acknowledgements

We gratefully acknowledge funding from NSERC, the Canada CIFAR AI Chair program, and the Alberta Machine Intelligence Institute (Amii). Special thanks as well to Nicolas Le Roux for comments on an earlier version of this work.

## Appendix A. Proofs

**Lemma 7.** *[Soft Performance Difference] For any policies  $\pi_{\text{old}}, \pi_{\text{new}}$ , the following is true for any  $\tau \geq 0$ .*

$$\eta_\tau(\pi_{\text{new}}) - \eta_\tau(\pi_{\text{old}}) = \frac{1}{1-\gamma} \mathbb{E}_{d^{\pi_{\text{new}}}} \left[ \mathbb{E}_{\pi_{\text{new}}} [A_\tau^{\pi_{\text{old}}}(S, A)] - \tau \text{KL}(\pi_{\text{new}}(\cdot | S) \parallel \pi_{\text{old}}(\cdot | S)) \right].$$

**Proof** When we write  $\mathbb{E}_{\rho_0}^{\pi_{\text{new}}}$ , we mean the expectation over the trajectory distribution induced by  $\rho_0$  and  $\pi_{\text{new}}$ .

$$\begin{aligned} \frac{1}{1-\gamma} \mathbb{E}_{d^{\pi_{\text{new}}}, \pi_{\text{new}}} [A_\tau^{\pi_{\text{old}}}(S, A)] &= \mathbb{E}_{\rho_0}^{\pi_{\text{new}}} \left[ \sum_{t=0}^{\infty} \gamma^t A_\tau^{\pi_{\text{old}}}(S_t, A_t) \right] \\ &= \mathbb{E}_{\rho_0}^{\pi_{\text{new}}} \left[ \sum_{t=0}^{\infty} \gamma^t (Q_\tau^{\pi_{\text{old}}}(S_t, A_t) - \tau \log \pi_{\text{old}}(\cdot | S_t) - V_\tau^{\pi_{\text{old}}}(S_t)) \right] \end{aligned}$$

where the first equality follows from the definition of the visitation distribution and the second from the definition of the soft advantage. We can simplify the term inside the expectation as follows.

$$\begin{aligned} \sum_{t=0}^{\infty} \gamma^t (Q_\tau^{\pi_{\text{old}}}(S_t, A_t) - \tau \log \pi_{\text{old}}(\cdot | S_t) - V_\tau^{\pi_{\text{old}}}(S_t)) \\ = \sum_{t=0}^{\infty} \gamma^t (r(S_t, A_t) + \gamma V_\tau^{\pi_{\text{old}}}(S_{t+1}) - \tau \log \pi_{\text{old}}(\cdot | S_t) - V_\tau^{\pi_{\text{old}}}(S_t)) \\ = \left( \sum_{t=0}^{\infty} \gamma^t (r(S_t, A_t) - \tau \log \pi_{\text{old}}(\cdot | S_t)) \right) - V_\tau^{\pi_{\text{old}}}(S_0), \end{aligned}$$

where the second line follows from expanding  $Q_\tau^{\pi_{\text{old}}}$  and the second from the telescoping series  $\gamma V_\tau^{\pi_{\text{old}}}(S_{t+1}) - V_\tau^{\pi_{\text{old}}}(S_t)$ . Plugging this back into the expectation, and using  $\mathbb{E}_{\rho_0}^{\pi_{\text{new}}} [V_\tau^{\pi_{\text{old}}}(S_0)] = \eta_\tau(\pi_{\text{old}})$  we get

$$\begin{aligned} \mathbb{E}_{\rho_0}^{\pi_{\text{new}}} \left[ \sum_{t=0}^{\infty} \gamma^t A_\tau^{\pi_{\text{old}}}(S_t, A_t) \right] &= -\eta_\tau(\pi_{\text{old}}) + \mathbb{E}_{\rho_0}^{\pi_{\text{new}}} \left[ \sum_{t=0}^{\infty} \gamma^t (r(S_t, A_t) - \tau \log \pi_{\text{old}}(\cdot | S_t)) \right] \\ &= -\eta_\tau(\pi_{\text{old}}) + \eta_\tau(\pi_{\text{new}}) + \mathbb{E}_{\rho_0}^{\pi_{\text{new}}} \left[ \sum_{t=0}^{\infty} \gamma^t \tau (\log \pi_{\text{new}}(\cdot | S_t) - \log \pi_{\text{old}}(\cdot | S_t)) \right] \\ &= -\eta_\tau(\pi_{\text{old}}) + \eta_\tau(\pi_{\text{new}}) + \frac{\tau}{1-\gamma} \mathbb{E}_{d^{\pi_{\text{new}}}} [\text{KL}(\pi_{\text{new}}(\cdot | S) \parallel \pi_{\text{old}}(\cdot | S))], \end{aligned}$$

where the second equality is obtained by adding and subtracting  $\tau \log \pi_{\text{new}}(\cdot | S_t)$ . ■

**Proposition 8.** *[Improvement Under Average RKL Reduction] For  $\pi_{\text{old}}, \pi_{\text{new}} \in \Pi$ , define*

$$\begin{aligned} \Delta \text{RKL}(\pi_{\text{old}}(\cdot | S), \pi_{\text{new}}(\cdot | S)) \\ := \text{RKL}(\pi_{\text{old}}(\cdot | S), \mathcal{B}_\tau Q_\tau^{\pi_{\text{old}}}(S, \cdot)) - \text{RKL}(\pi_{\text{new}}(\cdot | S), \mathcal{B}_\tau Q_\tau^{\pi_{\text{old}}}(S, \cdot)). \end{aligned}$$

For  $\tau > 0$ , we can write:

$$\eta_\tau(\pi_{\text{new}}) - \eta_\tau(\pi_{\text{old}}) = \frac{\tau}{1-\gamma} \mathbb{E}_{d^{\pi_{\text{new}}}} [\Delta \text{RKL}(\pi_{\text{old}}(\cdot|S), \pi_{\text{new}}(\cdot|S))]. \quad (14)$$

Furthermore,  $\eta_\tau(\pi_{\text{new}}) \geq \eta_\tau(\pi_{\text{old}})$  if and only if

$$\mathbb{E}_{d^{\pi_{\text{new}}}} [\text{RKL}(\pi_{\text{old}}(\cdot|S), \mathcal{B}_\tau Q_\tau^{\pi_{\text{old}}}(S, \cdot))] \geq \mathbb{E}_{d^{\pi_{\text{new}}}} [\text{RKL}(\pi_{\text{new}}(\cdot|S), \mathcal{B}_\tau Q_\tau^{\pi_{\text{old}}}(S, \cdot))], \quad (15)$$

or, equivalently,

$$\mathbb{E}_{d^{\pi_{\text{new}}}} [\Delta \text{RKL}(\pi_{\text{old}}(\cdot|S), \pi_{\text{new}}(\cdot|S))] \geq 0.$$

**Proof** We start by writing the RHS of Lemma 7.

$$\begin{aligned} & \frac{1}{1-\gamma} \mathbb{E}_{d^{\pi_{\text{new}}}, \pi_{\text{new}}} [A_\tau^{\pi_{\text{old}}}(S, A)] - \frac{\tau}{1-\gamma} \mathbb{E}_{d^{\pi_{\text{new}}}} [\text{KL}(\pi_{\text{new}}(\cdot|S) \parallel \pi_{\text{old}}(\cdot|S))] = \\ & \frac{\tau}{1-\gamma} \mathbb{E}_{d^{\pi_{\text{new}}}, \pi_{\text{new}}} \left[ \frac{Q_\tau^{\pi_{\text{old}}}(S, A)}{\tau} - \log(\pi_{\text{old}}(A|S)) - \frac{V_\tau^{\pi_{\text{old}}}(S)}{\tau} \right] \\ & \quad - \frac{\tau}{1-\gamma} \mathbb{E}_{d^{\pi_{\text{new}}}, \pi_{\text{new}}} [\log(\pi_{\text{new}}(A|S)) - \log(\pi_{\text{old}}(A|S))] = \\ & \frac{\tau}{1-\gamma} \left( \mathbb{E}_{d^{\pi_{\text{new}}}, \pi_{\text{new}}} \left[ \log \left( e^{\frac{Q_\tau^{\pi_{\text{old}}}(S, A)}{\tau}} \right) \right] - \mathbb{E}_{d^{\pi_{\text{new}}}, \pi_{\text{old}}} \left[ \frac{Q_\tau^{\pi_{\text{old}}}(S, A)}{\tau} - \log(\pi_{\text{old}}(A|S)) \right] \right) \\ & \quad - \frac{\tau}{1-\gamma} \mathbb{E}_{d^{\pi_{\text{new}}}, \pi_{\text{new}}} [\log(\pi_{\text{new}}(A|S))] = \\ & \frac{\tau}{1-\gamma} \mathbb{E}_{d^{\pi_{\text{new}}}, \pi_{\text{new}}} \left[ \log \left( e^{\frac{Q_\tau^{\pi_{\text{old}}}(S, A)}{\tau}} \right) - \log(\pi_{\text{new}}(A|S)) \right] \\ & \quad - \frac{\tau}{1-\gamma} \mathbb{E}_{d^{\pi_{\text{new}}}, \pi_{\text{old}}} \left[ \log \left( e^{\frac{Q_\tau^{\pi_{\text{old}}}(S, A)}{\tau}} \right) - \log(\pi_{\text{old}}(A|S)) \right] = \\ & \frac{\tau}{1-\gamma} \mathbb{E}_{d^{\pi_{\text{new}}}} [\Delta \text{RKL}(\pi_{\text{old}}(\cdot|S), \pi_{\text{new}}(\cdot|S))]. \end{aligned}$$

The last equality follows by adding and subtracting  $\mathbb{E}_{d^{\pi_{\text{new}}}} (\log(Z(S)))$  and rearranging. Plugging that in the equation from Lemma 7 we get:

$$\eta_\tau(\pi_{\text{new}}) - \eta_\tau(\pi_{\text{old}}) = \frac{\tau}{1-\gamma} \mathbb{E}_{d^{\pi_{\text{new}}}} [\Delta \text{RKL}(\pi_{\text{old}}(\cdot|S), \pi_{\text{new}}(\cdot|S))],$$

which can only be nonnegative if  $\mathbb{E}_{d^{\pi_{\text{new}}}} [\Delta \text{RKL}(\pi_{\text{old}}(\cdot|S), \pi_{\text{new}}(\cdot|S))] \geq 0$ . ■

**Proposition 9.** [Counterexample for Improvement with FKL] For any  $\tau \geq 0$ , and  $\gamma \in [0, 1)$ , there exists a pair of policies  $(\pi_{\text{old}}, \pi_{\text{new}})$  such that at every state  $s \in \mathcal{S}$  we have  $\Delta \text{FKL}(\pi_{\text{old}}(\cdot|s), \pi_{\text{new}}(\cdot|s)) > 0$  but the new policy has lower value:  $Q_\tau^{\pi_{\text{new}}}(s, a) < Q_\tau^{\pi_{\text{old}}}(s, a)$  at every state-action pair  $(s, a) \in \mathcal{S} \times \mathcal{A}$ ,  $V_\tau^{\pi_{\text{new}}}(s) < V_\tau^{\pi_{\text{old}}}(s)$  at every state  $s \in \mathcal{S}$ , and  $\eta_\tau(\pi_{\text{new}}) < \eta_\tau(\pi_{\text{old}})$ .



**Proof** Consider the environment with a single state  $s$  and two actions:  $a_1$  and  $a_2$ . Regardless of the action chosen, the agent always transition to  $s$ . We will omit dependency on the state in the following notation. The rewards are defined as

$$r(a_1) = -1 \quad , \quad r(a_2) = 1.$$

Take  $\pi_{\text{old}}$  and  $\pi_{\text{new}}$  as follows.

$$\begin{aligned} \pi_{\text{old}}(a_1) &= \epsilon_1 & , & \quad \pi_{\text{new}}(a_1) = 1 - \epsilon_2, \\ \pi_{\text{old}}(a_2) &= 1 - \epsilon_1 & , & \quad \pi_{\text{new}}(a_2) = \epsilon_2. \end{aligned}$$

We will prove the result by making  $\epsilon_1$  arbitrarily small, which we will show forces  $\text{FKL}(\pi_{\text{old}}, \mathcal{B}_\tau Q_\tau^{\pi_{\text{old}}})$  to  $\infty$  while keeping  $\epsilon_2$  fixed, causing  $\text{FKL}(\pi_{\text{new}}, \mathcal{B}_\tau Q_\tau^{\pi_{\text{old}}})$  to be finite. Note that

$$\begin{aligned} \text{FKL}(\pi_{\text{old}}, \mathcal{B}_\tau Q_\tau^{\pi_{\text{old}}}) &= \sum_{i=1}^2 \mathcal{B}_\tau Q_\tau^{\pi_{\text{old}}}(a_i) \log \left( \frac{\mathcal{B}_\tau Q_\tau^{\pi_{\text{old}}}(a_i)}{\pi_{\text{old}}(a_i)} \right) \\ &= -\mathcal{H}(\mathcal{B}_\tau Q_\tau^{\pi_{\text{old}}}) - \sum_{i=1}^2 \mathcal{B}_\tau Q_\tau^{\pi_{\text{old}}}(a_i) \log(\pi_{\text{old}}(a_i)), \\ \lim_{\epsilon_1 \rightarrow 0} \text{FKL}(\pi_{\text{old}}, \mathcal{B}_\tau Q_\tau^{\pi_{\text{old}}}) &= \underbrace{-\lim_{\epsilon_1 \rightarrow 0} \mathcal{H}(\mathcal{B}_\tau Q_\tau^{\pi_{\text{old}}}) - \lim_{\epsilon_1 \rightarrow 0} \mathcal{B}_\tau Q_\tau^{\pi_{\text{old}}}(a_1) \log(\epsilon_1)}_{\geq -\log 2 \text{ and } \leq 0} + 0. \end{aligned}$$

To calculate the limit of the middle summand, we note that if  $\lim_{\epsilon_1 \rightarrow 0} \mathcal{B}_\tau Q_\tau^{\pi_{\text{old}}}(a_1) > 0$ , the middle summand will go to infinity, since  $\lim_{\epsilon_1 \rightarrow 0} -\log(\epsilon_1) = \infty$ . We can verify that this is indeed the case.

$$\begin{aligned} \lim_{\epsilon_1 \rightarrow 0} Q_\tau^{\pi_{\text{old}}}(a_1) &= -1 + \frac{\gamma}{1-\gamma} & ; & \quad \lim_{\epsilon_1 \rightarrow 0} Q_\tau^{\pi_{\text{old}}}(a_2) = \frac{1}{1-\gamma} \\ \lim_{\epsilon_1 \rightarrow 0} \mathcal{B}_\tau Q_\tau^{\pi_{\text{old}}}(a_1) &= \frac{e^{(-1+\frac{\gamma}{1-\gamma})\frac{1}{\tau}}}{Z} & ; & \quad \lim_{\epsilon_1 \rightarrow 0} \mathcal{B}_\tau Q_\tau^{\pi_{\text{old}}}(a_2) = \frac{e^{(\frac{1}{1-\gamma})\frac{1}{\tau}}}{Z}, \end{aligned} \quad (20)$$

where  $Z := e^{(-1+\frac{\gamma}{1-\gamma})\frac{1}{\tau}} + e^{(\frac{1}{1-\gamma})\frac{1}{\tau}}$ . Since, for fixed  $\gamma$  and  $\tau$ , the quantities in Equation (20) are fixed, we have that  $\lim_{\epsilon_1 \rightarrow 0} -\mathcal{B}_\tau Q_\tau^{\pi_{\text{old}}}(a_1) \log(\epsilon_1) = \infty$ , causing  $\lim_{\epsilon_1 \rightarrow 0} \text{FKL}(\pi_{\text{old}}, \mathcal{B}_\tau Q_\tau^{\pi_{\text{old}}}) = \infty$ . Moreover,  $\text{FKL}(\pi_{\text{new}}, \mathcal{B}_\tau Q_\tau^{\pi_{\text{old}}})$  has a similar form of the above FKL, but, since  $\epsilon_2$  is assumed to be fixed, this quantity will be finite. The point is that for any  $\epsilon_2$ , we can find  $\epsilon_1$  such that  $\text{FKL}(\pi_{\text{old}}, \mathcal{B}_\tau Q_\tau^{\pi_{\text{old}}}) > \text{FKL}(\pi_{\text{new}}, \mathcal{B}_\tau Q_\tau^{\pi_{\text{old}}})$ .

It remains to be seen that we can have  $\epsilon_2$  that guarantees  $V_\tau^{\pi_{\text{new}}} < V_\tau^{\pi_{\text{old}}}$ . We write

$$\begin{aligned} V_\tau^{\pi_{\text{new}}} &= \mathbb{E} \left[ \sum_{t=0}^{\infty} \gamma^t (R + \tau \mathcal{H}(\pi_{\text{new}})) \right] = \mathbb{E} \left[ \sum_{t=0}^{\infty} \gamma^t R \right] + \frac{\tau \mathcal{H}(\pi_{\text{new}})}{1-\gamma} \\ &= \left( \sum_{t=0}^{\infty} \gamma^t \mathbb{E}[R] \right) + \frac{\tau \mathcal{H}(\pi_{\text{new}})}{1-\gamma} \\ &= \frac{2\epsilon_2 - 1}{1-\gamma} + \frac{\tau \mathcal{H}(\pi_{\text{new}})}{1-\gamma}. \end{aligned}$$

Additionally, we know that  $\lim_{\epsilon_1 \rightarrow 0} V_\tau^{\pi_{\text{old}}} = \frac{1}{1-\gamma}$ . If we can find  $\epsilon_2$  such that  $V_\tau^{\pi_{\text{new}}} < \frac{1}{1-\gamma}$ , then we can find  $\epsilon_1$  such that simultaneously  $V_\tau^{\pi_{\text{new}}} < V_\tau^{\pi_{\text{old}}}$  and  $\text{FKL}(\pi_{\text{old}}, \mathcal{B}_\tau Q_\tau^{\pi_{\text{old}}}) > \text{FKL}(\pi_{\text{new}}, \mathcal{B}_\tau Q_\tau^{\pi_{\text{old}}})$ .  $V_\tau^{\pi_{\text{new}}} < \frac{1}{1-\gamma}$  will hold if

$$\begin{aligned} \frac{1}{1-\gamma} (2\epsilon_2 - 1 + \tau \mathcal{H}(\pi_{\text{new}})) &< \frac{1}{1-\gamma} \\ 2\epsilon_2 - 1 + \tau(-(1-\epsilon_2)\log(1-\epsilon_2) - \epsilon_2 \log(\epsilon_2)) &< 1. \end{aligned} \quad (21)$$

We use  $f(\epsilon_2)$  to denote the LHS of eq. (21). We have

$$\lim_{\epsilon_2 \rightarrow 0} f(\epsilon_2) = -1,$$

which is less than the RHS of Equation (21). Formally, for any  $\epsilon > 0$ , we can find  $\delta > 0$  such that if  $|\epsilon_2| < \delta$ ,  $|f(\epsilon_2) - 1| < \epsilon$ . Any  $\epsilon < 2$  will suffice: we can conclude that, for any fixed  $\tau \geq 0$ , there is some  $\epsilon_2 \in (0, 1)$  satisfying eq. (21). ■

**Proposition 11** (Sufficient FKL Reduction in Bandits). *For two policies  $\pi_{\text{old}}, \pi_{\text{new}} \in \mathbb{R}^{|\mathcal{A}|}$  in the bandit setting, if*

$$\begin{aligned} &\Delta \text{FKL}(\pi_{\text{old}}, \pi_{\text{new}}) \\ &\geq \max \left\{ 0, \text{FKL}(\pi_{\text{old}}, \mathcal{B}_\tau Q) - \frac{1}{2} \left( \frac{\tau}{\|\mathbf{q}\|_\infty} \left( \text{RKL}(\pi_{\text{old}}, \mathcal{B}_\tau Q) + \mathcal{B}_\tau Q^\top \log(\pi_{\text{old}}) \right) \right)^2 \right\} \end{aligned}$$

and

$$\text{RKL}(\pi_{\text{old}}, \mathcal{B}_\tau Q) + \mathcal{B}_\tau Q^\top \log(\pi_{\text{old}}) \geq 0,$$

then  $\Delta \text{RKL}(\pi_{\text{old}}, \pi_{\text{new}}) \geq 0$  and  $\eta_\tau(\pi_{\text{new}}) \geq \eta_\tau(\pi_{\text{old}})$ .

**Proof** Start with the following.

$$\begin{aligned} 0 &\leq \text{FKL}(\pi_{\text{new}}, \mathcal{B}_\tau Q) \\ &\leq \mathcal{B}_\tau Q^\top \log \left( \frac{\mathcal{B}_\tau Q}{\pi_{\text{new}}} \right) \\ &= \mathcal{B}_\tau Q^\top \left( \frac{\mathbf{q}}{\tau} - \log(\pi_{\text{new}}) \right) - \log(Z) \\ &\quad \triangleright \text{Expanding the inner } \mathcal{B}_\tau Q \\ 0 &\leq \mathcal{B}_\tau Q^\top (\mathbf{q} - \tau \log(\pi_{\text{new}})) - \tau \log(Z) \\ &\quad \triangleright \text{Multiplying both sides by } \tau \\ &= \pi_{\text{new}}^\top (\mathbf{q} - \tau \log \pi_{\text{new}}) + \mathbf{q}^\top (\mathcal{B}_\tau Q - \pi_{\text{new}}) + \\ &\quad \tau \log \pi_{\text{new}}^\top (\pi_{\text{new}} - \mathcal{B}_\tau Q) - \tau \log(Z) \\ &\quad \triangleright \text{Adding and subtracting } \pi_{\text{new}}^\top \mathbf{q} \text{ and } \tau \pi_{\text{new}}^\top \log \pi_{\text{new}} \\ &= -\tau \text{RKL}(\pi_{\text{new}}, \mathcal{B}_\tau Q) + \mathbf{q}^\top (\mathcal{B}_\tau Q - \pi_{\text{new}}) + \\ &\quad \tau (\pi_{\text{new}}^\top \log(\pi_{\text{new}}) - \mathcal{B}_\tau Q^\top \log(\pi_{\text{new}})) \\ &\quad \triangleright \text{Absorbing the partition function.} \end{aligned} \quad (22)$$

We then analyze some of the summands from Equation (22) in turn.

$$\begin{aligned}
 \mathbf{q}^\top (\mathcal{B}_\tau Q - \boldsymbol{\pi}_{new}) &= \sum_i q_i (\mathcal{B}_\tau Q_i - \pi_{new i}) \\
 &\leq \left| \sum_i q_i (\mathcal{B}_\tau Q_i - \pi_{new i}) \right| \\
 &\leq \sum_i |q_i| |(\mathcal{B}_\tau Q_i - \pi_{new i})| \\
 &\leq \|\mathbf{q}\|_\infty \sum_i |(\mathcal{B}_\tau Q_i - \pi_{new i})|.
 \end{aligned}$$

By Pinsker's inequality (Pinsker, 1964),

$$\sum_i |(\mathcal{B}_\tau Q_i - \pi_{new i})| \leq \sqrt{2\text{FKL}(\boldsymbol{\pi}_{new}, \mathcal{B}_\tau Q)}.$$

Therefore,

$$\mathbf{q}^\top (\mathcal{B}_\tau Q - \boldsymbol{\pi}_{new}) \leq \|\mathbf{q}\|_\infty \sqrt{2\text{FKL}(\boldsymbol{\pi}_{new}, \mathcal{B}_\tau Q)}.$$

The other summand from Equation (22) can be written as

$$\tau(\boldsymbol{\pi}_{new}^\top \log(\boldsymbol{\pi}_{new}) - \mathcal{B}_\tau Q^\top \log(\boldsymbol{\pi}_{new})) \leq \tau(0 - \mathcal{B}_\tau Q^\top \log(\boldsymbol{\pi}_{old})),$$

where we used the fact that the negative entropy of  $\boldsymbol{\pi}_{new}$  is less than or equal to zero and that, since the underlying assumption is that we have non-negative FKL reduction, we also have  $-\mathcal{B}_\tau Q^\top \log(\boldsymbol{\pi}_{new}) \leq -\mathcal{B}_\tau Q^\top \log(\boldsymbol{\pi}_{old})$  (by the FKL definition).

We substitute these upper bounds into Equation (22).

$$\begin{aligned}
 0 &\leq -\tau \text{RKL}(\boldsymbol{\pi}_{new}, \mathcal{B}_\tau Q) + \mathbf{q}^\top (\mathcal{B}_\tau Q - \boldsymbol{\pi}_{new}) + \\
 &\quad \tau(\boldsymbol{\pi}_{new}^\top \log(\boldsymbol{\pi}_{new}) - \mathcal{B}_\tau Q^\top \log(\boldsymbol{\pi}_{new})) \\
 &\leq -\tau \text{RKL}(\boldsymbol{\pi}_{new}, \mathcal{B}_\tau Q) + \|\mathbf{q}\|_\infty \sqrt{2\text{FKL}(\boldsymbol{\pi}_{new}, \mathcal{B}_\tau Q)} + \\
 &\quad \tau(-\mathcal{B}_\tau Q^\top \log(\boldsymbol{\pi}_{old})),
 \end{aligned}$$

which then implies

$$\text{RKL}(\boldsymbol{\pi}_{new}, \mathcal{B}_\tau Q) \leq \frac{\|\mathbf{q}\|_\infty}{\tau} \sqrt{2\text{FKL}(\boldsymbol{\pi}_{new}, \mathcal{B}_\tau Q)} - \mathcal{B}_\tau Q^\top \log(\boldsymbol{\pi}_{old}). \quad (23)$$

If the RHS of Equation (23) is less than or equal to  $\text{RKL}(\boldsymbol{\pi}_{old}, \mathcal{B}_\tau Q)$ , we will have  $\text{RKL}(\boldsymbol{\pi}_{new}, \mathcal{B}_\tau Q) \leq \text{RKL}(\boldsymbol{\pi}_{old}, \mathcal{B}_\tau Q)$ , which in turn implies improvement. The assumption that the RHS of Equation (23) is  $\leq \text{RKL}(\boldsymbol{\pi}_{old}, \mathcal{B}_\tau Q)$  can be written as

$$\frac{\|\mathbf{q}\|_\infty}{\tau} \sqrt{2\text{FKL}(\boldsymbol{\pi}_{new}, \mathcal{B}_\tau Q)} - \mathcal{B}_\tau Q^\top \log(\boldsymbol{\pi}_{old}) \leq \text{RKL}(\boldsymbol{\pi}_{old}, \mathcal{B}_\tau Q).$$

With some algebraic manipulation, we get that this assumption is equivalent to

$$\frac{\tau}{\|\mathbf{q}\|_\infty}(\text{RKL}(\boldsymbol{\pi}_{old}, \mathcal{B}_\tau Q) + \mathcal{B}_\tau Q^\top \log(\boldsymbol{\pi}_{old})) \geq \sqrt{2\text{FKL}(\boldsymbol{\pi}_{new}, \mathcal{B}_\tau Q)}.$$

Assuming that  $\text{RKL}(\boldsymbol{\pi}_{old}, \mathcal{B}_\tau Q) + \mathcal{B}_\tau Q^\top \log(\boldsymbol{\pi}_{old}) \geq 0$ , the above is equivalent to

$$\left( \frac{\tau}{\|\mathbf{q}\|_\infty}(\text{RKL}(\boldsymbol{\pi}_{old}, \mathcal{B}_\tau Q) + \mathcal{B}_\tau Q^\top \log(\boldsymbol{\pi}_{old})) \right)^2 \geq 2\text{FKL}(\boldsymbol{\pi}_{new}, \mathcal{B}_\tau Q).$$

Dividing by 2, adding  $\text{FKL}(\boldsymbol{\pi}_{old}, \mathcal{B}_\tau Q)$ , and rearranging yields that the assumption is equivalent to the following.

$$\Delta\text{FKL}(\boldsymbol{\pi}_{old}, \boldsymbol{\pi}_{new}) \geq \text{FKL}(\boldsymbol{\pi}_{old}, \mathcal{B}_\tau Q) - \frac{1}{2} \left( \frac{\tau}{\|\mathbf{q}\|_\infty} \left( \text{RKL}(\boldsymbol{\pi}_{old}, \mathcal{B}_\tau Q) + \mathcal{B}_\tau Q^\top \log(\boldsymbol{\pi}_{old}) \right) \right)^2. \quad (24)$$

The claim follows. ■

**Proposition 13** (Improvement Under Average Sufficient FKL Reduction). *Assume the action set is finite. If*

$$\mathbb{E}_{d^{\pi_{new}}} [\text{RKL}(\pi_{old}(\cdot | S), \mathcal{B}_\tau Q_\tau^{\pi_{old}}(S, \cdot))] + \mathbb{E}_{d^{\pi_{new}}} [\mathbb{E}_{\mathcal{B}_\tau Q_\tau^{\pi_{old}}} [\log(\pi_{old}(\cdot | S))]] \geq 0 \quad (17)$$

and

$$\mathbb{E}_{d^{\pi_{new}}} [\Delta\text{FKL}(\pi_{old}(\cdot | S), \pi_{new}(\cdot | S))] \geq \mathbb{E}_{d^{\pi_{new}}} [\text{FKL}(\pi_{old}(\cdot | S), \mathcal{B}_\tau Q_\tau^{\pi_{old}}(S, \cdot))] - \frac{1}{2} \left( \frac{\tau}{\|Q_\tau^{\pi_{old}}\|_\infty} \left( \mathbb{E}_{d^{\pi_{new}}} [\text{RKL}(\pi_{old}(\cdot | S), \mathcal{B}_\tau Q_\tau^{\pi_{old}}(S, \cdot))] + \mathbb{E}_{d^{\pi_{new}}} [\mathbb{E}_{\mathcal{B}_\tau Q_\tau^{\pi_{old}}} [\log(\pi_{old}(\cdot | S))]] \right) \right)^2,$$

then  $\eta_\tau(\pi_{new}) \geq \eta_\tau(\pi_{old})$ .

**Proof** We know from Proposition 8 that if we have

$$\mathbb{E}_{d^{\pi_{new}}} [\Delta\text{RKL}(\pi_{old}(\cdot | S), \pi_{new}(\cdot | S))] \geq 0,$$

then  $\eta_\tau(\pi_{new}) \geq \eta_\tau(\pi_{old})$ . We also know from Equation (23) that the following is true for all states.

$$\begin{aligned} & \frac{\|Q_\tau^{\pi_{old}}(s, \cdot)\|_\infty}{\tau} \sqrt{2\text{FKL}(\pi_{new}(\cdot | s), \mathcal{B}_\tau Q_\tau^{\pi_{old}}(s, \cdot))} - \mathbb{E}_{\mathcal{B}_\tau Q_\tau^{\pi_{old}}} [\log(\pi_{old}(\cdot | s))] \\ & \geq \text{RKL}(\pi_{new}(\cdot | s), \mathcal{B}_\tau Q_\tau^{\pi_{old}}(s, \cdot)). \end{aligned}$$

The above inequality implies that

$$\begin{aligned} & \mathbb{E}_{d^{\pi_{new}}} \left[ \frac{\|Q_\tau^{\pi_{old}}(S, \cdot)\|_\infty}{\tau} \sqrt{2\text{FKL}(\pi_{new}(\cdot | S), \mathcal{B}_\tau Q_\tau^{\pi_{old}}(S, \cdot))} - \mathbb{E}_{\mathcal{B}_\tau Q_\tau^{\pi_{old}}} [\log(\pi_{old}(\cdot | S))] \right] \\ & \geq \mathbb{E}_{d^{\pi_{new}}} [\text{RKL}(\pi_{new}(\cdot | S), \mathcal{B}_\tau Q_\tau^{\pi_{old}}(S, \cdot))]. \end{aligned}$$

If we can show that the LHS is smaller than

$$\mathbb{E}_{d^{\pi_{\text{new}}}} [\text{RKL}(\pi_{\text{old}}(\cdot | S), \mathcal{B}_\tau Q_\tau^{\pi_{\text{old}}}(S, \cdot))],$$

then, by Proposition 8, we will be guaranteed improvement. The condition can be written as

$$\begin{aligned} & \mathbb{E}_{d^{\pi_{\text{new}}}} [\text{RKL}(\pi_{\text{old}}(\cdot | S), \mathcal{B}_\tau Q_\tau^{\pi_{\text{old}}}(S, \cdot))] \geq \\ & \mathbb{E}_{d^{\pi_{\text{new}}}} \left[ \frac{\|Q_\tau^{\pi_{\text{old}}}(S, \cdot)\|_\infty}{\tau} \sqrt{2\text{FKL}(\pi_{\text{new}}(\cdot | S), \mathcal{B}_\tau Q_\tau^{\pi_{\text{old}}}(S, \cdot))} - \mathbb{E}_{\mathcal{B}_\tau Q_\tau^{\pi_{\text{old}}}} [\log(\pi_{\text{old}}(\cdot | S))] \right]. \end{aligned} \quad (25)$$

This inequality will imply:

$$\begin{aligned} \mathbb{E}_{d^{\pi_{\text{new}}}} [\text{RKL}(\pi_{\text{old}}(\cdot | S), \mathcal{B}_\tau Q_\tau^{\pi_{\text{old}}}(S, \cdot))] & \geq \mathbb{E}_{d^{\pi_{\text{new}}}} [\text{RKL}(\pi_{\text{new}}(\cdot | S), \mathcal{B}_\tau Q_\tau^{\pi_{\text{old}}}(S, \cdot))] \\ & \Leftrightarrow \mathbb{E}_{d^{\pi_{\text{new}}}} [\Delta \text{RKL}(\pi_{\text{old}}(\cdot | S), \pi_{\text{new}}(\cdot | S))] \geq 0, \end{aligned}$$

which will in turn imply improvement. We will start from Equation (25) and do the derivation backwards: each subsequent step will always imply the previous step, but the converse may or may not be true. In the end, the final inequality will imply all those preceding it and, in turn, also imply the desired result. When two consecutive steps imply each other, we will write  $\Leftrightarrow$ ; otherwise, we will write  $\Leftarrow$ .

We begin by writing out what we desire and rearranging.

$$\begin{aligned} & \mathbb{E}_{d^{\pi_{\text{new}}}} [\text{RKL}(\pi_{\text{old}}(\cdot | S), \mathcal{B}_\tau Q_\tau^{\pi_{\text{old}}}(S, \cdot))] \\ & \geq \mathbb{E}_{d^{\pi_{\text{new}}}} \left[ \frac{\|Q_\tau^{\pi_{\text{old}}}(S, \cdot)\|_\infty}{\tau} \sqrt{2\text{FKL}(\pi_{\text{new}}(\cdot | S), \mathcal{B}_\tau Q_\tau^{\pi_{\text{old}}}(S, \cdot))} - \mathbb{E}_{\mathcal{B}_\tau Q_\tau^{\pi_{\text{old}}}} [\log(\pi_{\text{old}}(\cdot | S))] \right], \\ & \Leftarrow \mathbb{E}_{d^{\pi_{\text{new}}}} [\text{RKL}(\pi_{\text{old}}(\cdot | S), \mathcal{B}_\tau Q_\tau^{\pi_{\text{old}}}(S, \cdot))] \geq \\ & \frac{\|Q_\tau^{\pi_{\text{old}}}\|_\infty}{\tau} \mathbb{E}_{d^{\pi_{\text{new}}}} \left[ \sqrt{2\text{FKL}(\pi_{\text{new}}(\cdot | S), \mathcal{B}_\tau Q_\tau^{\pi_{\text{old}}}(S, \cdot))} \right] + \mathbb{E}_{d^{\pi_{\text{new}}}} \left[ -\mathbb{E}_{\mathcal{B}_\tau Q_\tau^{\pi_{\text{old}}}} [\log(\pi_{\text{old}}(\cdot | S))] \right], \\ & \Leftrightarrow \frac{\tau}{\|Q_\tau^{\pi_{\text{old}}}\|_\infty} \left( \mathbb{E}_{d^{\pi_{\text{new}}}} [\text{RKL}(\pi_{\text{old}}(\cdot | S), \mathcal{B}_\tau Q_\tau^{\pi_{\text{old}}}(S, \cdot)) + \mathbb{E}_{\mathcal{B}_\tau Q_\tau^{\pi_{\text{old}}}} [\log(\pi_{\text{old}}(\cdot | S))] \right] \\ & \geq \mathbb{E}_{d^{\pi_{\text{new}}}} \left[ \sqrt{2\text{FKL}(\pi_{\text{new}}(\cdot | S), \mathcal{B}_\tau Q_\tau^{\pi_{\text{old}}}(S, \cdot))} \right]. \end{aligned}$$

Now, we square both sides. The following is an  $\Leftrightarrow$  because we assumed

$$\mathbb{E}_{d^{\pi_{\text{new}}}} [\text{RKL}(\pi_{\text{old}}(\cdot | S), \mathcal{B}_\tau Q_\tau^{\pi_{\text{old}}}(S, \cdot))] + \mathbb{E}_{d^{\pi_{\text{new}}}} [\mathbb{E}_{\mathcal{B}_\tau Q_\tau^{\pi_{\text{old}}}} [\log(\pi_{\text{old}}(\cdot | S))] ] \geq 0.$$

Hence,

$$\begin{aligned} & \Leftrightarrow \left( \frac{\tau}{\|Q_\tau^{\pi_{\text{old}}}\|_\infty} \left( \mathbb{E}_{d^{\pi_{\text{new}}}} [\text{RKL}(\pi_{\text{old}}(\cdot | S), \mathcal{B}_\tau Q_\tau^{\pi_{\text{old}}}(S, \cdot)) + \mathbb{E}_{\mathcal{B}_\tau Q_\tau^{\pi_{\text{old}}}} [\log(\pi_{\text{old}}(\cdot | S))] \right] \right)^2 \\ & \geq \left( \mathbb{E}_{d^{\pi_{\text{new}}}} \left[ \sqrt{2\text{FKL}(\pi_{\text{new}}(\cdot | S), \mathcal{B}_\tau Q_\tau^{\pi_{\text{old}}}(S, \cdot))} \right] \right)^2. \end{aligned}$$

The above is implied by the following because of Jensen's inequality which gives us

$$\left( \mathbb{E}_{d^{\pi_{\text{new}}}} \left[ \sqrt{2\text{FKL}(\pi_{\text{new}}(\cdot|S), \mathcal{B}_\tau Q_\tau^{\pi_{\text{old}}}(S, \cdot))} \right] \right)^2 \leq \mathbb{E}_{d^{\pi_{\text{new}}}} [2\text{FKL}(\pi_{\text{new}}(\cdot|S), \mathcal{B}_\tau Q_\tau^{\pi_{\text{old}}}(S, \cdot))].$$

$$\begin{aligned} &\Leftarrow \left( \frac{\tau}{\|Q_\tau^{\pi_{\text{old}}}\|_\infty} \left( \mathbb{E}_{d^{\pi_{\text{new}}}} [\text{RKL}(\pi_{\text{old}}(\cdot|S), \mathcal{B}_\tau Q_\tau^{\pi_{\text{old}}}(S, \cdot)) + \mathbb{E}_{\mathcal{B}_\tau Q_\tau^{\pi_{\text{old}}}} [\log(\pi_{\text{old}}(\cdot|S))]] \right) \right)^2 \\ &\geq \mathbb{E}_{d^{\pi_{\text{new}}}} [2\text{FKL}(\pi_{\text{new}}(\cdot|S), \mathcal{B}_\tau Q_\tau^{\pi_{\text{old}}}(S, \cdot))]. \end{aligned}$$

Dividing by two and rearranging once more,

$$\begin{aligned} &\Leftrightarrow \frac{1}{2} \left( \frac{\tau}{\|Q_\tau^{\pi_{\text{old}}}\|_\infty} \left( \mathbb{E}_{d^{\pi_{\text{new}}}} [\text{RKL}(\pi_{\text{old}}(\cdot|S), \mathcal{B}_\tau Q_\tau^{\pi_{\text{old}}}(S, \cdot)) + \mathbb{E}_{\mathcal{B}_\tau Q_\tau^{\pi_{\text{old}}}} [\log(\pi_{\text{old}}(\cdot|S))]] \right) \right)^2 \\ &\geq \mathbb{E}_{d^{\pi_{\text{new}}}} [\text{FKL}(\pi_{\text{new}}(\cdot|S), \mathcal{B}_\tau Q_\tau^{\pi_{\text{old}}}(S, \cdot))], \\ &\Leftrightarrow -\frac{1}{2} \left( \frac{\tau}{\|Q_\tau^{\pi_{\text{old}}}\|_\infty} \left( \mathbb{E}_{d^{\pi_{\text{new}}}} [\text{RKL}(\pi_{\text{old}}(\cdot|S), \mathcal{B}_\tau Q_\tau^{\pi_{\text{old}}}(S, \cdot)) + \mathbb{E}_{\mathcal{B}_\tau Q_\tau^{\pi_{\text{old}}}} [\log(\pi_{\text{old}}(\cdot|S))]] \right) \right)^2 \\ &\quad + \mathbb{E}_{d^{\pi_{\text{new}}}} [\text{FKL}(\pi_{\text{old}}(\cdot|S), \mathcal{B}_\tau Q_\tau^{\pi_{\text{old}}}(S, \cdot))] \\ &\leq \mathbb{E}_{d^{\pi_{\text{new}}}} [\Delta\text{FKL}(\pi_{\text{old}}(\cdot|S), \pi_{\text{new}}(\cdot|S))]. \end{aligned}$$

The claims thus follows, as we have recovered the assumption in the statement of the Proposition.  $\blacksquare$

## Appendix B. Additional Experimental Results

### B.1 Exploration in a Discrete Maze

For these experiments, we use Gym-maze<sup>14</sup>, choosing their fixed  $10 \times 10$  maze to plot the changes in state-visitation distribution throughout training. This way, some of the differences we may be able to inspect are: if any one of the divergences becomes deterministic quicker than the other; if any of the divergences get stuck in local optima while the other succeeds in finding the optimal policy; how spread-out the state-visitation distribution is in the early phases of training, when the agent is more likely to be exploring; if there are different priorities between regions of the maze when the agents are exploring.

For the Gym-maze, the dynamics  $\Pr(s_{t+1} | s_t, a_t)$  are deterministic and the actions are the four directions. The agent remains in place if it tries to move to a position where there is a wall. The reward is -0.1 divided by the total number of cells if  $s_{t+1}$  is not the goal state and is 1.0 for the goal state. There is a timeout if the agent does not reach the goal after 10,000 steps. The agent is given a tabular representation: a one-hot encoding of the (x,y) position. This means that the agent has to create some sort of mental map of the maze from the positions it visited, causing the environment to be a harder exploratory problem than it might seem at first glance. We use the same agent that will be used in Section 9, based on Algorithm 1, which was introduced in Section 4.

14. <https://github.com/MattChanTK/Gym-maze>

On each iteration, one gradient descent step is performed to update the policy, for a given value function.

### B.1.1 EXPLORATION WITH TRUE VALUES

We want to understand differences in exploration when minimizing the KL divergences with respect to the estimated value functions. Even so, it is important to also study how the state-visitation distribution changes when using accurate value functions, which we will henceforth refer to as true values, noting that they are still only approximations of the actual values that are calculated more precisely. In this setting, the agent does not need to explore or even interact with the environment directly; the dynamics are given. These studies make clear not only how entropy affects the convergence of policies but also make it easier to disentangle which behaviors and results are due to the use of estimated values and which happen even with true values.

By hand annotating the dynamics, we can use dynamic programming to compute more accurate estimates of the value function, as opposed to the common approach of using gradient descent methods based on the Bellman equation and least squares. The gradient for the greedification step is computed over all states, as opposed to using a buffer, and the learning rate is set to 0.1 with RMSprop. The total number of iterations is 100.

The stopping condition for dynamic programming is when the relative difference between successive Q's is less than 0.01% for 10 consecutive iterations. The policy update, for either FKL or RKL, requires both Q and V. We compute V directly from Q, by summing over all four actions weighted by the current policy. The most representative timesteps are illustrated in Figure 15.

### B.1.2 EXPLORATION WITH ESTIMATED VALUES

In this section, we use the more practical approach of updating value function estimates via expected semi-gradient updates. The optimizer used was RMSprop with learning rate 0.001 and the total number of iterations is 20000. We use a mini-batch of 32 states sampled from a buffer. The buffer size is 10000.

Results are illustrated in Figure 16, where we show only the subset of timesteps most representative of changes and only the plots corresponding to  $\tau = 0$ . The start state is in the top left position and the goal state is in the bottom right. To obtain these images, 30 seeds were used for each temperature-divergence combination and trained for the full number of iterations. The image at timestep  $t$  corresponds to 100 trajectories generated from each of the 30 policies at that timestep. Particularly, we take the visitation counts of each of these  $30 \times 100$  trajectories, normalize them and average them, producing an image representative of the overall exploratory behavior of that divergence-temperature combination. The figure shows that, given a certain temperature, both RKL and FKL have state-visitation distributions that evolve very similarly, as can be seen by comparing the pairwise green and blue images for each timestep.

Figure 17 makes it clear that, for this setting, entropy regularization seems to do more harm than good: the agents converge to policies that tend to go to the correct trajectory, but waste time exploring when they already have all information they need. This is one

example where the maximization of entropy conflicts with the true objective, ideally, one would prefer to have a deterministic policy for this environment at the end of training.

## B.2 Exploration in a Continuous Maze

This section gives a more in-depth view of the experiments from Section 8.2. Figure 18 plots the cumulative number of times both the misleading and the correct exits are reached throughout training using 30 seeds and 2M steps, instead of 500k. For  $\tau = 1000$ , RKL and FKL have very similar curves; for  $\tau = 100$  and  $\tau = 10$  the RKL visits the misleading exit more and the correct exit less. For the remaining temperatures, FKL visits both exits more than the RKL. For lower temperatures, the misleading exit is visited orders of magnitude more than the regular one. These all corroborate with the conclusion that the FKL is more exploratory in this setting.

## B.3 Performance

Implementation details are the same as in Section 9. We perform 30 runs for all hyperparameter settings and plot the mean return averaged over the past 20 episodes. Shaded areas represent standard errors.

### B.3.1 CONTINUOUS-ACTIONS RESULTS

We compare agents on Pendulum (Brockman et al., 2016), Reacher, Swimmer and HalfCheetah (Todorov et al., 2012), with results shown in Figure 19. We exclude Hard FKL in our comparison since it requires access to  $\max_a Q(s, a)$ , which is difficult to obtain with continuous actions. The leftmost plot shows all temperatures from RKL, the middle plot shows all temperatures for FKL and the rightmost plot averages all high temperatures and all low temperatures for each divergence. Temperatures  $[1.0, 0.5, 0.1]$  were considered high and  $[0.05, 0.01, 0.005, 0.001, 0.0]$  were considered low.

Except for Pendulum, which is the simplest environment and where FKL seems to perform more consistently across temperatures, the overall behavior of both divergences is very similar, with performance being much more dependent on the choice of temperature than on the choice of divergence. On Reacher, Swimmer and Pendulum, FKL and RKL with high temperatures have the worst performance, but on HalfCheetah this pattern is reversed, meaning the benefits of entropy regularization are environment dependent.

It is difficult to comment on the importance of the policy parameterization for these experiments relative to our microworld experiments. Any influence from the Gaussian policy parameterization is conflated with function approximation. Moreover, as we will see below, no stark pattern seems to divide continuous and discrete action settings, as one did in our microworld experiments.

### B.3.2 DISCRETE-ACTIONS RESULTS

We report results for environments from the OpenAI Gym (Brockman et al., 2016) and MinAtar (Young and Tian, 2019). Analogously to the continuous action setting, the OpenAI Gym results reported in Figure 20 show that both FKL and RKL behave similarly for any given choice of temperature, with the left and middle plots being similar to one another.



The main difference is that, for some of the non-optimal temperatures for each problem, FKL seemed to learn faster than RKL, this becomes specially clear on Acrobot. The higher temperatures performed better on CartPole and LunarLander, but worse on Acrobot, confirming that the influence of this hyperparameter is highly environment dependent.

Finally, for the MinAtar results represented in Figure 21, there is once more no consistent dominance of either KL over the other: the plots of both FKL and RKL are again highly similar to each other. The slight superiority of FKL for non-optimal temperatures is present only on Breakout and Seaquest. On Asterix, Freeway, Seaquest and Space Invaders highest temperatures performed the worse, but they performed the best on Breakout, showing a pattern opposite of the one seen in the continuous environments of Figure 19 and confirming that the optimal temperature is going to vary according to the environment.

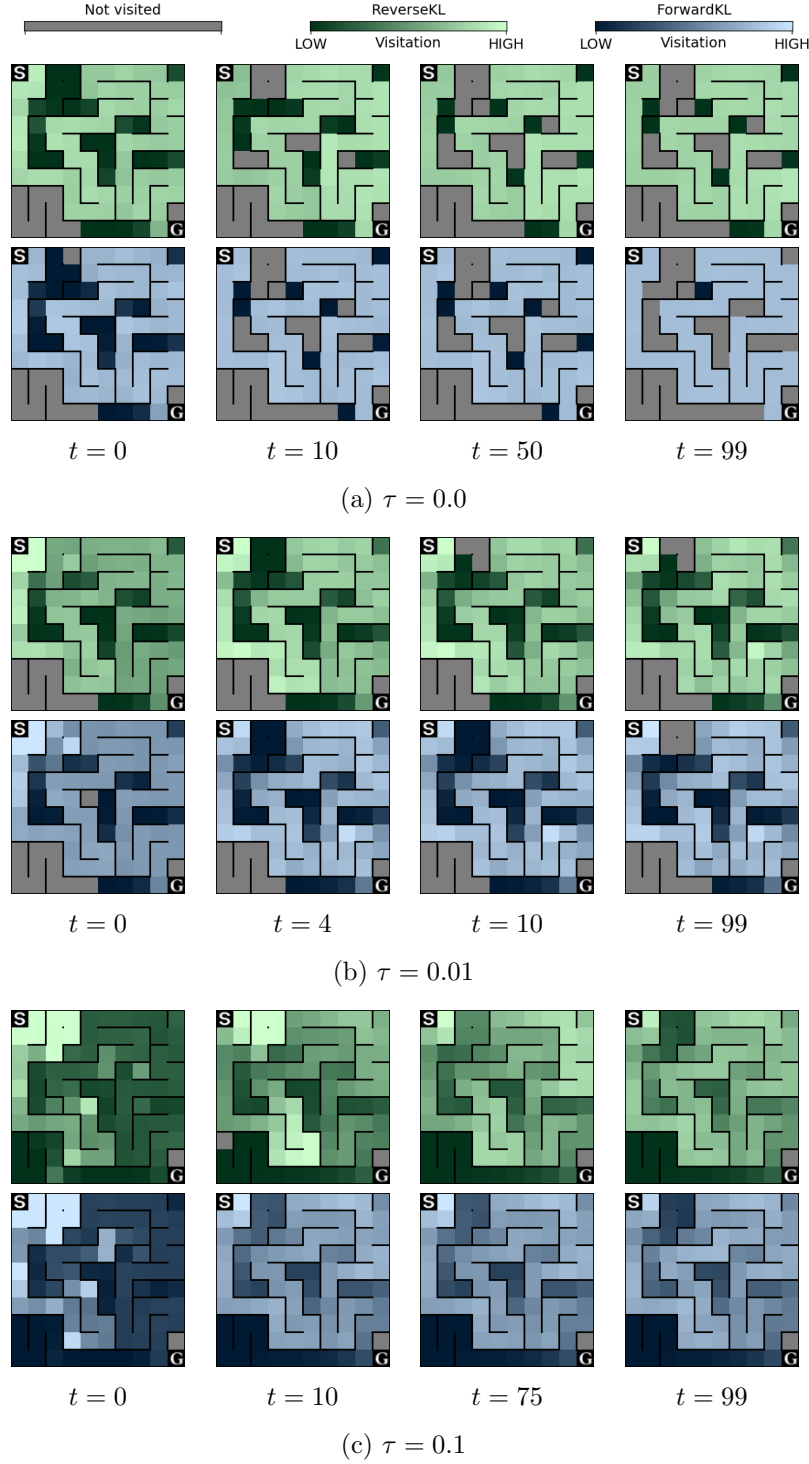


Figure 15: Evolution of state-visitation distributions throughout training for each temperature with true values.

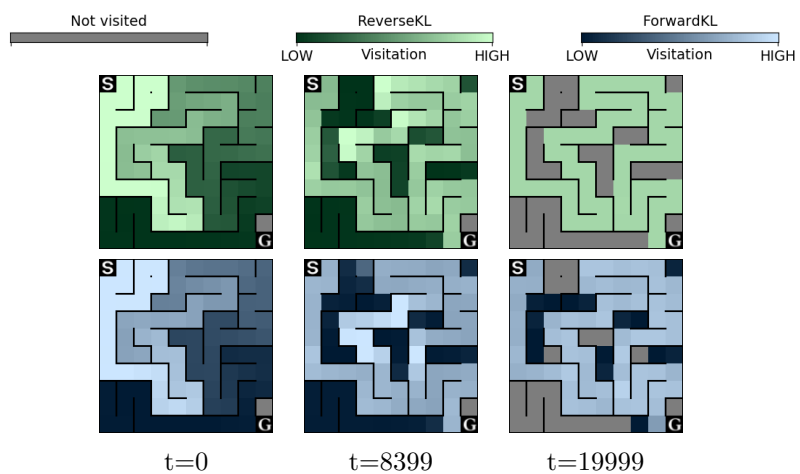


Figure 16: Evolution of state-visitation distributions throughout training for  $\tau = 0$

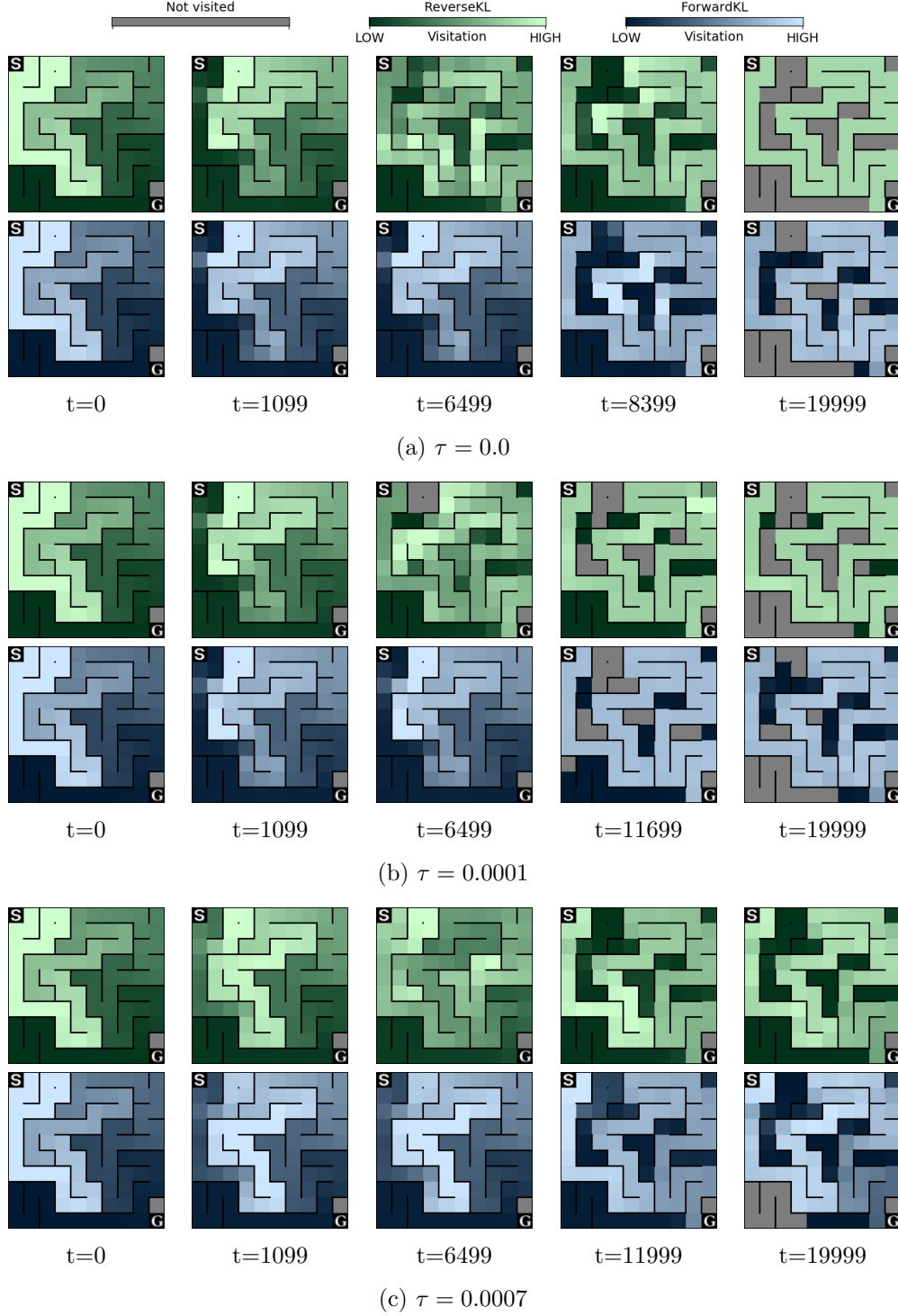


Figure 17: Evolution of state-visitation distributions throughout training for each temperature with estimated values.

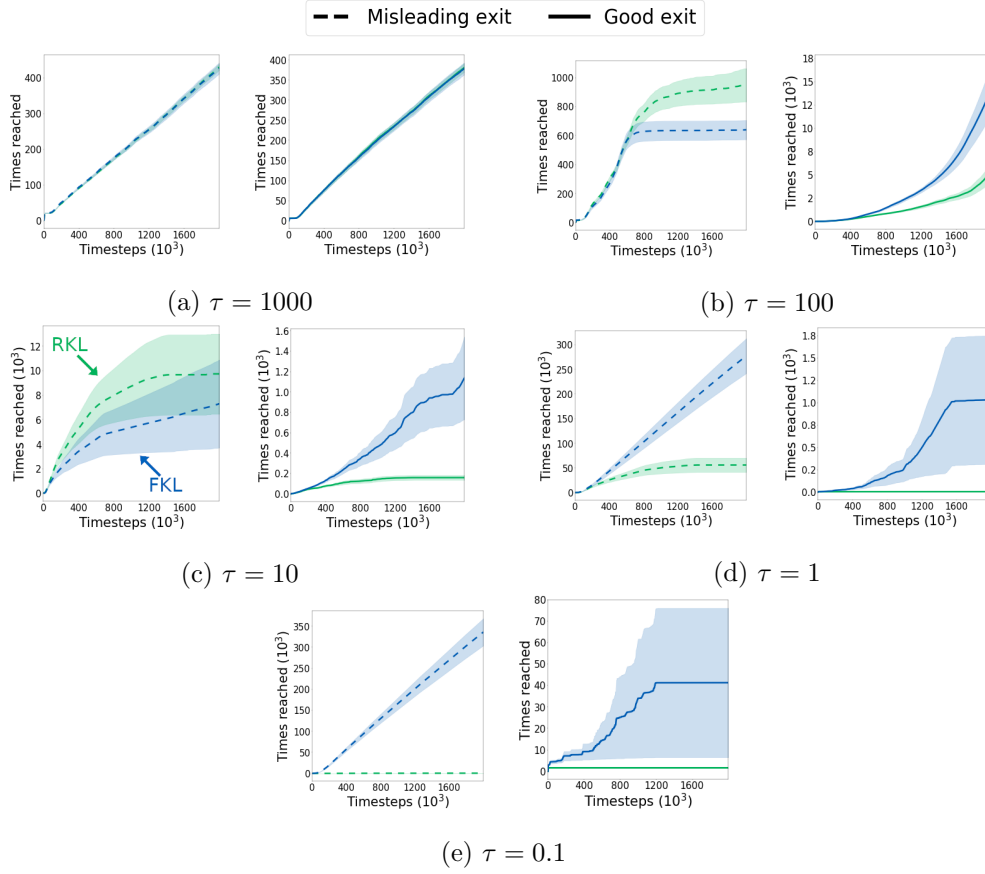


Figure 18: Cumulative number of times the each exit is reached throughout training for multiple temperatures plotted separately. RKL corresponds to green curves and FKL to blue curves.

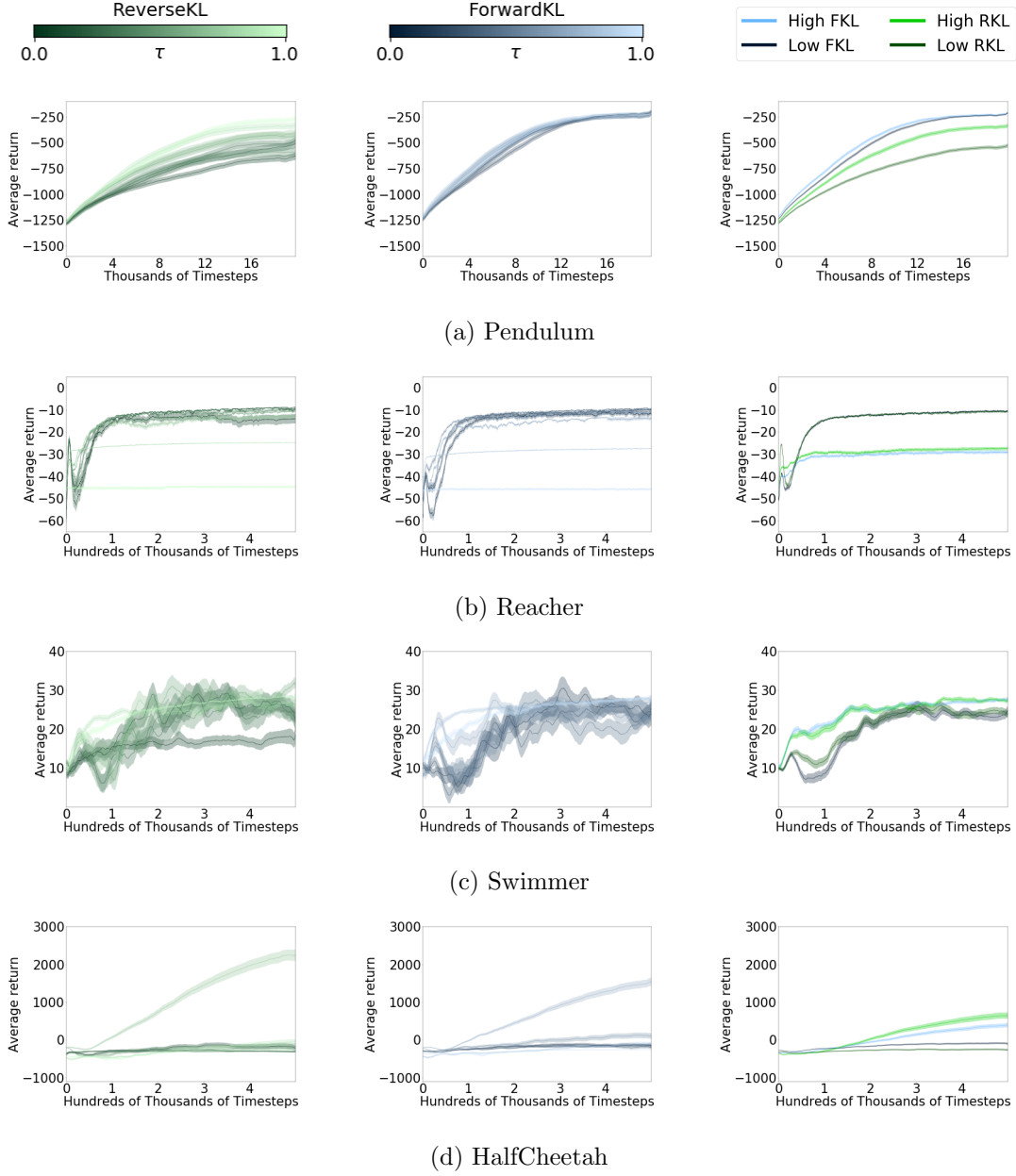


Figure 19: Continuous-action environments. Shown are the averaged top 20% performing hyperparameter settings for each algorithm, which are selected by largest area under the last half of the learning curve. In the left we have RKL, in the middle we have FKL and in the right we grouped the high and low temperatures for both FKL and RKL. Temperatures for the curves in the left and middle plots correspond to the respective colormaps and in the rightmost plot the curves correspond to the legend

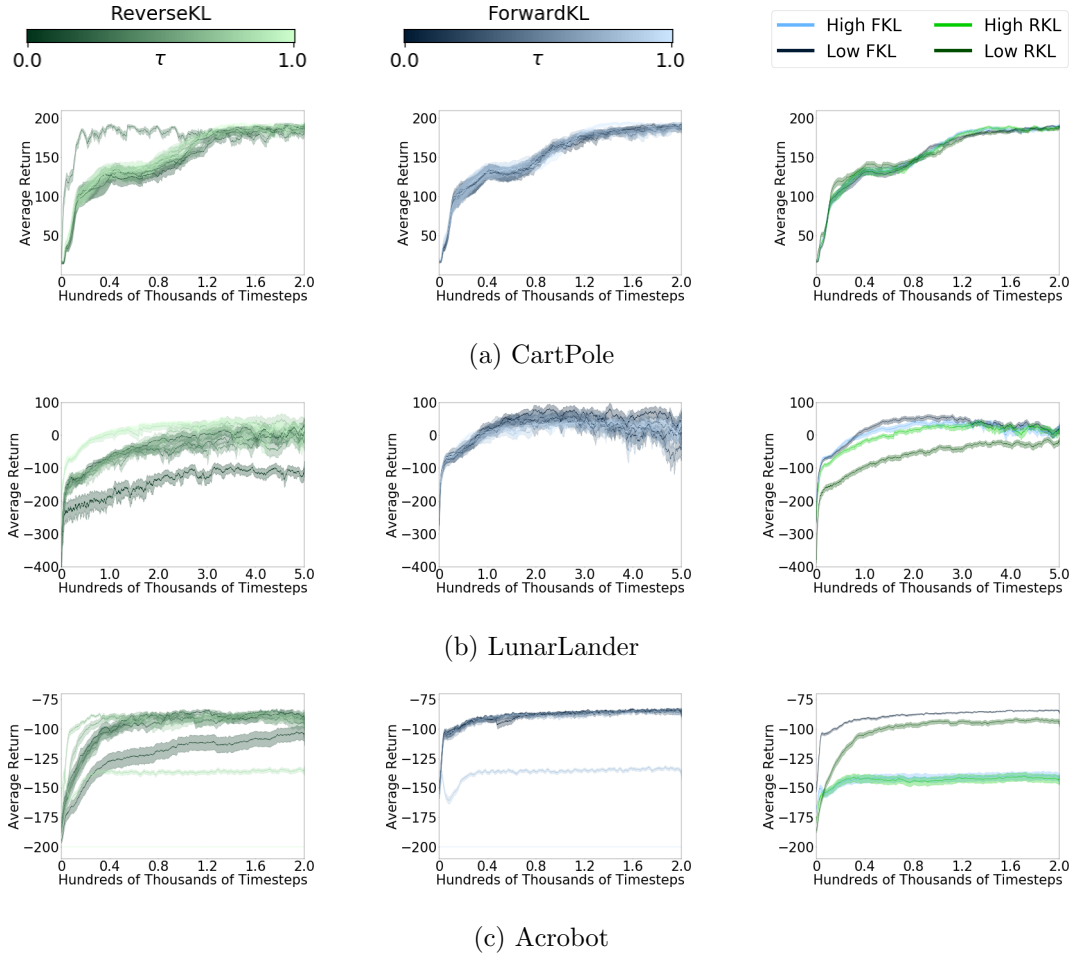


Figure 20: OpenAI Gym discrete-action environments. Plot settings are identical to Figure 19.

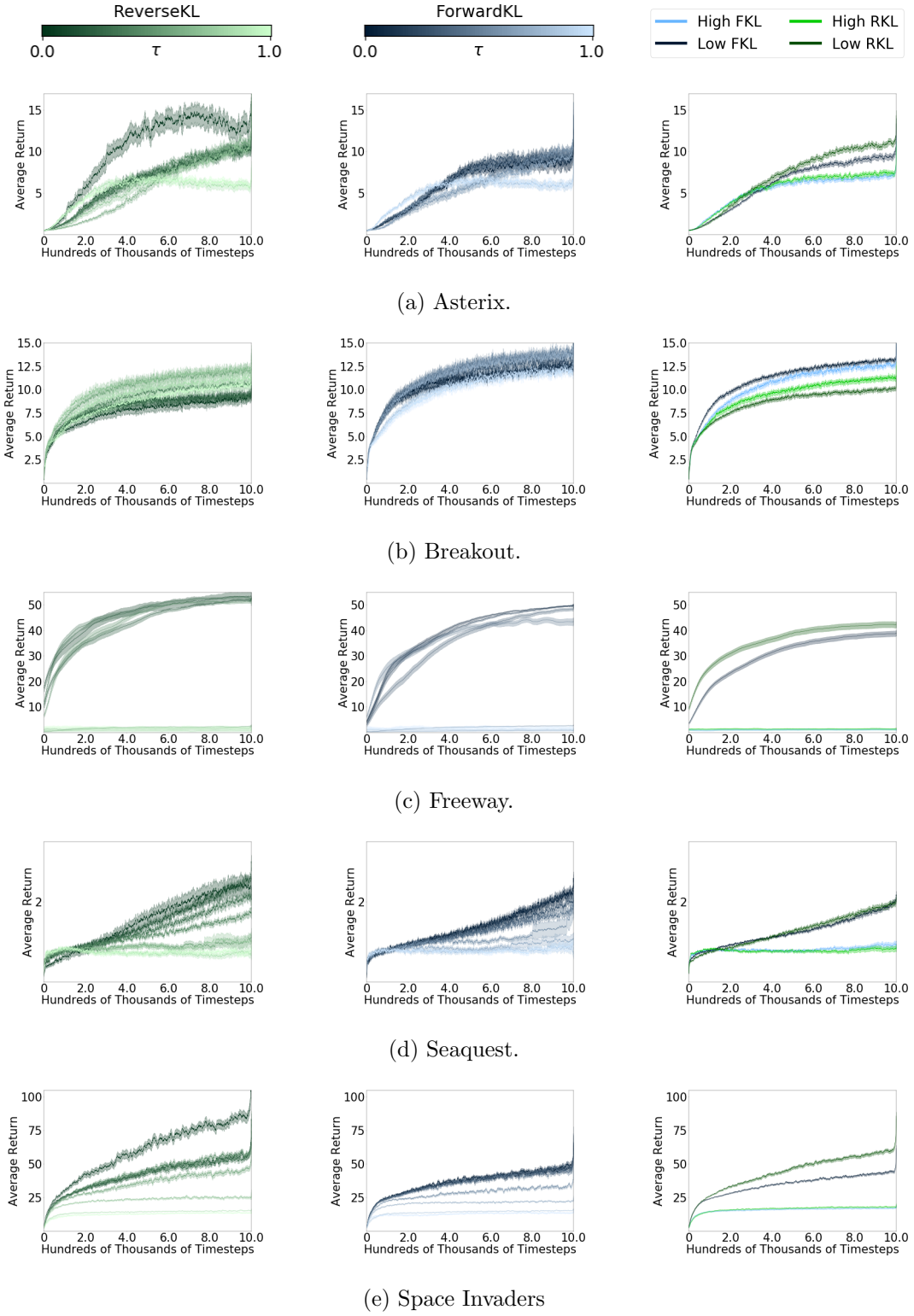


Figure 21: MinAtar discrete-action environments. Plot settings are identical to those in Figure 19.



## References

- Yasin Abbasi-Yadkori, Peter Bartlett, Kush Bhatia, Nevena Lazic, Csaba Szepesvari, and Gellért Weisz. Politex: Regret bounds for policy iteration using expert prediction. In *International Conference on Machine Learning*, 2019.
- Abbas Abdolmaleki, Jost Tobias Springenberg, Yuval Tassa, Remi Munos, Nicolas Heess, and Martin Riedmiller. Maximum a posteriori policy optimisation. In *International Conference on Learning Representations*, 2018.
- Alekh Agarwal, Sham M Kakade, Jason D Lee, and Gaurav Mahajan. On the theory of policy gradient methods: Optimality, approximation, and distribution shift. *arXiv:1908.00261*, 2019a.
- Rishabh Agarwal, Chen Liang, Dale Schuurmans, and Mohammad Norouzi. Learning to generalize from sparse and underspecified rewards. In *International Conference on Machine Learning*, 2019b.
- Zafarali Ahmed, Nicolas Le Roux, Mohammad Norouzi, and Dale Schuurmans. Understanding the impact of entropy on policy optimization. In *International Conference on Machine Learning*, 2019.
- Martin Arjovsky, Soumith Chintala, and Léon Bottou. Wasserstein generative adversarial networks. In *International Conference on Machine Learning*, 2017.
- Kavosh Asadi and Michael L. Littman. An alternative softmax operator for reinforcement learning. In *International Conference on Machine Learning*, 2017.
- Boris Belousov and Jan Peters. Entropic regularization of markov decision processes. *Entropy*, 21(7), 2019.
- Dimitri P. Bertsekas. Approximate policy iteration: A survey and some new methods. *Journal of Control Theory and Applications*, 9(3), 2011.
- Dimitri P Bertsekas. *Reinforcement learning and optimal control*. Athena Scientific Belmont, MA, 2019.
- Jalaj Bhandari and Daniel Russo. Global optimality guarantees for policy gradient methods. *arXiv:1906.01786*, 2019.
- Patrick Billingsley. *Probability and Measure*. John Wiley & Sons, 2008.
- Christopher M. Bishop. *Pattern Recognition and Machine Learning*. Springer-Verlag, Berlin, Heidelberg, 2006.
- Greg Brockman, Vicki Cheung, Ludwig Pettersson, Jonas Schneider, John Schulman, Jie Tang, and Wojciech Zaremba. Openai gym. *arXiv:1606.01540*, 2016.
- Minmin Chen, Ramki Gummati, Chris Harris, and Dale Schuurmans. Surrogate objectives for batch policy optimization in one-step decision making. In *Advances in Neural Information Processing Systems*, 2019.

- Po-Wei Chou, Daniel Maturana, and Sebastian Scherer. Improving stochastic policy gradients in continuous control with deep reinforcement learning using the beta distribution. In *International Conference on Machine Learning*, 2017.
- Charles W Clenshaw and Alan R Curtis. A method for numerical integration on an automatic computer. *Numerische Mathematik*, 2(1), 1960.
- Robert Dadashi, Adrien Ali Taiga, Nicolas Le Roux, Dale Schuurmans, and Marc G. Bellemare. The value function polytope in reinforcement learning. In *International Conference on Machine Learning*, 2019.
- Logan Engstrom, Andrew Ilyas, Shibani Santurkar, Dimitris Tsipras, Firdaus Janoos, Larry Rudolph, and Aleksander Madry. Implementation matters in deep rl: A case study on ppo and trpo. In *International Conference on Learning Representations*, 2019.
- Amir-massoud Farahmand, Doina Precup, André MS Barreto, and Mohammad Ghavamzadeh. Classification-based approximate policy iteration. *IEEE Transactions on Automatic Control*, 60(11), 2015.
- Matthew Fellows, Anuj Mahajan, Tim GJ Rudner, and Shimon Whiteson. Virel: A variational inference framework for reinforcement learning. In *Advances in Neural Information Processing Systems*, 2019.
- Justin Fu, Katie Luo, and Sergey Levine. Learning robust rewards with adversarial inverse reinforcement learning. In *International Conference on Learning Representations*, 2018.
- Matthieu Geist, Bruno Scherrer, and Olivier Pietquin. A theory of regularized markov decision processes. In *International Conference on Machine Learning*, 2019.
- Seyed Kamyar Seyed Ghasemipour, Richard Zemel, and Shixiang Gu. A divergence minimization perspective on imitation learning methods. In *Conference on Robot Learning*, 2020.
- Dibya Ghosh, Marlos C. Machado, and Nicolas Le Roux. An operator view of policy gradient methods. In *Advances in Neural Information Processing Systems*, 2020.
- Shixiang Gu. *Sample-efficient deep reinforcement learning for continuous control*. PhD thesis, University of Cambridge, 2019.
- Tuomas Haarnoja, Haoran Tang, Pieter Abbeel, and Sergey Levine. Reinforcement learning with deep energy-based policies. In *International Conference on Machine Learning*, 2017.
- Tuomas Haarnoja, Aurick Zhou, Pieter Abbeel, and Sergey Levine. Soft actor-critic: Off-policy maximum entropy deep reinforcement learning with a stochastic actor. In *International Conference on Machine Learning*, 2018.
- Peter Henderson, Riashat Islam, Philip Bachman, Joelle Pineau, Doina Precup, and David Meger. Deep reinforcement learning that matters. In *AAAI Conference on Artificial Intelligence*, 2018.

- Jonathan Ho and Stefano Ermon. Generative adversarial imitation learning. In *Advances in Neural Information Processing Systems*, 2016.
- Andrew Ilyas, Logan Engstrom, Shibani Santurkar, Dimitris Tsipras, Firdaus Janoos, Larry Rudolph, and Aleksander Madry. A closer look at deep policy gradients. In *International Conference on Learning Representations*, 2020.
- Ehsan Imani, Eric Graves, and Martha White. An off-policy policy gradient theorem using emphatic weightings. In *Advances in Neural Information Processing Systems*, 2018.
- Riashat Islam, Raihan Seraj, Pierre-Luc Bacon, and Doina Precup. Entropy regularization with discounted future state distribution in policy gradient methods. *arXiv:1912.05104*, 2019.
- Ghassen Jerfel, Serena Lutong Wang, Clara Fannjiang, Katherine A Heller, Yian Ma, and Michael Jordan. Variational refinement for importance sampling using the forward kullback-leibler divergence. In *Advances in Approximate Bayesian Inference*, 2021.
- Sham Kakade and John Langford. Approximately optimal approximate reinforcement learning. In *International Conference on Machine Learning*, 2002.
- Diederik P Kingma and Jimmy Ba. Adam: A method for stochastic optimization. *International Conference on Learning Representations*, 2015.
- Jens Kober and Jan R Peters. Policy search for motor primitives in robotics. In *Advances in Neural Information Processing Systems*, 2008.
- Daphne Koller and Nir Friedman. *Probabilistic graphical models: principles and techniques*. MIT press, 2009.
- Vijay R Konda and John N Tsitsiklis. Actor-critic algorithms. In *Advances in Neural Information Processing Systems*, 2000.
- Tadashi Kozuno, Eiji Uchibe, and Kenji Doya. Theoretical analysis of efficiency and robustness of softmax and gap-increasing operators in reinforcement learning. In *International Conference on Artificial Intelligence and Statistics*, 2019.
- Michail G Lagoudakis and Ronald Parr. Reinforcement learning as classification: Leveraging modern classifiers. In *International Conference on Machine Learning*, 2003.
- Alessandro Lazaric, Mohammad Ghavamzadeh, and Rémi Munos. Analysis of a classification-based policy iteration algorithm. In *International Conference on Machine Learning*, 2010.
- Alessandro Lazaric, Mohammad Ghavamzadeh, and Rémi Munos. Finite-sample analysis of least-squares policy iteration. *Journal of Machine Learning Research*, 13(98), 2012.
- Alessandro Lazaric, Mohammad Ghavamzadeh, and Rémi Munos. Analysis of classification-based policy iteration algorithms. *Journal of Machine Learning Research*, 17(19), 2016.
- Sergey Levine. Reinforcement learning and control as probabilistic inference: Tutorial and review. *arXiv:1805.00909*, 2018.

- Timothy P Lillicrap, Jonathan J. Hunt, Alexander Pritzel, Nicolas Heess, Tom Erez, Yuval Tassa, David Silver, and Daan Wierstra. Continuous control with deep reinforcement learning. In *International Conference on Learning Representations*, 2016.
- Sungsu Lim, Ajin Joseph, Lei Le, Yangchen Pan, and Martha White. Actor-expert: A framework for using q-learning in continuous action spaces. *arXiv:1810.09103*, 2018.
- Boyi Liu, Qi Cai, Zhuoran Yang, and Zhaoran Wang. Neural trust region/proximal policy optimization attains globally optimal policy. In *Advances in Neural Information Processing Systems*, 2019.
- Tyler Lu, Dale Schuurmans, and Craig Boutilier. Non-delusional q-learning and value-iteration. In *Advances in Neural Information Processing Systems*, 2018.
- Jincheng Mei, Chenjun Xiao, Ruitong Huang, Dale Schuurmans, and Martin Müller. On principled entropy exploration in policy optimization. In *International Joint Conference on Artificial Intelligence*, 2019.
- Jincheng Mei, Chenjun Xiao, Csaba Szepesvari, and Dale Schuurmans. On the global convergence rates of softmax policy gradient methods. In *International Conference on Machine Learning*, 2020.
- Volodymyr Mnih, Adria Puigdomenech Badia, Mehdi Mirza, Alex Graves, Timothy Lillicrap, Tim Harley, David Silver, and Koray Kavukcuoglu. Asynchronous methods for deep reinforcement learning. In *International Conference on Machine Learning*, 2016.
- Ofir Nachum, Mohammad Norouzi, and Dale Schuurmans. Improving policy gradient by exploring under-appreciated rewards. In *International Conference on Learning Representations*, 2017a.
- Ofir Nachum, Mohammad Norouzi, Kelvin Xu, and Dale Schuurmans. Bridging the gap between value and policy based reinforcement learning. In *Advances in Neural Information Processing Systems*, 2017b.
- Ofir Nachum, Bo Dai, Ilya Kostrikov, Yinlam Chow, Lihong Li, and Dale Schuurmans. Algaedice: Policy gradient from arbitrary experience. *arXiv:1912.02074*, 2019.
- Gergely Neu, Anders Jonsson, and Vicenç Gómez. A unified view of entropy-regularized markov decision processes. *arXiv:1705.07798*, 2017.
- Gerhard Neumann. Variational inference for policy search in changing situations. In *International Conference on Machine Learning*, 2011.
- Mohammad Norouzi, Samy Bengio, zhifeng Chen, Navdeep Jaitly, Mike Schuster, Yonghui Wu, and Dale Schuurmans. Reward augmented maximum likelihood for neural structured prediction. In *Advances in Neural Information Processing Systems*, 2016.
- Chris Nota and Philip S. Thomas. Is the policy gradient a gradient? In *International Conference on Autonomous Agents and Multiagent Systems*, 2020.

- Brendan O’Donoghue, Remi Munos, Koray Kavukcuoglu, and Volodymyr Mnih. Combining policy gradient and q-learning. *International Conference on Learning Representations*, 2017.
- Fabio Pardo, Arash Tavakoli, Vitaly Levдик, and Petar Kormushev. Time limits in reinforcement learning. In *International Conference on Machine Learning*, 2018.
- Theodore J. Perkins and Mark D. Pendrith. On the existence of fixed points for q-learning and sarsa in partially observable domains. In *International Conference on Machine Learning*, 2002.
- Theodore J Perkins and Doina Precup. A convergent form of approximate policy iteration. In *Advances in Neural Information Processing Systems*, 2003.
- Jan Peters, Katharina Mülling, and Yasemin Altün. Relative entropy policy search. In *AAAI Conference on Artificial Intelligence*, 2010.
- Mark S Pinsker. *Information and information stability of random variables and processes*. Holden-Day, 1964.
- Konrad Rawlik, Marc Toussaint, and Sethu Vijayakumar. On stochastic optimal control and reinforcement learning by approximate inference. In *International Joint Conference on Artificial Intelligence*, 2013.
- Oliver Richter and Roger Wattenhofer. Learning policies through quantile regression. *arXiv:1906.11941*, 2019.
- Moonkyung Ryu, Yinlam Chow, Ross Anderson, Christian Tjandraatmadja, and Craig Boutilier. Caql: Continuous action q-learning. In *International Conference on Learning Representations*, 2020.
- Igal Sason and Sergio Verdú.  $f$ -divergence inequalities. *IEEE Transactions on Information Theory*, 62(11), 2016.
- Bruno Scherrer. Approximate policy iteration schemes: A comparison. In *International Conference on Machine Learning*, 2014.
- Bruno Scherrer and Matthieu Geist. Local policy search in a convex space and conservative policy iteration as boosted policy search. In *Joint European Conference on Machine Learning and Knowledge Discovery in Databases*, 2014.
- Bruno Scherrer, Mohammad Ghavamzadeh, Victor Gabillon, Boris Lesner, and Matthieu Geist. Approximate modified policy iteration and its application to the game of tetris. *Journal of Machine Learning Research*, 16(49), 2015.
- John Schulman, Sergey Levine, Pieter Abbeel, Michael Jordan, and Philipp Moritz. Trust region policy optimization. In *International Conference on Machine Learning*, 2015.
- John Schulman, Philipp Moritz, Sergey Levine, Michael Jordan, and Pieter Abbeel. High-dimensional continuous control using generalized advantage estimation. *International Conference on Learning Representations*, 2016.

- John Schulman, Xi Chen, and Pieter Abbeel. Equivalence between policy gradients and soft q-learning. *arXiv:1704.06440*, 2017a.
- John Schulman, Filip Wolski, Prafulla Dhariwal, Alec Radford, and Oleg Klimov. Proximal policy optimization algorithms. *arXiv:1707.06347*, 2017b.
- Lior Shani, Yonathan Efroni, and Shie Mannor. Adaptive trust region policy optimization: Global convergence and faster rates for regularized mdps. In *AAAI Conference on Artificial Intelligence*, 2020.
- David Silver, Guy Lever, Nicolas Heess, Thomas Degris, Daan Wierstra, and Martin Riedmiller. Deterministic policy gradient algorithms. In *International Conference on Machine Learning*, 2014.
- Richard S. Sutton. *Temporal Credit Assignment in Reinforcement Learning*. PhD thesis, University of Massachusetts Amherst, 1984.
- Richard S. Sutton and Andrew G. Barto. *Reinforcement Learning: An Introduction*. MIT press, 2018.
- Richard S. Sutton, David A. McAllester, Satinder P. Singh, and Yishay Mansour. Policy gradient methods for reinforcement learning with function approximation. In *Advances in Neural Information Processing Systems*, 1999.
- Philip Thomas. Bias in natural actor-critic algorithms. In *International Conference on Machine Learning*, 2014.
- Tijmen Tieleman and Geoffrey Hinton. Lecture 6.5-rmsprop: Divide the gradient by a running average of its recent magnitude. *Coursera: Neural Networks for Machine Learning*, 2012.
- Emanuel Todorov, Tom Erez, and Yuval Tassa. Mujoco: A physics engine for model-based control. In *International Conference on Intelligent Robots and Systems*, 2012.
- Nino Vieillard, Tadashi Kozuno, Bruno Scherrer, Olivier Pietquin, Remi Munos, and Matthieu Geist. Leverage the average: an analysis of kl regularization in reinforcement learning. In *Advances in Neural Information Processing Systems*, 2020a.
- Nino Vieillard, Olivier Pietquin, and Matthieu Geist. Deep conservative policy iteration. In *AAAI Conference on Artificial Intelligence*, 2020b.
- Paul Wagner. A reinterpretation of the policy oscillation phenomenon in approximate policy iteration. In *Advances in Neural Information Processing Systems*, 2011.
- Paul Wagner. Optimistic policy iteration and natural actor-critic: A unifying view and a non-optimality result. In *Advances in Neural Information Processing Systems*, 2013.
- Ziyu Wang, Victor Bapst, Nicolas Heess, Volodymyr Mnih, Remi Munos, Koray Kavukcuoglu, and Nando de Freitas. Sample efficient actor-critic with experience replay. *International Conference on Learning Representations*, 2017.

- Patrick Nadeem Ward, Ariella Smofsky, and Avishek Joey Bose. Improving exploration in soft-actor-critic with normalizing flows policies. *Workshop on Invertible Neural Networks and Normalizing Flows at International Conference for Machine Learning*, 2019.
- Christopher J.C.H. Watkins and Peter Dayan. Q-learning. *Machine Learning*, 8(3-4), 1992.
- Ronald J Williams. Simple statistical gradient-following algorithms for connectionist reinforcement learning. *Machine Learning*, 8(3-4), 1992.
- Kenny Young and Tian Tian. Minatar: An atari-inspired testbed for more efficient reinforcement learning experiments. *arXiv:1903.03176*, 2019.
- B. Ziebart. Modeling purposeful adaptive behavior with the principle of maximum causal entropy. *PhD thesis, Carnegie Mellon University*, 2010.
- Brian D Ziebart, Andrew L Maas, J Andrew Bagnell, and Anind K Dey. Maximum entropy inverse reinforcement learning. In *AAAI Conference on Artificial Intelligence*, 2008.